VODOHOSPODÁŘSKÉ TECHNICKO-EKONOMICKÉ INFORMACE
(WATER MANAGEMENT TECHNICAL AND ECONOMIC INFORMATION)

VTEI / 2022 / 1

2nd February – World Wetlands Day

Wetlands are among of the world's most significant and threatened ecosystems. They take part in the water cycle in nature, retain water in the landscape, have a positive impact on the climate through high evaporation, sequester excess carbon dioxide from the air, and are a source of food for more than a third of the planet (fishing, rice cultivation). Peat bogs are an important carbon sink. The importance of wetlands is therefore in mitigating climate change, too. At the same time, wetlands are cores of biodiversity; they are biotopes for specific communities and endemic or very rare species of plants, animals, fungi, and micro-organisms. Unfortunately, due to human influence, wetlands are becoming increasingly scarce on Earth.

The Ramsar Convention is thus the first global intergovernmental convention for the protection and wise use of natural resources and the only convention that protects a specific type of biotope. The Convention on Wetlands of International Importance Especially as Waterfowl Habitat, known as the Ramsar Convention on Wetlands, was signed by the first States on 2nd February 1971 in Ramsar, Iran. This day was subsequently declared the World Wetlands Day.

So far, 169 states have joined the Convention. The Czech Republic has been a party to the Convention since 1990. The Ministry of Environment (MoE) is responsible for the implementation of the Convention in the Czech Republic. The Czech Ramsar Committee (established in 1993), which is composed of representatives of the Ministry of Environment, nature conservation officers, scientists, researchers and NGOs, acts as an advisory body on wetland protection. The Convention obliges member countries to designate at least one wetland of international importance on their territory, whose natural values meet the approved criteria, and to include it in the list of wetlands of international importance. It also commits the state to guarantee increased care and protection to the listed wetlands.

Did you know that the Czech Republic has included a total of 14 sites on the Ramsar List?

- Šumava peat bogs
- Třeboň Ponds
- Novozámecký and Břehyňský Ponds
- Lednice Ponds
- Litovelské Pomoraví (protected landscape area)
- The Odra floodplain (Poodří)
- Krkonoše peat bogs
- Třeboň peat bogs
- Wetlands of the lower Dyje floodplain
- The Liběchovka and Pšovka wetlands
- The underground Punkva river
- Ore Mts. peat bogs
- The upper Jizera river
- Slavkov Forest springs and peat bogs

Mgr. Zuzana Řehořová
VTEI expert editor

Photo: Shutterstock.com

Contents


Photo: i3rf.com

Dear readers,

I am certain that you feel the same way I do. It was looking like winter was finally going to be what we have been waiting for. The beginning was full of hope – it was freezing and there was snow even in towns and cities. Then, suddenly, something went wrong, and we entered the new year with temperature records. Those above zero, of course. Some days saw the highest temperatures ever recorded, with only the temperatures of the 1930^{s} getting closer. The thaw deprived us of valuable snow, so we have to rely on rain and hope that it will be sufficient to create the necessary water supplies for the summer with drought expected again. On the other hand, we are not yet out of winter, so it is too early to draw any conclusions. With some exaggeration, it will be interesting to see which of the articles in the VTEI February issue will ultimately be more relevant - the one addressing the zero isochion, i.e. the snow line, or the article about the detection of wetlands and waterlogged areas.

I am sure most of you have heard of seven-year climate cycles. They were based on ancient farmers´ empirical experience, and the symbolism of seven fat and thin cows is found even in the Old Testament. The cycles may not have been exactly seven years long, fluctuating between six and ten years, but they have worked for centuries. So we still may hope that we will swing into the watery and cold season, although with energy prices rising dramatically there probably is not much to yearn for either.

Nonetheless, I would like to end on a positive note: there is still hope that all these weather fluctuations are part of a natural process and we have more time to reverse climate change, which - if it is not already here - is sure to come. Like new variants of covid, which I didn't want to mention at all this time.

I wish everyone good health and every success.

Ing. Tomáš Urban
Director of TGM Water Research Institute

Automatic watershed delineation in the Czech Republic using ArcGIS Pro

VÍT ŠŤOVÍČEK

Keywords: automatic delineation — watershed — watershed divide — GIS — ArcHydro

SUMMARY

Manual watershed delineation by watershed divides has traditionally been performed by means of an analysis of topographic maps and contour lines. With the availability of digital elevation models, watershed and streams delineation is performed automatically, which reduces the time spent on manual delineation. In this study, we introduce the process of automatic delineation and the models available within the toolbox Arc Hydro Tool Pro, created by the company ESRI for the ArcGIS Pro software. Automatic delineation was implemented by means of different methods for selected watersheds in the Czech Republic, varying in area and elevation. Digital elevation models with different resolutions, from pixel size of 2 × 2 m to 50 × 50 m, were used as the input layer. Next, these delineated watersheds were compared with the current layer of fourth-order watershed divides (valid in 2019). Results of automatic delineation for each watershed, except those in lowlands, show a high overall accuracy. Automatic delineation can be applied not only as an input to hydrological models but also in consequent watershed analysis, for example, with the use of other tools in ArcGIS Pro.

INTRODUCTION

Watershed delineation is the basis for hydrological modelling and analysis. Traditionally, it is carried out by analysing topographic maps and contour lines, which is often a lengthy and challenging process. By using the digital elevation model (here-in-after DEM), which represents the relief of the Earth's surface, the whole process can be carried out automatically, thus reducing its time demands significantly. Techniques for automatic watershed delineation have been available since the mid-1980[s] and have been used in several geoinformation systems (GIS) and other applications. The development of these techniques, as well as the emergence of new higher resolution DEMs, form the basis for accurate and rapid analysis. Another important factor is the development of computer technology, which allows more powerful and comprehensive operations to be performed locally and quickly enough. This gradually increases the demand for automated systems which must provide accurate and rapidly available results [1–3].

ArcHydro is a data model, a set of tools and procedures that have been developed over the years to support specific GIS implementations in the area of water resources. Since 2002, it has expanded with more than 300 new tools from the original 30 and it has been widely used in many different projects by a range of users including government institutions, private companies, schools, and general users interested in water resources [4].

This article serves as an introduction to the automatic delineation process that can be performed using the tools in the Arc Hydro Tools Pro toolbox, created by the company ESRI for the ArcGIS Pro software. The automatic delineation itself was then implemented using different methods for selected watersheds in the Czech Republic varying in area and elevation to verify its accuracy and shortcomings in different types of relief.

METHODOLOGY

The basis of ArcHydro is the Hydrology toolset, which is stored in the Spatial Analyst toolbox. The new Arc Hydro Tools toolbox has been extended with new tools and improvements to existing ones. The newest Arc Hydro Tools Pro toolbox, which was used for the purposes of this article, was created for the transition to ArcGIS Pro.

The basic process of delineating and creating a river network using the Terrain Preprocessing toolset is partially illustrated in *Fig. 1* and can be summarized in a few steps [6]:

1. The Level DEM function – assigns the cells of the input DEM the same value as the values in the polygons of the embedded water bodies layer.
2. The DEM Reconditioning – reshapes the relief by "burning" the stream (linear feature) using the AGREE method [7], where the streams surroundings are lowered by entered values. This creates a more distinct cross-sectional profile that may not be completely clear in the input DEM due to the lack of elevation data in the vicinity of the streams.
3. Fill Sinks – modifies the terrain´s unevenness by increasing or decreasing the cell value depending on the surrounding cells so that the generated river network is continuous.
4. Flow Direction – determines the flow direction for each cell according to the largest difference in values (largest slope) between adjacent cells and produces a raster (D8 method). D-Infinity or Multiple Flow Direction methods can also be selected.
5. Flow Accumulation – based on the Flow Direction raster, it adds the number of cells from which water flows into a given cell and assigns this resulting value to the cell. It then creates a raster from all the values.
6. Stream Definition – based on Flow Accumulation grid and a user specified treshlod (the number of cells or minimum watershed area), it computes a stream grid. All cells above the threshold value are then assigned the value of 1, all cells below the value are assigned the blank value of "Null". The smaller threshold value leads to a denser stream network and a higher number of catchments.

7. Stream Segmentation – divides streams into individual segments (to the confluence of two streams or between confluences) and assigns a unique identifier to them. All cells in a given segment can thus be distinguished unequivocally from others by a specific "Grid Code".

8. Catchment Grid Delineation – assigns each cell a value that matches the catchment to which it belongs. This value is identical to the value of each stream's segment. The resulting raster is then converted to a polygon layer using the Catchment Polygon Processing function.

9. Drainage line Processing – converts the generated river network raster from step 6 to a line feature class.

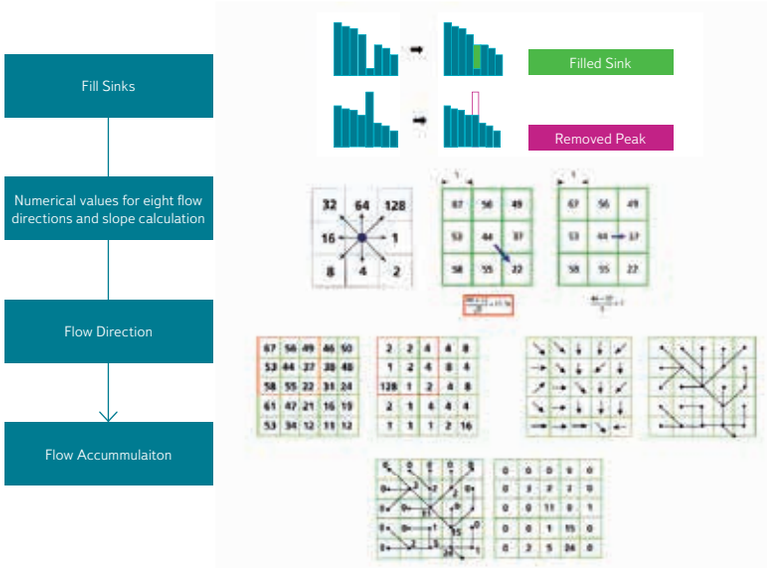

Fig. 1. Automatic watershed delineation process [5]

Steps 1 and 2 require the input polygon (water areas) and line (streams) features, respectively, which may make the functions described in the following steps different, but the whole process works without them, too.

To speed up the whole process, the Terrain Preprocessing Workflows toolset [8] can be used, which contains several models from which the user chooses based on the available input data and the type of river network in a given relief. The input data is divided into four categories:

1. The user has only DEM (no stream or sink information),

2. DEM and known sinks,

3. DEM and known streams and sinks,

4. DEM and known streams.

The river network type is then divided into three categories: dendritic, deranged, or combined.

Six watersheds varying in area and elevation were selected to create watershed divides using automatic delineation and the Skořenický potok watershed (*Fig. 2*) was selected to compare automatic delineation over DEMs with different resolutions and the actual watershed divide layer. Specifically, these were pairs of watersheds, always smaller and larger in area, located in lowlands (Blatnice, Čepel), uplands (Jívka, Třebovka) and mountains (Říčka, Malé Labe). Firstly, polygons (a certain extent or window, identical to *Fig. 2*) were created around all the

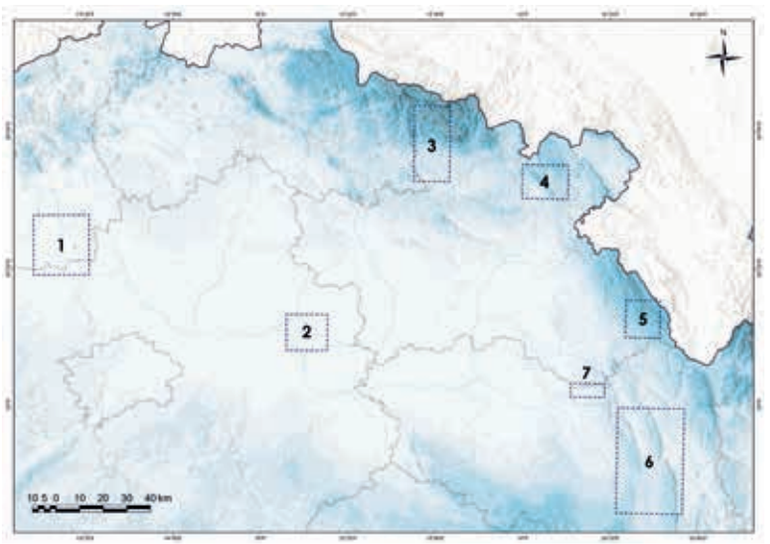

Fig. 2. Map of selected watersheds: 1 – Čepel, 2 – Blatnice, 3 – Malé Labe, 4 – Jívka, 5 – Říčka, 6 – Třebovka, 7 – Skořenický potok (Source: DIBAVOD, ArcČR 500 and DMR5G)

watersheds, in which the actual delineation was carried out. Only DMR 5G was used as a base for all watersheds within this delineation. The first model was chosen to be a dendritic river network with DEM only (no stream or sink information), followed by the second model with the layer of streams burnt into the relief model. The stream layer was used from the DIBAVOD digital database [9]. Polygons were generated between these two layers to show the deviation between the actual and generated watershed divides. Finally, the accuracy of the whole delineation was evaluated according to the size of their areas. The current watershed divides layer can be downloaded from: http://voda.chmi.cz/opv/stahnout.html.

To compare the automatic delineation over DEM with different resolutions and the actual watershed divide layer in the Skořenický potok watershed, four relief models were used – DMR 5G, DMR 4G, DMÚ 25, available from the Czech Geodetic and Cadastral Office´s website (https://geoportal.cuzk.cz) and ArcČR 500 available from Arcdata Prague (https://www.arcdata.cz/produkty/geograficka-data/arccr-4-0) with pixel sizes of 2, 10, 25 and 50 m. Again, the model for dendritic river network with no stream or sink information was chosen.

RESULTS AND DISCUSSION

The first aspect evaluated was the effect of DEM resolution on the automatic watershed delineation. The Skořenický potok watershed was selected as the testing territory, with an area of 17.1 km^2, an average slope of 3.72% and an average elevation of 361 m above sea level. It is clear from the resulting values in *Tab. 1* that as the DEM resolution decreases, the accuracy of the delineation itself decreases, too. While the deviation from the actual watershed divide is higher than 4% when using DMR 4G, it is more than double for the 25 × 25 m resolution and reaches 12.8% for the lowest resolution of 50 × 50 m.

Therefore, it is confirmed that accurate delineation of a watershed depends largely on the quality of the initial DEM, and more precisely, on its resolution [10–12]. A more detailed view of the difference between the generated watershed divides is provided in *Fig. 3*. It shows that when using a DEM with a lower resolution, a kind of "teeth" due to the pixel size are created, which prevents detailed and accurate delineation.

However, the overall deviation is quite significant for such a small watershed for all DEM types. In this case this is caused by the small area in the western part of the watershed with a low slope and a complicated river network. The

Tab. 1. Results of the automatic delineation in the Skořenický potok watershed

DEM resolution [m]	Area difference [km²]	Deviation [%]*
2 × 2	0.87	5.11
10 × 10	0.95	5.55
25 × 25	1.82	10.66
50 × 50	2.19	12.79

**Ratio of area difference to total watershed area*

automatic delineation did not generate a range of the stream and the watershed divide took a different direction. Such an error can be avoided by burning the actual streams into the relief itself. If we used the terrain with burnt streams in the Skořenický potok watershed as an illustration, we would get the overall deviation for DMR 5G slightly higher than 4%.

The delineation results for the six selected watersheds are shown in *Tab. 2*. The smallest difference was achieved for the largest watershed in terms of area, the Třebovka, where the deviation (excluding burnt streams) was only 0.89%. The two mountain watersheds of the Říčka and Malé Labe had slightly more, with deviations of 1.34 and 1.85% respectively, while another upland watershed, the Jívka, still had a small deviation of 2.35%. The lowland watersheds were generated with the least accuracy. The Blatnice watershed had a deviation of 7.55% and the larger Čepel watershed´s deviation was high – 9.13%.

The terrain with burnt stream features has reduced the deviation in all watersheds except the Čepel, where, on the contrary, has been an increase by almost 2%. The high deviations in the Čepel watershed, as in other lowland watersheds, may be caused by the fact that the area is crossed by linear features (mainly motorways and railway linear features) which significantly encroach on the terrain that is otherwise lowland. If the elevation of the feature is then particularly below or above the surrounding terrain, the model may evaluate it as a watershed divide, or as the stream itself, thereby fundamentally altering the course of the watershed, as is the case of the Čepel watershed (*Fig. 4*). Literature [13] states, inter alia, that features such as artificial streams, low dams or large lakes can form significant sinks in the terrain that affect the accuracy of the results, especially in lowland areas and river floodplains. This results in the generation of an unreal river network, which is further limited by the resolution of the DEM used. The Fill Sinks function is used to remove sinks, but the question is to what

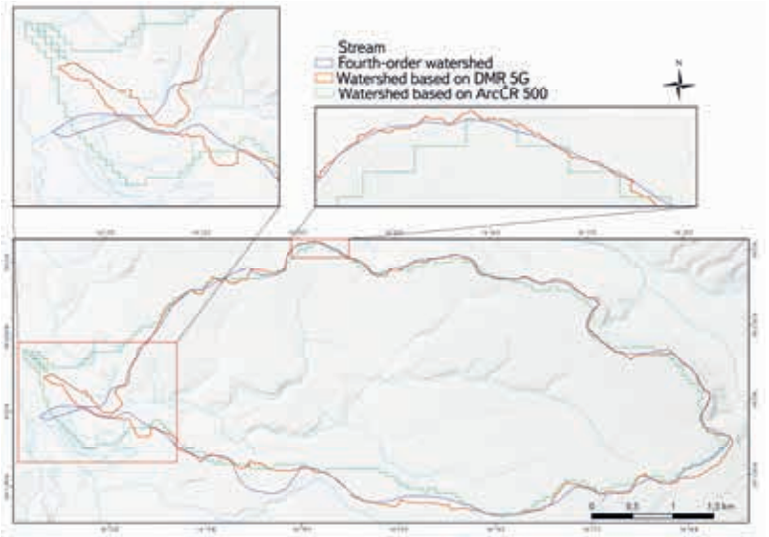

Fig. 3. Delineated watersheds of Skořenický potok using different digital elevation models

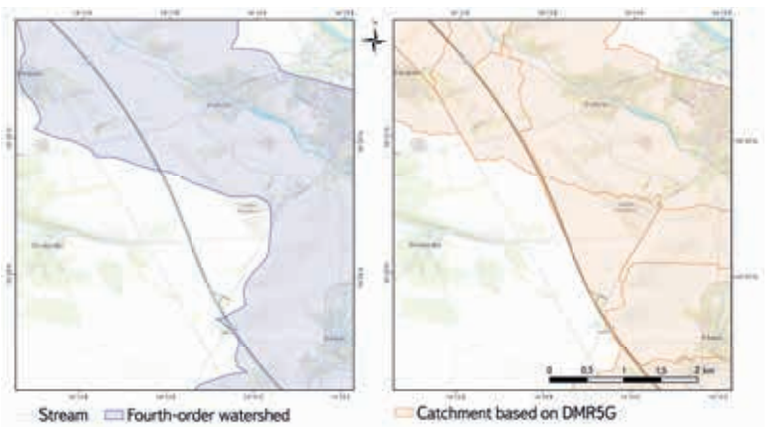

Fig. 4. Impact of a motorway on the automatic delineation of the Čepel watershed and catchments (Source map: Esri World Topographic Map)

Tab. 2. Results of automatic delineation in the individual watersheds

				Area difference [km²]		Deviation [%]*	
Name of watershed	Average altitude [m a. s. l.]	Average slope [%]	Area [km²]	Model without burnt streams	Model with burnt streams	Model without burnt streams	Model with burnt streams
Říčka	740.35	10.76	33.52	0.45	0.45	1.34	1.34
Malé Labe	689.51	12.17	73.36	1.36	1.21	1.85	1.65
Blatnice	193.32	1.47	33.55	2.53	1.32	7.55	3.95
Čepel	226.88	2.72	98.97	9.04	10.83	9.13	10.94
Jívka	555.5	11.82	27.96	0.66	0.62	2.35	2.20
Třebovka	476.18	6.14	195.85	1.74	1.73	0.89	0.88

**Ratio of area difference to total watershed area*

extent the given relief should be smoothed. On the one hand, some smoothing is necessary as it removes inaccuracies in the input DEM and a more real surface can be achieved while preserving the topographic characteristics, on the other hand, too much smoothing can change or remove the actual (natural) sinks that are important for the correct description of the relief. Thus, in this case, a proper smoothing of the DEM goes through a well-chosen threshold value to lower or raise the sinks. However, a single chosen value cannot, in the end, correspond to the whole study territory and therefore the intention and scope of the whole study must also be taken into account [14, 15].

Although the burning of the streams into the terrain reduced the deviation in the other basins, in all cases it was only a slight change in the order of tenths or even hundredths of a percent, except in the Blatnice watershed, where it was refined by 3.6%. The results may thus suggest that the burning of streams into the terrain is meaningless in some watersheds, but a closer examination of the resulting watershed divides reveals that the refinement is obvious mainly in the individual catchments, not in the whole selected watershed. In this case, the burning of the streams does not affect the resulting accuracy but could affect subsequent analyses of the watershed or catchment. Thus, the use of stream layers can significantly increase the accuracy of watershed delineation, especially in flat lowland areas [16, 17].

Other refining factors may include the use of the layer of water areas, thus providing a link between the river network and lakes, coastal lagoons or estuaries [18]. For example, the freely available SRTM (Shuttle Radar Topography Mission) Water Body Dataset layer from the USGS at 30 × 30 m resolution can be used for this purpose (https://earthexplorer.usgs.gov). Methods for automatic delineation in drainage-free areas using the SRTM DEM (Digital Elevation Model) are presented, for example, by Liu [10].

Last but not least, setting the threshold value to generate a river network can play a role. In the models used for this study, this value is the default one (automatically evaluated by the model on the basis of raw DEM). However, selecting a lower value, thereby densifying the river network, may result in a more accurate delineation [19].

Although the "accuracy" of watershed delineations is compared throughout the article, the layer of the actual watershed divides cannot be taken as a basis free of any errors. It is a layer that is regularly updated but contains a large number of areas where the course of the watershed divides is not entirely clear. The automatic delineation, on the other hand, respects the relief exactly and determines the flow direction precisely for each pixel. On the other hand, it cannot correctly evaluate certain specifics, such as streams flowing under the surface or man-made channels, which are taken into account when watershed divides are created manually. The results should therefore be taken with a grain of salt and seen as a possibility of using ArcHydro Pro tools in the latest view of the Czech Republic´s relief. In the future, it would be useful to analyse a larger number of watersheds with different areas, on differently rugged relief, and to find out what threshold values (for filling/adjusting sinks or river network density) would best describe the given terrain and thus provide the basis for the most efficient automatic delineation. At the same time, more attention needs to be paid to watersheds in the lowlands, in areas with flat terrain, where studies have shown the greatest deviations from the actual watershed divides. Consequently, more evaluation criteria based on the shape or length characteristics of the watershed divides should be used to assess the accuracy of the delineation. The lengths of watershed divides in the Skořenický potok watershed (*Fig. 3*) can be used as an illustration. Here, the length of the actual watershed divide is 21.2 km, the DEM-generated length with a resolution of 25 × 25 m is almost 27 km, and the DEM-generated length with a resolution of 2 × 2 m is almost 31 km, which at first glance does not correspond to the map or the resulting deviations. The high resolution of DMR 5G results in many small "teeth" on the generated watershed divide, which increase its overall length. If we wanted to evaluate according to this criterion, we would first have to choose the most appropriate level of generalization of the watershed divide. For example, if we smoothed this watershed divide according to the Smooth Line function with a tolerance of 100 m, the resulting length would be 22.1 km, just under a kilometre longer than the actual length of the watershed divide.

USES

Automatic watershed delineation can be used mainly as an input to hydrological models such as SWAT, HBV, HEC-GeoHMS or ILWIS. The studies that have been completed focus on comparisons of different delineation methods and procedures rather than on differences in accuracy between models, so it is not possible to say unequivocally which model is more appropriate. However, in general, their conclusions are in agreement with the results of this study, especially in that the largest differences in delineation are formed in lowland areas with flat terrain (or coastal areas) and delineation accuracy is highly dependent on the resolution of the input DEM [20, 16, 17]. Larger scale applications can be found, for example, in the Pan-European River and Catchment Database [18], which contains data on river networks, lakes and watershed boundaries across Europe. These are based on DEMs with 100 m resolution, thus creating the conditions for medium- and small-scale modelling. SRTM elevation data, a derived shoreline layer and selected natural sinks served as additional input data for the watershed delineation and the generation of the river network. If necessary, in a very flat terrain where it was not possible to unambiguously determine the course of the stream according to the DEM, a reference network of streams was used. The network of streams and its related watershed were generated according to the classical D8 method to determine the flow direction and the Soille and Gratin algorithm [21] to determine the flow accumulation. Three new algorithms [22] were used to solve the problem of stream flow in a flat terrain, and a part of the terrain in the flow direction at artificial sinks was cut out instead of filling the sink itself, thus preventing further extension of the flat terrain. Similar or additional methods and algorithms for optimum sink removal have been the focus of studies [23, 24], which could also provide guidance on how to refine delineation and could be applied to the territories selected in this study.

The Czech Hydrometeorological Institute is currently in the process of updating the watershed divides over DMR 5G. The editing is being done manually in ArcGIS Pro with the ZABAGED stream layer and using automatically generated contour lines and contour lines derived and provided by the Czech Geodetic and Cadastral Office [25]. At the same time, editors can use the HydroDEM toolbox to generate watershed divides automatically. Thus, automatic delineation is mainly used as an auxiliary tool in this case, especially in flat lowland areas where the watershed divides are not as clear as in watersheds with a higher slope.

CONCLUSION

This paper has presented the possibility of automatic delineation of watersheds and river networks using the tools in the Arc Hydro Tool Pro package in ArcGIS Pro environment. The process of automatic delineation itself was described and applied to selected watersheds in the Czech Republic within evaluation of its functionality and accuracy. The most accurate watersheds were generated in the mountainous and hilly areas (deviation of watershed size from the actual watershed divides up to a maximum of 2.4%), and the least ones in the lowland areas. The results are consistent with the results of other studies to date, where the largest deviations also occur in lowland areas with flat terrain. Furthermore, the decreasing accuracy of delineation with lower resolution of the input DEM was also confirmed. Possible ways of modifying the DEM and changes in the

watershed divide generation procedure to improve delineation accuracy were discussed. Within further research, it was proposed to apply automatic delineation to a larger number of watersheds with a focus on lowland areas. In particular, the resulting accuracy could be influenced by modifying the DEM – both through the input layer of water areas and through different options of sink modification. Thus, automatic delineation using the tools in the Arc Hydro Tool Pro package together with a DEM of a sufficiently high resolution for the purpose of the given study can be recommended as a powerful and sufficiently accurate tool.

References

[1] DJOKIC, D., YE, Z. DEM Preprocessing for Efficient Watershed Delineation [on-line] In: *Proceedings of the 19th Esri Users Conference, San Diego, CA. 1999.* Available from: https://proceedings.esri.com/library/userconf/proc99/proceed/papers/pap676/p676.htm

[2] GARBRECHT, J., MARTZ L. W. Digital Elevation Model Issues in Water Resources Modeling [on-line] In: *Proceedings of the 19th Esri Users Conference, San Diego, CA. 1999.* Available from: https://proceedings.esri.com/library/userconf/proc99/proceed/papers/pap866/p866.htm

[3] MERWADE, V. *Terrain Processing Using ArcHydro/GeoHMS* [on-line]. School of Civil Engineering, Purdue University, 2019. Available from: https://web.ics.purdue.edu/~vmerwade/education/terrain_processing.pdf

[4] DJOKIC, D. Arc Hydro in ArcGIS Pro: The Next Generation of Tools for Water Resources, In: *Esri Federal GIS Conference Proceedings*, Washington D. C. 2020.

[5] MAIDMENT, D. R. *Arc Hydro: GIS for Water Resources*. Redlans, Calif.: ASRI Press, 2002. ISBN 1589480341.

[6] *ESRI. Arc Hydro Tools v2.0 – Tutorial* [on-line]. 2011, p. 184. Available from: http://downloads.esri.com/archydro/archydro/Tutorial

[7] FERDI, H. *AGREE – DEM Surface Reconditioning Systém* [on-line]. 1997. Available from: https://www.ce.utexas.edu/prof/maidment/GISHYDRO/ferdi/research/agree/agree.html

[8] *ESRI. Arc Hydro: Overview of Terrain Preprocessing Workflows* [on-line]. 2019, p. 18. Available from: https://www.esri.com/content/dam/esrisites/en-us/media/whitepaper/archydro-overviewofterrainprocessingworkflows.pdf

[9] *DIBAVOD – Digitální báze vodohospodářských dat* [on-line]. Available from: http://www.dibavod.cz

[10] LIU, K., SONG, CH., KE, L., JIANG, L., MA, R. Automatic Watershed Delineation in the Tibetan Endorheic Basin. A Lake-Oriented Approach Based on Digital Elevation Models. *Geomorphology* [on-line]. 2020, 358, 107127. ISSN 0169555X. Available from: doi: 10.1016/j.geomorph.2020.107127

[11] WILSON, J. P. Digital Terrain Modeling. *Geomorphology* [on-line]. 2012, 137(1), p. 107–121. ISSN 0169555X. Available from: doi: 10.1016/j.geomorph.2011.03.012

[12] ALCARAZ, S. A., SANNIER, CH. C. T., VITORINO, A., DANIEL, O. Comparison of Methodologies for Automatic Generation of Limits and Drainage Networks for Hidrographic Basins. *Revista Brasileira de Engenharia Agrícola e Ambiental* [on-line]. 2009, 13(4), p. 369–375. ISSN 1415-4366. Available from: doi: 10.1590/S1415-43662009000400001

[13] LI, L., YANG, J., WU, J. A Method of Watershed Delineation for Flat Terrain Using Sentinel-2A Imagery and DEM: A Case Study of the Taihu Basin. *ISPRS International Journal of Geo-Information* [on-line]. 2019, 8(12), 528. ISSN 2220-9964. Available from: doi: 10.3390/ijgi8120528

[14] LI, S., MACMILLAN, R. A., LOBB, D. A., MCCONKEY, B. G., MOULIN, A., FRASER, W. R. Lidar DEM Error Analyses and Topographic Depression Identification in a Hummocky Landscape in the Prairie Region of Canada. *Geomorphology* [on-line]. 2011, 129(3–4), p. 263–275. ISSN 0169555X. Available from: doi: 10.1016/j.geomorph.2011.02.020

[15] GRIMALDI, S., NARDI, F., Di BENEDETTO, F., ISTANBULLUOGLU, E., BRAS, R. L. A Physically-Based Method for Removing Pits in Digital Elevation Models. *Advances in Water Resources* [on-line]. 2007, 30(10), p. 2151–2158. ISSN 03091708. Available from: doi: 10.1016/j.advwatres.2006.11.016

[16] RAY, L. K. Limitation of Automatic Watershed Delineation Tools in Coastal Region. *Annals of GIS* [on-line]. 2018, 24(4), p. 261–274. ISSN 1947-5683. Available from: doi: 10.1080/19475683.2018.1526212

[17] BAKER, M. E., WELLER, D. E., JORDAN, T. E. Comparison of Automated Watershed Delineations: Effects on Land Cover Areas, Percentages, and Relationships to Nutrient Discharge. *Photogrammetric Engineering and Remote Sensing*. 2006, 72, p. 159–168.

[18] VOGT, J., SOILLE, P., DE JAGER, A., RIMAVICIUTE, E., MEHL, W., FOISNEAU, S., BODIS, K., DUSART, J., PARACCHINI, M., HAASTRUP, P., BAMPS, C. *A Pan-European River and Catchment Database. EUR 22920 EN*. Luxembourg (Luxembourg): OPOCE, 2007. JRC40291

[19] LI, Z. Watershed Modeling Using Arc Hydro Based on DEMs: A Case Study in Jackpine Watershed. *Environmental Systems Research* [on-line]. 2014, 3(11). ISSN 2193-2697. Available from: doi: 10.1186/2193-2697-3-11

[20] BALASUBRAMANI, K., SARAVANABAVAN, V., KANNADSAN, K. *A Comparison of Approaches for Automated Watershed Delineation: A Case Study of NagalAr Watershed.* [on-line]. 2012. Available from: https://www.researchgate.net/publication/267601581_A_Comparison_of_Approaches_for_Automated_Watershed_Delineation_A_Case_study_of_NagalAr_Watershed

[21] SOILLE, P., GRATIN, C. An Efficient Algorithm for Drainage Network Extraction on DEMs. *Journal of Visual Communication and Image Representation*. 1994, 5, p. 181–189.

[22] SOILLE, P. *Morphological Image Analysis*. 2nd Edition. Berlin, Heidelberg, New York: Springer 2003.

[23] WANG, Y., QIN, CH., ZHU, A. Review on Algorithms of Dealing with Depressions in Grid DEM. *Annals of GIS* [on-line]. 2019, 25(2), p. 83–97. ISSN 1947-5683. Available from: doi: 10.1080/19475683.2019.1604571

[24] JACKSON, S. *Designing an Optimal Pit Removal Tool for Digital Elevation Models* [on-line]. 2012, p. 11. Available from: https://www.caee.utexas.edu/prof/maidment/giswr2012/TermPaper/Jackson.pdf

[25] MATULOVÁ, J., TYL, R. *Aktualizace rozvodnic ČR nad digitálním modelem reliéfu 5G* [on-line]. Available from: https://storymaps.arcgis.com/stories

The author

Bc. Vít Šťovíček
✉ vit.stovicek@chmi.cz
ORCID: 0000-0002-4997-8056

Czech Hydrometeorological Institute,
Hydrology Database and Water Budget Department, Prague

The paper has been peer-reviewed.

DOI: 10.46555/VTEI.2021.11.002

Photo: Shutterstock.com

Zero isochion in the framework of geomorphological regions in Czechia: its extraction from the MODIS imagery and its dynamics

LIBOR DUCHÁČEK, ONDŘEJ LEDVINKA

Keywords: remote sensing (RS) — geographical information systems (GIS) — snow cover — snow water storage — Czech Hydrometeorological Institute (CHMI) — hydrology — geomorphology in Czechia

SUMMARY

Since December 2012, during every winter season, the altitude of the zero isochion (snowline) has been determined at the Czech Hydrometeorological Institute for the purposes of operational hydrology. The reason is the estimation of the amount of water stored in snow cover, which is inevitable activity for Czech hydrologists who naturally want their forecasting models to give relevant results. In order to get a better idea about current spatial distribution of snow cover in Czechia, the information on the zero isochion has been extracted from the MODIS imagery coming from the Terra satellite. The obtained time series represents a relatively long period (currently until May 2021), which offers the possibility of analyzing the spatial and temporal dynamics of the zero isochion in Czechia. In this study, the information about the isochion was divided into 27 geomorphological regions and the winter season was divided into the accumulation period and the melting period. The focus was on possible differences between individual regions and time periods, as well as on relationships between zero isochion dynamics and selected factors derived from other geographical data, such as the digital elevation model. Due to different reasons, the data on the isochion were incomplete and did not satisfy the requirements for fitting the models which need regularly/evenly spaced sampling. Therefore, missing daily values were estimated so that the series finally covered the winter seasons from November to May. This was accomplished by the application of a suitable modified EM algorithm that respected both the temporal and the spatial structure of the multivariate time series. Correlation and regression analyses followed, where the main aim was to find out if the belonging to a geomorphological region (with its selected attributes) has an influence, and if there are significant interannual changes.

INTRODUCTION

For more than ten years, the zero isochion has been a practical tool for calculating snow water storage as part of regular hydrological forecast analyses within the Czech Hydrometeorological Institute. The main benefit of determining the isochion is the definition of the areas where we can expect snow cover to be present and where snow cover will be absent, or where we need to take into account snow water equivalent and where it can be neglected. Defining such a boundary within the homogeneous regions of Czechia allows better interpolation of snow cover depth values recorded in the CHMI station network. A more detailed description of hydrological forecast analyses, including the application of the zero isochion in the calculations, is offered by [1, 2]. The content of this paper is related to work [3], where the basic procedures of extracting the zero isochion using satellite images and information on its distribution within the geomorphological regions of Czechia have been summarized. It is the search for correlations and other relationships that can be inferred from the observed series that are the main topic of the following text. One of the key areas of the study is quantifying the degree of dependence of the variability of the average altitude of the zero isochion on the terrain characteristics of the geomorphological regions. The long-term altitude of the zero isochion is analyzed for the entire winter season defined by the months of November to May (for nine years 2013–2021), as well as for parts of the winter season that are typical of snow accumulation, of snow melt and for the rest of this season (for four years 2018–2021). An attempt was made to trace the degree of influence of the factors related to the terrain configuration in different periods of the winter season. Since the length of the collected time series is already quite sufficient (in the sense of an undivided winter season), an equally important task was to see how the altitude of the zero isochion changes with time, i.e., in each year, and whether a significant trend can be observed for some geomorphological regions. In extracting the altitude of the zero isochion and respecting its definition according to [4], a procedure similar to that in [3] was followed for the sake of necessary consistency. New problems were addressed using a variety of statistical techniques, with regression analysis and the selection of significant explanatory variables playing a central role, in addition to descriptive statistics and methods for filling in missing values.

DATA AND METHODOLOGY

Satellite data

A significant portion of the data analyzed in this project comes from the National Snow and Ice Data Center (NSIDC) portal, which supports research on the cryosphere, i.e., snow, ice, glaciers, and frozen ground, as well as the climatic

interactions that take place in the cryosphere. The NSIDC administers and distributes scientific data, creates tools for accessing the data, supports data users, conducts scientific research, and educates the public about the cryosphere. As a platform for data originating from the National Aeronautics and Space Administration (NASA), it is also certified as a CoreTrustSeal Regular Member of the World Data System, an interdisciplinary body of the International Science Council (ISC; formerly ICSU). The portal has been distributing data free of charge to the entire scientific community since 1976 in a variety of formats known in the field of RS and in sizes ranging from small text files to terabytes of data. Further information on products, tools and published outputs can be found at [5].

The specific dataset used for the purposes of the zero isochion analysis is designated MODIS/Terra Snow Cover 5-Min L2 Swath 500m, Version 61, and is available, including metadata, from [6]. The name of the dataset contains basic descriptive information about the sensed data. The images are collected using the Moderate Resolution Imaging Spectroradiometer (MODIS) sensor installed on the Terra satellite. Terra is a NASA multinational scientific research satellite in a Sun-synchronous orbit around the Earth that makes simultaneous measurements of the Earth's atmosphere, soil, and water to contribute to the understanding of how the Earth is changing and to identify implications for life on Earth [7]. The location of the MODIS sensor on the Terra satellite is shown in *Fig. 1.*

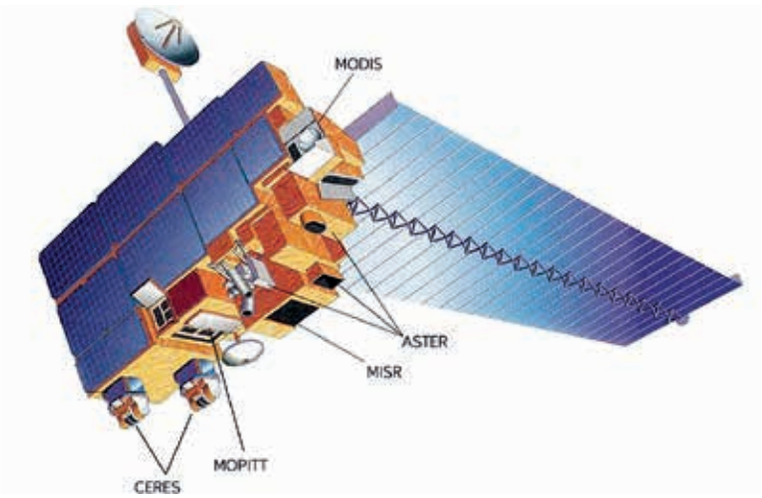

Fig. 1. Terra satellite, launched 18th December 1999 (orbit height: 713 km; orbital velocity: 7,503 km.s^{-1}; maximum velocity: 27,010 km.h^{-1}) and the position of the MODIS sensor (source: [8])

The images tagged with the MOD10_L2 identifier provide information about the snow cover in daily steps. Detection is done using the Normalized Difference Snow Index (NDSI). Another product is a series of correction images that are designed to mitigate errors and mark the detection of uncertain snow cover. Snow-covered landscapes typically have very high reflectance in the visible bands and very low reflectance for the shortwave infrared bands. The NDSI reveals the magnitude of this difference. Each data granule contains 5 minutes of swath data observed at a resolution of 500 m. Data collection began on 24th February 2000 and data revision is now underway for current version 61, which is expected to be completed in spring 2022.

Satellite data download and processing in a GIS environment

The practical aspect of the processing of these data at the CHMI consists in pre-setting the parameters of the area of interest to a rectangle covering the territory of Czechia. If the acquired image is in intersection with this rectangle, the CHMI staff is informed by e-mail as soon as possible about its availability together with a link to download the given data file. The time of sending the notification depends on the image's complexity. If the image has many classes, there may be a delay. However, most often notifications are sent within 12 hours after acquisition.

Tab. 1. Classes of the NDSI_Snow_Cover output

NDSI snow cover values and data flag values (saved as 8-bit unsigned integers)
0-100: NDSI snow cover
200: missing data
201: no decision
211: night
237: inland water
239: ocean
250: cloud
254: detector saturated
255: fill

Data is provided in the HDF-EOS2 format and is stored as 8-bit unsigned integers. The Hierarchical Data Format (HDF) allows for efficient storage of large, yet quite diverse data and metadata [9]. For the area of interest covering Czechia, the size of such files is approximately 5-25 MB, reflecting the area and spatial distribution of snow in the landscape. Each HDF file is composed of several parameters, of which the output "NDSI_Snow_Cover" is essential for snow detection as it contains attributes divided into nine classes listed in *Tab. 1.*

For further work in the GIS environment, it is necessary to extract the individual classes first into a raster form and then into polygons, from which the essential boundary between snow and snow-free areas is exploited. In the first stage of the extraction, it is necessary to use the HEG tool (HDF-EOS To GeoTIFF Conversion Tool), which is freely available as supporting software from the NASA portal [10]. It allows a sufficiently accurate conversion from the HDF format to the GeoTIFF format so that, when projecting to UTM and specifying the corresponding zone (for Czechia 33N or 34N in the east), there is a correct overlay with a Czech Digital Elevation Model (DEM; see below). The local reflections

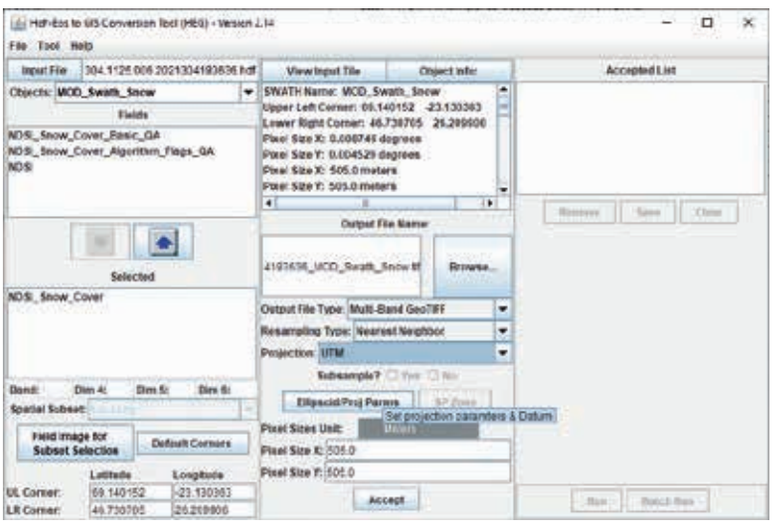

Fig. 2. Parameter settings for conversion in the HEG tool

in class 237, i.e., inland water bodies that overlap with the hydrographic base in the GIS (e.g., Rozkoš or Nové Mlýny water reservoirs) are the best verification of the overlay quality. An example of a HEG tool setup is shown in *Fig. 2*.

The processing of images in ArcGIS Desktop can be divided into several phases, with the use of each tool adapting to the capabilities of the ArcGIS Desktop license within the CHMI. Future adaptation to newer versions and products can also be expected:

A. **Extraction of the data of interest from the RS image**. The GeoTIFF image is imported with the parameters set in the HEG tool (projection, range). Most often the image is taken in the morning for Czechia, which includes the area from approximately southern Scandinavia to the Alps. In less frequent cases, images with only a partial overlap can also be used, based on the orbital path of the satellite, which may record the territory of Czechia from multiple fly-bys. Images that have an intersection with the preset rectangular mask for Czechia are subjected to cropping to reduce the complexity of the partial calculations. The resulting raster must be first reclassified with respect to the delineation of snow and snow-free areas. The original data up to 2017 were classified more generally into three basic groups: snow, no snow and cloud cover. After 2017, the quality of reflectance from snow cover is broken down in more detail into classes from 0 to 100 (according to the NDSI index), where 0 is a guaranteed snow-free area and 100 is the highest possible reflectance from snow cover. For the purposes of the CHMI hydrology, all snow reflectance values between 1 and 100 are treated as snow in order to provide the largest possible data package for evaluating the zero isochion. As a result, all values 1–100 are reclassified to a value of 50 and values of 0 are treated as snow-free areas. A significant feature based on actual weather conditions is the class value of 201, which is the area of questionable evaluation (NDSI internal calculation), and the class value of 250, which is cloud cover, the most common limiting factor for a full evaluation. The other classes can be considered complementary and can be omitted from further operations. The reclassified raster is further generalized by the Boundary Clean tool to suppress sub-regions of unit pixel sizes, and then the classes are colour coded to make the primary visual overview of the dataset stand out. For further operations, it is necessary to first convert the raster layer to a polygon layer and then to a line layer using the Feature to Line tool. This creates a dataset of lines that have a specific gridcode according to the original raster they surrounded. Specifically, at the contact of two polygons, where one comes with the value of 0 (no snow) and the other with a value of 50 (snow), two lines will be created, one with gridcode 0 and the other with gridcode 50. The element being searched for is then the layer created by the intersection of the selections (Intersect tool) of these two lines and contains all visible boundaries between the snow and no-snow areas. This discontinuous line bounding the recorded snow cover can be referred to as the zero isochion. This line already provides some spatial idea of the position of the snow boundary within the Czech territory. For a more detailed indication of the position, it is necessary to find the approximate value of the altitude at which this line is located. Pixel extraction using a mask was chosen as the simplest method where the isochion line is considered the mask. This is how the altitude values are extracted from the raster base, which is a DEM with a resolution of 25 m (see below).

B. **Spatial data analysis**. Geomorphological regions were chosen as the most appropriate division of the Czech territory for the definition of the zero isochion. These areas best reflect the relief features, relative and absolute ruggedness (mountains/lowlands) and the distribution of slope orientation to the cardinal directions (north/south, west/east), i.e., factors that are expected to have a major influence on snow cover accumulation and melting. Within Czechia, there are 27 such treatment regions (see *Tab. 2* and *Fig. 3* for details). For each of these regions, the extracted set of pixels belonging to the given geomorphological region is evaluated using the Zonal Statistics as Table tool, and the output is a statistic containing information on the number of pixels, their minimum and maximum values, the range of values, the sum of values and, above all, the average value, which is the item that is processed subsequently. The vector layer with geomorphological regions replaces the function of the zero isochion position database, as a column of values is created for each day analyzed, where each geomorphological region is assigned an average position value if it was recorded on that day. The Join Field tool is used to link the statistical output to the region layer attribute table.

C. **Visual interpretation of data**. Visualization of the values can be done by showing labels with these values for each region, possibly with an underlying choropleth map. The situation where an average value is defined for each or at least for most of the geomorphological regions is rather rare during observations, as the cloud factor is often present and in the absence of cloud cover the snow is either limited to mountain areas or, on the contrary, covers the whole territory of Czechia. As mentioned above, the snow boundaries are based on different NDSI reflectance index intensities and each of the average values needs to be critically analyzed (i.e., validated) to see if it is an objective value and can represent the conditions in the region. The evaluation is based not only on internal snow cover data coming from the CHMI observation network (automatic stations, observers, field measurements), but also, for example, on web camera outputs or historical correlations between regions. The position of the zero isochion enters the snow water storage calculation as a limiting value for the spatial interpolation of snow cover parameters, where a fictitious network of zero points is generated for each of the regions, which prevents the interpolation from estimating a non-zero (positive) snow cover depth or snow water equivalent below this position. For this analysis in a GIS environment, the ClidataGIS tool is used, which allows the import of measured data, a more detailed visual inspection, and the setting of parameters for interpolation. The final output is a map, including a supplementary table reflecting changes in snow occurrence over the previous weeks, which is posted on the CHMI portal, and the public can see the predicted water volume in the sub-basins of interest (water reservoirs, major outlet sections of watercourses). Currently, such an output, based on Monday's measured values, is generated once a week, on Tuesday. In the future, however, it will be possible to produce similar analyses more frequently during the week thanks to the automated network of snow gauging stations combined with satellite imagery.

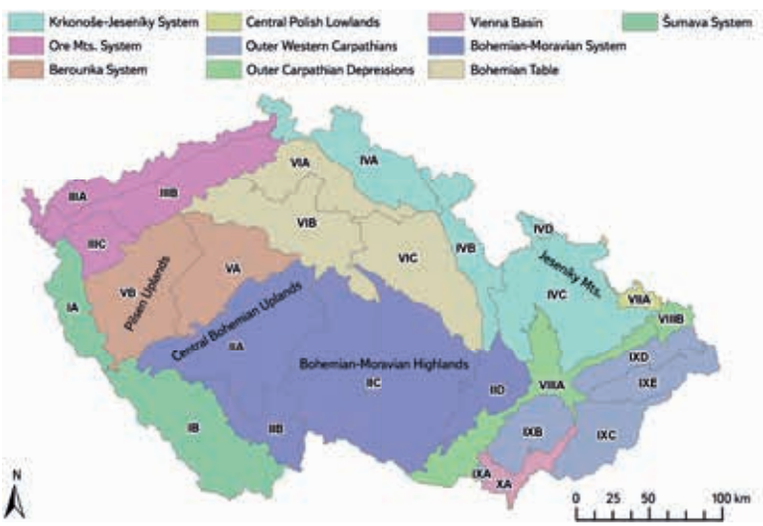

Fig. 3. Geomorphological regions (for ID see *Tab. 2*) and their parent subprovinces in Czechia (adapted from [11])

Tab. 2. Geomorphological regions for which, in the winter season, the CHMI determines the average altitude of the zero isochion, and their identifiers (adapted from [11])

ID	Region	Subprovince	Province	System
IA	Bohemian Forest Region	Šumava System	Bohemian Upland	Hercynian
IB	Šumava Region	Šumava System	Bohemian Upland	Hercynian
IIA	Central Bohemian Hilly land	Bohemian-Moravian System	Bohemian Upland	Hercynian
IIB	South Bohemian Basins	Bohemian-Moravian System	Bohemian Upland	Hercynian
IIC	Bohemian-Moravian Highlands	Bohemian-Moravian System	Bohemian Upland	Hercynian
IID	Brno Highlands	Bohemian-Moravian System	Bohemian Upland	Hercynian
IIIA	Ore Mts. Region	Ore Mts. System	Bohemian Upland	Hercynian
IIIB	Ore Mts. Piedmont Region	Ore Mts. System	Bohemian Upland	Hercynian
IIIC	Karlovy Vary Highlands	Ore Mts. System	Bohemian Upland	Hercynian
IVA	Giant Mts. Region	Krkonoše-Jeseníky System	Bohemian Upland	Hercynian
IVB	Orlice Region	Krkonoše-Jeseníky System	Bohemian Upland	Hercynian
IVC	Jeseníky Region	Krkonoše-Jeseníky System	Bohemian Upland	Hercynian
IVD	Krkonoše-Jeseníky Piedmont	Krkonoše-Jeseníky System	Bohemian Upland	Hercynian
IXA	South Moravian Carpathians	Outer Western Carpathians	Western Carpathians	Alpine-Himalayan
IXB	Central Moravian Carpathians	Outer Western Carpathians	Western Carpathians	Alpine-Himalayan
IXC	Slovak-Moravian Carpathians	Outer Western Carpathians	Western Carpathians	Alpine-Himalayan
IXD	Western Beskids Piedmont	Outer Western Carpathians	Western Carpathians	Alpine-Himalayan
IXE	Western Beskids	Outer Western Carpathians	Western Carpathians	Alpine-Himalayan
VA	Brdy Region	Berounka System	Bohemian Upland	Hercynian
VB	Pilsen Hilly land	Berounka System	Bohemian Upland	Hercynian
VIA	North Bohemian Table	Bohemian Table	Bohemian Upland	Hercynian
VIB	Central Bohemian Table	Bohemian Table	Bohemian Upland	Hercynian
VIC	East Bohemian Table	Bohemian Table	Bohemian Upland	Hercynian
VIIA	Silesian Lowland	Central Polish Lowlands	Central European Lowland	Hercynian
VIIIA	Western Outer Carpathian Depressions	Outer Carpathian Depressions	Western Carpathians	Alpine-Himalayan
VIIIB	Northern Outer Carpathian Depressions	Outer Carpathian Depressions	Western Carpathians	Alpine-Himalayan
XA	South Moravian Basin	Vienna Basin	West Pannonian Basin	Alpine-Himalayan

Basic geographical material for obtaining terrain explanatory variables

The spatial (but also temporal) variability of the altitude of the zero isochion is influenced by the terrain configuration. Temporal variability will certainly be more related to the climatic conditions of the territorial units for which the study is conducted. Since these territorial units were geomorphological regions for the above-mentioned reasons, it was necessary to obtain a vector layer with polygons representing these regions. This was downloaded from the Geoportal of the Czech Office for Surveying, Mapping and Cadastre, where it is part of the Data200 database (specifically the Description layer) [12]. This layer is based on the geomorphological division described in publication [11], which in fact refers to 28 regions. However, at the CHMI, only 27 regions are traditionally considered, as the Záhorská Lowland is merged with the South Moravian Basin (row with ID XA in *Tab. 2*). The layer of geomorphological regions has been adjusted accordingly before further analyses.

The Digital Elevation Model (DEM) in the form of a raster, which was the source of information on elevation and other terrain parameters in the geomorphological regions, is based on the Digital Model of Territory prepared at a scale of 1 : 25,000 (DMU 25), which the CHMI purchased from the Military

Geographical and Hydrometeorological Office in 2001. This raster with square cells representing an areas of 25^2 m was created from the original data directly at the CHMI, and contour lines were essential for its creation. The DEM was thus created by suitable interpolation in the then S-42 system. However, because the CHMI switched over time to the UTM zone 33/34N system, the raster was reprojected and resampled into this system (more precisely only zone 33). Similarly, the geometry of the polygon layer of the geomorphological regions was transformed to the UTM zone 33N system.

Using the polygon and raster layers, several terrain features were then extracted for each geomorphological region. These were to serve as explanatory variables in the planned regression analysis. Their list and meaning are presented in *Tab. 3*. Special attention should be paid to the SDASP indicator, which is not well known in the Czech literature. It is the so-called directional standard deviation expressing the variability of slope orientation in individual regions expressed in radians [13]. The R package circular [14] was used to calculate terrain characteristics related to angles. The vector layer was manipulated during extraction using the R package sf [15], while the raster layer was manipulated using the R package terra [16].

Statistical processing of the extracted data on the altitude of the zero isochion

Fig. 4 reveals how many values of zero isochion altitude were available in the original database from December 2012 to May 2021, when the CHMI staff had already evaluated the data completely on their own. Naturally, zero isochion altitude information was only available for the winter seasons, which are usually divided into two calendar years. However, this division is not very suitable for further processing of the time series, so winter seasons were next assigned to years with a larger proportion of months. As the winter season was considered to be November to May, the months of November and December were assigned to the following calendar years. As a result, the winter seasons could be analyzed for the period 2013–2021, i.e., for nine years. For various reasons described earlier, the original database was not complete for the individual geomorphological regions, and even the equidistant weekly step was not followed, since, for example, due to cloud cover, one of the following cloud-free days of the week had to be selected. Missing values and not keeping the same time step make such data quite problematic for subsequent statistical processing, since the vast majority of statistical models require completeness and constancy of the time step (especially when time series models are involved). Although models for this type of data are also being developed (e.g., [17]), it is generally recommended to get rid of their above-mentioned shortcomings so that traditional models can be applied. Finally, the database of zero isochion altitude values was supplemented with estimated values to produce a time series in a daily time step for each geomorphological region that represented all winter seasons of the period 2013–2021 without any missing values. This result was achieved by means of a modified Expectation-Maximization (EM) algorithm that treats the incomplete time series as a multivariate series, where a vector of univariate series with relationships between them is thus considered, while a spline method is applied to all its elements as a filter.

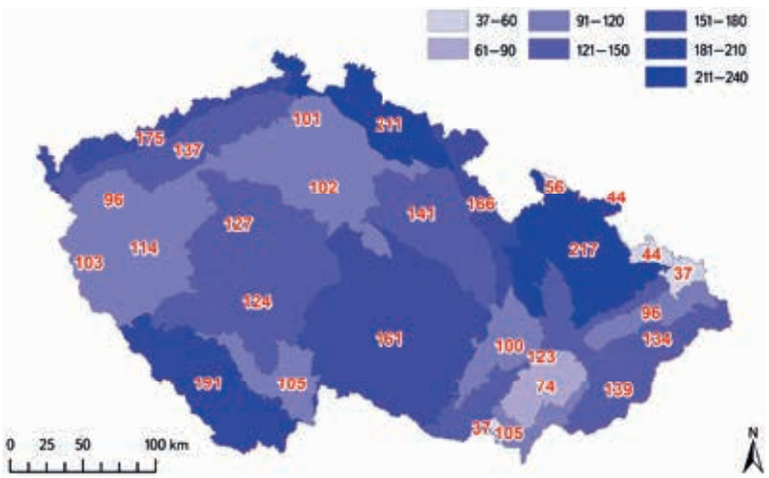

Fig. 4. Total number of days (values) with the detected zero isochion for all winter seasons 2013–2021

Tab. 3. Characteristics of geomorphological regions of Czechia obtained as explanatory variables for next regression analysis

Variable	Meaning
X	*X* coordinate of the centroid of the polygon representing the geomorphological region (for UTM zone 33N projection)
Y	*Y* coordinate of the centroid of the polygon representing the geomorphological region (for UTM zone 33N projection)
MIN	minimum elevation of the geomorphological region derived from the DEM
MAX	maximum elevation of the geomorphological region derived from the DEM
RANGE	range between the maximum and minimum elevation
MEDIAN	median elevation of the geomorphological region as determined from the DEM
SD	standard deviation of the elevations determined for each DEM cell falling into the geomorphological region
MEDSLOPE	median slope gradient determined from the DEM for the geomorphological region
MEANASP	mean orientation of slopes in the geomorphological region (categories North, East, South and West) as determined from the DEM
SDASP	standard deviation of the radians determining orientation of slopes in the geomorphological region determined from the DEM (according to [13])
PREVASP	prevailing orientation of slopes in the geomorphological region (categories North, East, South and West) as determined from the DEM

Tab. 4. Values of selected explanatory variables related to terrain of the 27 geomorphological regions of Czechia

Region	*X* [m]	*Y* [m]	MIN [m]	MAX [m]	RANGE [m]	MEDIAN [m]	SD [m]	MEDSLOPE [°]	MEANASP	SDASP [rad]	PREVASP
IA	336085.9	5501474.3	371	1039	668	532	96.2	4.12	East	2	East
IB	424956.4	5423466	387	1373	986	704	187.5	6.32	North	2.09	North
IIA	453643.9	5489265.7	190	723	533	453	71.8	3.82	East	2.39	South
IIB	470010	5433611.5	361	576	215	436	35.6	1.15	East	1.94	East
IIC	546326.6	5472446.7	193	836	643	517	99.6	3.62	East	2.4	East
IID	622653.7	5467326.5	186	731	545	386	113.4	4.87	East	2.18	East
IIIA	367418.7	5593028.7	112	1242	1130	651	183.8	6.45	South	2.06	South
IIIB	394800.1	5587386.7	115	929	814	354	136.6	3.82	East	2.03	East
IIIC	347914.8	5546078.6	373	980	607	642	88.7	4.73	East	2.38	North
IVA	522349.7	5617564.5	211	1595	1384	476	211	7.18	South	2.24	South
IVB	600425.4	5562851.7	291	1111	820	485	131.8	5.74	South	2.09	South
IVC	667559.9	5532656.7	200	1491	1291	510	191.4	6.45	East	2.14	East
IVD	649892	5580222.8	220	517	297	307	48.6	2.06	North	1.36	North
IXA	621997.1	5409837.4	159	543	384	250	55.9	5.82	East	2.3	East
IXB	653086.3	5440624.5	162	583	421	269	66.9	5.17	East	2.74	East
IXC	703041	5442909.3	174	1014	840	383	141	7.75	West	2.03	West
IXD	723701.4	5496110.8	206	954	748	327	72.5	3.98	North	1.95	North
IXE	736095.5	5484037.7	268	1318	1050	575	161.9	13.3	West	2.49	West
VA	433084.5	5535094.7	169	861	692	391	122.8	3.62	East	2.08	North
VB	379855	5516508.7	231	770	539	435	71.1	3.43	East	2.24	North
VIA	493822	5599526.8	146	656	510	305	55.9	3.46	South	2.06	South
VIB	478917.2	5567738.2	133	455	322	219	47.3	1.22	East	1.95	East
VIC	570293.1	5545613.1	193	692	499	276	104	1.46	East	2.35	East
VIIA	718084.5	5539710.4	200	316	116	255	22	1.81	East	1.83	East
VIIIA	645831.3	5461667.5	161	382	221	222	31.8	1.15	East	1.76	East
VIIIB	743139.7	5525269.4	192	331	139	240	28.7	1.28	East	1.92	East
XA	651910	5415331.2	145	300	155	177	21.4	0.91	East	2.04	East

The algorithm is described in much more detail in [18], and the same authors implemented it in the R package mtsdi [19], whose mnimput function was also used to fill in the missing daily values.

The daily values were then aggregated for each year (i.e., winter season) using an alpha-trimmed mean to avoid sensitivity to extremes (see, e.g., [20] for more details on its properties). 10% of extreme values were trimmed. In addition, for those years where it was possible, the values were aggregated to represent, in addition to the complete season (labelled as COMPLETE), the different stages of the winter seasons (i.e., ACCUMULATION, MELT and the indistinguishable REST between accumulation and melting). For the definition of the accumulation and melting periods, respectively, the evolution of the snow cover in the border mountains, especially in the Giant Mountains and the Jizera Mountains, was used as a reference. Possible overlaps of these periods caused by possible thawing were not taken into account. However, the different durations of the different seasons in different years were guaranteed. Then, aggregation over all years was also carried out to obtain "long-term" values as explained variables for the regression models to be prepared. The dates defining the periods of snow accumulation and snowmelt were naturally not the same in all years, and

Tab. 5. Long-term averages of the zero isochion altitude for winter seasons (November–May) for the 27 geomorphological regions of Czechia

Region	ALL (2013–2021) [m]	ALL (2018–2021) [m]	ACCUMULATION (2018–2021) [m]	MELT (2018–2021) [m]	REST (2018–2021) [m]
IA	616	625	601	648	667
IB	808	808	748	914	782
IIA	450	445	440	454	442
IIB	439	437	439	436	432
IIC	539	537	516	572	545
IID	450	453	445	472	452
IIIA	699	697	626	842	705
IIIB	404	396	388	400	422
IIIC	663	682	654	724	685
IVA	651	638	568	818	573
IVB	612	618	555	750	606
IVC	683	678	570	873	699
IVD	351	360	359	357	363
IXA	212	201	193	204	228
IXB	282	280	295	264	265
IXC	500	511	448	594	554
IXD	391	386	366	414	439
IXE	627	625	575	700	622
VA	493	495	498	503	465
VB	459	465	464	463	473
VIA	322	319	313	328	319
VIB	254	247	248	247	248
VIC	352	342	330	348	370
VIIA	251	249	248	251	240
VIIIA	212	209	212	208	203
VIIIB	241	236	236	235	235
XA	182	178	178	178	178

therefore the procedure was strictly based on what was observed by a combination of satellite imagery and field survey. For the MELT period, the date of its start was not available for several geomorphological regions and was therefore replaced by the last date of the REST period. Period overlaps were not considered, rather the longer nature of the period was targeted.

For several reasons, including the amount of data obtained, determined by the number of geomorphological regions, a linear model (multivariate additive with parameter estimation using ordinary least squares) and a random forest model were finally chosen for the regression analysis itself. In the former case, terrain explanatory variables were selected based on the Akaike Information Criterion (using a combination of forward and backward variable selection; see [21, 22] for details). Specifically, the selection of explanatory variables was done through the stepAIC function implemented in the R package MASS, which is part of [23]. Before applying the linear models, the possible collinearity between the proposed explanatory variables was specifically investigated using Pearson correlation coefficients. In the case of random forests, the forward feature selection algorithm was applied using the ffs function implemented in the R package CAST [24–26], which mainly needs the R packages caret [27, 28] and randomForest [29] to make it work.

Tab. 6. Best linear models according to the Akaike Information Criterion

	Coefficient	Estimate	Std. error	*t*	P(> |t|)
ALL (2013–2021)	intercept	-73.65	35.43	-2.08	0.05
(R^2 = 0.99	*X*	0.000	0.000	1.39	0.18
F = 297.5	MIN	0.22	0.09	2.61	0.02
p < 0.01)	MAX	0.12	0.05	2.65	0.02
	MEDIAN	0.75	0.07	10.16	< 0.01
	SD	0.81	0.27	2.97	0.01
	MEDSLOPE	-9.28	2.83	-3.28	< 0.01
ACCUMULATION (2018–2021)	intercept	-701.23	536.17	-1.31	0.21
(R^2 = 0.99	*Y*	0.000	0.000	1.3	0.21
F = 174.7	MIN	0.35	0.1	3.52	< 0.01
p < 0.01)	MEDIAN	0.73	0.08	9.72	< 0.01
	SD	0.88	0.18	4.74	< 0.01
	MEDSLOPE	-4.79	3.05	-1.57	0.13
MELT (2018–2021)	intercept	-229.44	95.66	-2.4	0.03
(R^2 = 0.99	*X*	0.000	0.000	3.41	< 0.01
F = 112.5	MIN	0.21	0.15	1.42	0.17
p < 0.01)	MAX	0.25	0.08	3.08	0.01
	MEDIAN	0.94	0.12	7.76	< 0.01
	SD	0.96	0.45	2.11	0.05
	MEDSLOPE	-16.43	7.28	-2.26	0.04
	MEANASPEast	53.18	28.32	1.88	0.08
	MEANASPSouth	90.72	30.27	3	0.01
	MEANASPWest	65.25	45.08	1.45	0.17
	SDASP	-63.21	37.96	-1.67	0.12
REST (2018–2021)	intercept	-9.28	29.79	-0.31	0.76
(R^2 = 0.97	MAX	0.25	0.04	6.14	< 0.01
F = 115.2	MEDIAN	0.82	0.08	10.62	< 0.01
p < 0.01)	MEDSLOPE	-17.03	5.59	-3.04	0.01
	MEANASPEast	-9.63	21.8	-0.44	0.66
	MEANASPSouth	-29.39	26.61	-1.1	0.28
	MEANASPWest	86.3	43.79	1.97	0.06

Student t-distribution quantile; P – probability; F – Fisher-Snedecor F-distribution quantile; p – p-value

To determine whether a significant interannual monotonic trend can be observed in the altitude of the zero isochion, the non-parametric Mann–Kendall test was applied to each geomorphological region. Since this test, despite its non-parametric nature, is sensitive to autocorrelation in the time series, its trend-free pre-whitening (TFPW) modification implemented in the R package zyp [30] was chosen for the COMPLET series (2013–2021). The theoretical foundations of this test modification can be studied in references [31–33]. Other parts of the winter periods could not be studied in this way because the obtained time series were very short.

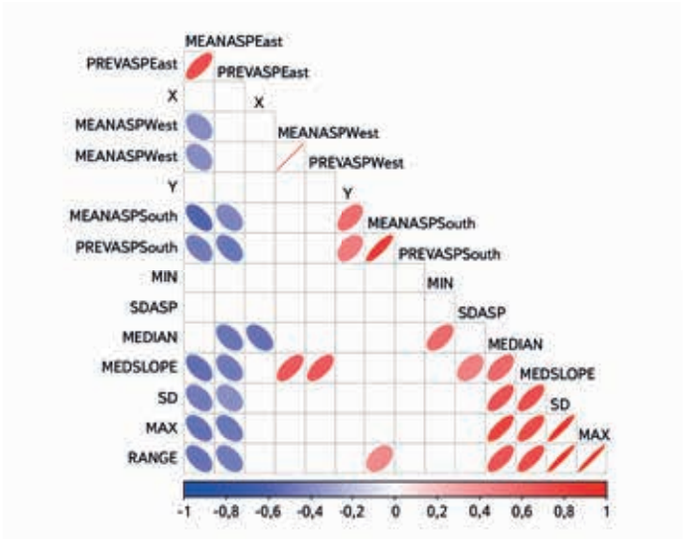

Fig. 5. Pearson correlations between the selected terrain explanatory variables (only correlations significant at the 0.05 level are shown by ellipses and colours)

RESULTS AND DISCUSSION

Fig. 4. shows the total number of zero isochion altitude values that have been derived from MODIS imagery for each of the 27 geomorphological regions used in the CHMI hydrology practice. A total of 3,216 such values were available for the period December 2012 to May 2021, which amounts to about 6.24% of the theoretically complete daily values (considering all winter seasons contained in the period November 2012 to May 2021, i. e., 51,570 values). This is not solely due to the fact that CHMI hydrologists traditionally focus on obtaining only one value per week for each region, but also because some regions are affected by cloud cover much more frequently than others. At the same time, it should be noted that lowland areas are much less likely to experience snowfall than areas characterised by more mountainous relief. In *Fig. 4*, this fact is highlighted by the method of a pseudo choropleth map, where geomorphological regions are classified into groups characterised by different intensities of blue. The difference, which is certainly due to the typical altitude or ruggedness within the regions, is very visible. In addition to the above, it must be taken into account that, in terms of spatial and temporal ocurrence of snow cover, the winters of the previous five years can be judged to have been below average, as can be seen from the continuous statistics [2].

Tab. 4 presents results regarding the extraction of selected terrain variables that were hypothesized to explain the spatial variation in the altitude of the zero isochion and, therefore, to be relevant for the construction of regression models. The list of variables that can be derived from the DEM in this way is certainly not exhaustive, but it was assumed to represent at least the most important factors related to latitude, longitude, and mean, minimum and maximum elevation, terrain ruggedness and slope gradient as well as the slope orientation to the cardinal directions. Particularly important here are the characteristics relating to the variability of elevation, but also the orientation of the slopes to the cardinal directions. The indicators related to slope orientation could have been expressed in angles, but in the end, it was decided that they would enter the regression models as categorical variables resulting from reclassification, since it is not easy to account for angular variables in such models and a transformation is recommended here anyway, usually by applying trigonometric functions.

Tab. 5 provides at least a basic idea of the long-term (or rather longer-term) values of the zero isochion altitude in the territory of individual geomorphological

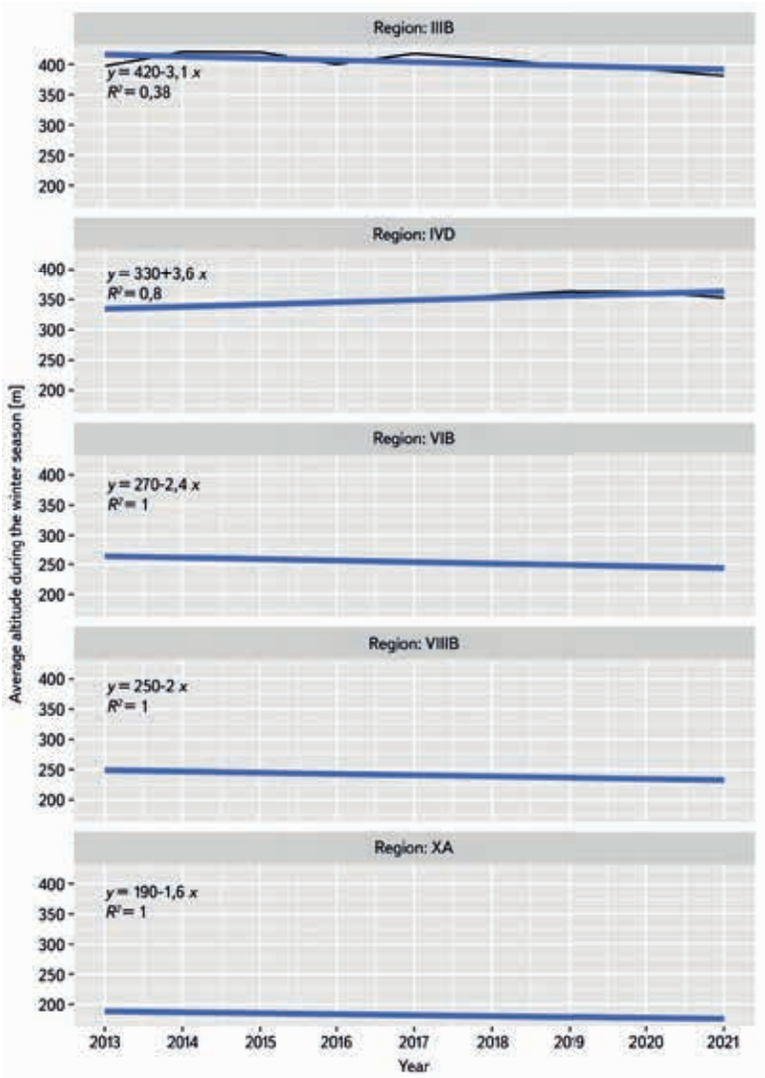

Fig. 6. Course of the annual series of average zero isochion altitude (2013–2021) in five geomorphological regions in Czechia for which a statistically significant monotonic trend was found at the 0.01 level (black line: specific altitude values; blue line: linear trend obtained by the ordinary least squares method)

regions of Czechia. In addition, *Tab. 5* shows how these long-term characteristics vary according to the different stages of the winter season (i.e., accumulation, melting and middle periods when accumulation or melting cannot be distinguished), at least for the years 2018–2021. It should be noted that the full (completed) multivariate series could also include values greater than the maximum and less than the minimum elevation occurring in the geomorphological regions due to extrapolations, which occurred for 16 regions in the supplemented data (in other words, for 1.3% of the total daily values). However, this was not an obstacle when subsequently using the models to identify which terrain features influence the variability of zero isochion altitude. Moreover, these values could be considered realistic if, for example, the highest parts of the regions reached the estimated positions. It is also assumed that these situations were reduced by applying the alpha-trimmed mean.

Before applying linear models, it is recommended to pay particular attention to the likely collinearity between the explanatory variables, i.e., the phenomenon where two or more variables provide very similar information. *Fig. 5* shows through Pearson correlations that, despite the incomplete list of terrain variables, collinearity was very likely present in the set of explanatory variables. In

Tab. 7. Explanatory variables selected by the algorithm according to [25] for random forest models

	Explanatory variable
ALL (2013–2021)	MAX
(R^2 = 0.93	MEDIAN
RMSE = 45.79	*X*
RRMSE = 10.18)	
ACCUMULATION (2018–2021)	MEDIAN
(R^2 = 0.93	SD
RMSE = 40.44	MIN
RRMSE = 9.49)	
MELT (2018–2021)	MAX
(R^2 = 0.92	MEDIAN
RMSE = 61.09	SDASP
RRMSE = 12.5)	
REST (2018–2021)	MAX
(R^2 = 0.92	MEDIAN
RMSE = 49.4	*X*
RRMSE = 10.92)	

RMSE – root mean squared error
RRMSE – relative root mean squared error

particular, we note a very close correlation (and statistically significant correlation at the 0.05 level) between the elevation maximum and the range between minimum and maximum. Furthermore, a very close relationship between the two variables related to slope orientation can be observed. For these reasons, the range between maximum and minimum elevation and the prevailing slope orientation were not further accounted for in the linear models. An alternative (while retaining all available explanatory variables) could be regression models in which the explanatory variables are principal components instead of the original variables (see, e.g. [34]). For the random forest models, all obtained terrain explanatory variables were deliberately retained before selection. Let us also note that for the random forest models, the original parameter settings were retained as, e.g., in [35].

Tab. 6 and *7* already reveal which terrain variables were specifically selected for the linear models (using the Akaike Information Criterion) and random forest models (using the forward feature selection algorithm of [25]), respectively. It can be seen that linear models are much more complex in terms of the inclusion of explanatory variables. Some variables are not significant according to the *t* statistic, but still contribute to the significance of the whole models. These are even significant at levels smaller than 0.05 according to the *F* statistic. Also, the values of the coefficients of determination (R^2) clearly indicate that the explanation of the variability of the long-term altitude of the zero isochion is more than good here. At the cost of reducing R^2 values, the algorithm selected fewer explanatory variables in the case of random forest models. Longitude and elevation extremes stand out very often here. The constantly occurring explanatory variable here is the characteristic related to the mean elevation of the geomorphological regions, which confirms the situation in *Fig. 4.* Characteristics associated with the variance of elevation (in the case of accumulation) and slope orientation (in the case of melting) also seem to be important for the snow accumulation and snowmelt periods, which sounds quite logical. It should be noted, however, that the random forest is a model based on resampling techniques, so a different run of the algorithm may result in a slightly different choice of variables. Nevertheless, we believe that even so, these selections would be very similar. For example, for snowmelt, the variance of slope orientation related to favourable or unfavourable conditions during the daylight hours will be important.

The analysis of trends, and thus interannual temporal variability of zero isochion altitude, was conducted only for the longest time series, designated as ALL, because the four-year period for which a phase-by-phase distribution discriminating between snow cover gains and losses is available cannot yet be considered representative for this type of analysis. It is clear from *Tab. 8* that the zero isochion was rather stable during the 2013–2021 winter seasons. Nevertheless, it is possible to note that five regions are likely to experience a decrease (Ore Mts. Piedmont Region, Central Bohemian Table, Northern Outer Carpathian Depressions, South Moravian Basin) or an increase in zero isochion altitude (Krkonoše-Jeseníky Piedmont). The reasons for such trends may vary from actual increases or decreases in snow cover to the fact that the data for some of these regions may not have been sufficient. For example, from *Fig. 6*, where the black line shows the time series for only the regions with a significant monotonic trend, it is clear that at least three of these results are quite implausible. Situations where $R^2 = 1$ almost never occur. Moreover, the courses of these suspect series show almost no variability (e.g., the black lines are covered by the blue regression lines), suggesting that the EM algorithm may have failed in filling in the missing values, working with only a few observed values that may have been burdened with large uncertainty on top of that. Let us add that while in *Fig. 6* the regression lines are constructed using linear models, in *Tab. 8* the regression coefficient and the intercept are related to so-called Sen's non-parametric estimator [36] to compare the results.

In order to update the table of differences between altitudes of the zero isochion in different geomorphological regions presented in [3], its new version has been compiled (see *Tab. 9*). It is obvious that the current figures are quite different from those published in the past. For example, there may have been some refinement, where the applied alpha-trimmed mean took the extreme values into account in a different way. However, from the practical point of view of the methodology for calculating snow water storage, the relationship between the mountain border regions where snow cover is longest and most frequent, is the most important for CHMI forecasters. Nevertheless, it is also necessary to mention the risk of significant spring flooding from melting snow, which is more associated with snow cover in the lowlands, i.e., in the tables surrounding the Elbe River. In such situations, the zero isochion is either completely suppressed and snow occurs over the whole territory, or the boundary is quite sharp and delimits the warmest areas and heat islands. *Tab. 9* only confirms the experience from the zero isochion analyses, especially the most widely used relationship, namely that between the Giant Mountains Region and the Šumava Region. This can be characterised simply by the fact that the snow cover in the Bohemian Forest always starts 100 metres or more higher as compared with the snowline in the Giant Mountains. The reasons for this can be seen in the ruggedness of the local regions, with the Giant Mountains representing steeper slopes and the Czech part of the Bohemian Forest representing a more gradual transition to lower areas.

Fig. 7 demonstrates an example of the output obtained with MODIS imagery and it also documents the conditions of snow cover loss in early April 2021. It shows the most common situation where snow cover is present only at the highest elevations of the mountains, where it is also partially covered by clouds. In contrast, the lowlands no longer have snow at all, just as the uncertainly definable areas with snow are no longer present at the end of winter, as characterised by code 201 (see *Tab. 1*).

Tab. 8. Results of trend analysis for all 27 geomorphological regions of Czechia (↑: statistically significant increasing trend at the 0.01 level; ↓: statistically significant decreasing trend at the 0.01 level)

Region	Kendall's tau	*p*-value	Sen's slope	Intercept	Graphical trend expression
IA	0.43	0.17	3.74	598.18	–
IB	0.14	0.71	4.06	782.19	–
IIA	-0.36	0.27	-1.01	456.15	–
IIB	-0.36	0.27	-0.25	439.8	–
IIC	-0.14	0.71	0.34	534.1	–
IID	0	1	1.69	447.65	–
IIIA	-0.14	0.71	3.3	674.8	–
IIIB	-0.79	< 0.01	-4.19	427.01	↓
IIIC	0.5	0.11	7.33	624.57	–
IVA	-0.29	0.39	0.23	657.84	–
IVB	-0.07	0.9	4.32	595.99	–
IVC	0	1	0.59	670.03	–
IVD	0.79	< 0.01	4.29	329.09	↑
IXA	-0.57	0.06	-4.39	236.98	–
IXB	-0.21	0.54	-3.3	301.42	–
IXC	0.14	0.71	4.65	469.41	–
IXD	-0.5	0.11	-1.1	401.11	–
IXE	-0.07	0.9	0.56	629.08	–
VA	-0.14	0.71	0.22	489.92	–
VB	0.29	0.39	1.27	451.72	–
VIA	-0.07	0.9	0.12	322.8	–
VIB	-1	< 0.01	-2.44	265.85	↓
VIC	-0.5	0.11	-3.48	368.05	–
VIIA	-0.43	0.17	-0.41	252.38	–
VIIIA	-0.29	0.39	-1.74	219.8	–
VIIIB	-1	< 0.01	-2.04	251	↓
XA	-1	< 0.01	-1.6	189.88	↓

CONCLUSION

This paper presents updated findings concerning the altitude of the zero isochion, i.e., the line representing the boundary between the snow and snow-free areas, in 27 geomorphological regions of Czechia, which are used in hydrological practice of the CHMI for estimating the snow water equivalent. Since snow represents a significant component of runoff in Czechia, this activity is necessary before running hydrological models used at the CHMI for both operational purposes and balance calculations. Field surveys are costly and time-consuming, and do not provide a sufficiently detailed picture of the spatial distribution of snow in regions that are often quite rugged in Czechia. Therefore, satellite imagery has been successfully used to refine this picture, and after appropriate

Tab. 9. Differences between long-term averages of the zero isochion altitude for winter seasons (November–May) across all 27 geomorphological regions of Czechia (in m)

XA	VIIIB	VIIIA	VIIA	VIC	VIB	VIA	VB	VA	IXE	IXD	IXC	IXB	IXA	IVD	IVC	IVB	IVA	IIIC	IIIB	IIIA	IID	IIC	IIB	IIA	IB	IA	
434	375	403	366	265	362	294	156	116	-10	220	116	333	404	266	-71	-2	-41	-48	207	-80	165	77	176	163	-194	0	**IA**
626	567	594	558	457	554	486	349	311	187	415	314	525	596	461	116	189	151	147	401	110	357	273	369	356	0		**IB**
267	208	235	199	99	196	130	-10	-41	-178	60	-49	167	235	102	-233	-165	-205	-211	45	-249	1	-84	12	0			**IIA**
257	198	227	188	87	186	117	-20	-54	-188	48	-60	157	227	88	-243	-173	-212	-224	35	-260	-11	-99	0				**IIB**
357	298	325	288	182	285	215	76	43	-88	146	38	252	324	189	-146	-80	-118	-124	130	-165	84	0					**IIC**
268	209	236	201	95	196	129	-7	-42	-175	60	-46	165	237	102	-230	-163	-202	-211	46	-247	0						**IID**
517	458	485	450	347	445	377	236	200	83	305	200	415	488	351	10	80	37	34	285	0							**IIIA**
222	163	188	153	56	150	83	-54	-87	-218	13	-90	120	191	56	-272	-209	-245	-254	0								**IIIB**
482	423	450	413	310	410	342	203	165	39	268	159	380	452	314	-23	48	11	0									**IIIC**
469	410	438	401	301	398	330	192	157	37	260	154	367	441	306	-35	34	0										**IVA**
430	371	399	362	264	358	293	157	123	-4	221	117	328	402	266	-72	0											**IVB**
500	441	469	433	326	428	358	223	186	69	285	185	397	470	340	0												**IVC**
169	110	138	100	1	98	29	-110	-146	-275	-45	-153	69	137	0													**IVD**
31	-28	0	-39	-141	-41	-109	-245	-281	-414	-181	-282	-71	0														**IXA**
100	41	67	31	-70	28	-41	-178	-210	-345	-106	-212	0															**IXB**
318	259	285	251	142	246	176	40	4	-120	104	0																**IXC**
209	151	178	140	40	138	68	-69	-102	-231	0																	**IXD**
445	386	415	377	272	373	304	168	132	0																		**IXE**
311	252	280	243	143	239	168	36	0																			**VA**
277	218	244	209	108	205	137	0																				**VB**
140	82	108	72	-29	69	0																					**VIA**
72	13	41	3	-98	0																						**VIB**
170	111	139	102	0																							**VIC**
69	10	37	0																								**VIIA**
31	-28	0																									**VIIIA**
59	0																										**VIIIB**
0																											**XA**

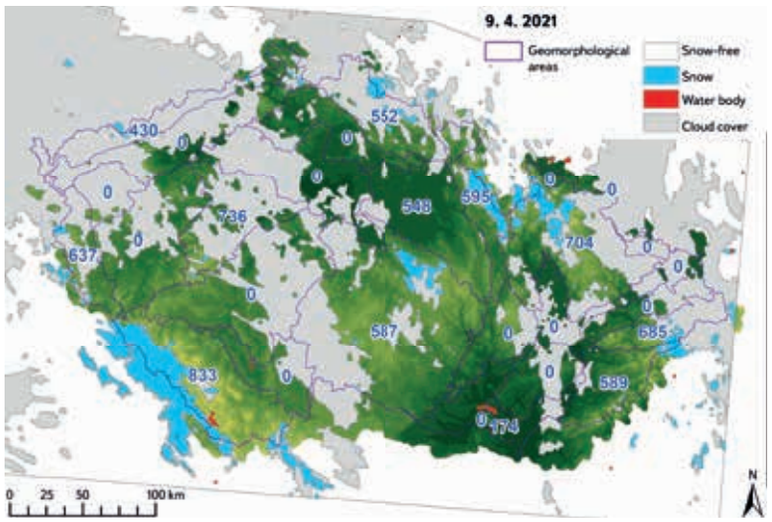

Fig. 7. Analyzed situation on 9th April 2021 where the selected classes from *Tab. 1* are depicted above the digital elevation model (values determine the average position of the zero isochion in m a. s. l. and 0 determines the area without recorded zero isochion)

calibration with data collected in the field, it can be very helpful in determining the boundary between snow and snow-free regions (see, e.g., [1] and [37]). The study thus built on previous research and, using an extended time series of zero isochion altitudes to May 2021, sought to answer the questions outlined in the conclusions of [3]. In particular, the spatial variability of the zero isochion altitude was studied and it was examined through regression models which terrain-related factors (determined in a GIS environment from the DEM based on the DMU 25 work) matter most for the variation of the zero isochion. The alpha-trimmed mean calculated from daily values was taken as the representative explained variable here, as it was assumed to reduce the influence of uncertainty in the determination of the position of the zero isochion. Moreover, the average zero isochion altitude in each region represents to some extent a limiting position below which non-zero (positive) values of snow cover depth and hence snow water equivalent can no longer be expected in interpolation processes. Given the uncertainties associated with MODIS imagery, we believe that if the derivation of the zero isochion is appropriately combined with the interpolation of values obtained from ground-based measurements, some of these uncertainties can be reduced to a great extent. Thus, the regression models constructed here to explain spatial variability can be very useful, for example, in estimating the (average) position of the zero isochion in situations where regions are mostly covered by clouds. It has been found that mean but also extreme values of elevation have a large influence. Longitude also seems to play a role. In the case of snow accumulation, the standard deviation calculated from the elevations occurring in a given geomorphological region is added to the explanatory variables in the regression models. In the case of snowmelt, the standard deviation obtained from all angles determining slope orientation appears to be significant. The study of the temporal variability of the zero isochion altitude was carried out by trend analysis in order to determine whether the presence of monotonic deterministic trends can be observed. In order to reduce the influence of autocorrelation, the TFPW modification of the Mann–Kendall test was applied. The results show that snow cover, and hence the zero isochion, behaved stably during the winter seasons. A statistically significant interannual trend was found only in five geomorphological regions. However, the results of the analyses should be interpreted with caution. For example, in three areas the coefficient of determination was suspiciously equal to one, which is a very rare phenomenon. Instead of indicating reality, this fact rather indicates that the Expectation-Maximization (EM) algorithm used to fill in the missing values of the zero isochion altitude failed in some cases. This was due to lack of information, which was certainly caused by the small amount of data obtained from MODIS images or derived products.

As indicated above, revisions to the NDSI index-based product are due to be completed in spring 2022. This could subsequently provide some sort of verification at the CHMI whether the relationships presented in this paper are still valid. Naturally, the deployment of (semi)automatic processing of data coming from MODIS imagery is proposed, provided that the CHMI staff deepen their scripting skills. It is highly recommended to extend the time series towards history, considering that products related to snow detection on the Earth's surface have been available since 2000. It is also suggested to complement the data considering that MODIS imagery has a much finer time step than one week. This may also allow the application of more sophisticated time series models than simple trend analysis. This will refine the notion of the temporal dynamics of the zero isochion if the explanatory variables also include a number of climatological features along with the terrain characteristics. The explanation for the differences in the position of the zero isochion can also be found in different climatic conditions, especially in the occurrence of rainfall situations, which mainly affect the south-west part of Czechia, while they do not reach such intensities towards the northern mountain ranges anymore. It is also worth looking at other characteristics related to the zero isochion that may enter the models as explanatory variables. For example, the gradient of change of the zero isochion or the change in the duration of the zero isochion presence a certain elevation zone can provide interesting information to hydrologists. Similar variables have already been studied in [38], and especially the period of snow-melt and its effect on runoff was the focus of study [39]. The method by which the zero isochion is extracted in these publications is also worth mentioning. This method differs from the methodology presented here, and therefore a comparison of the two approaches using data for Czechia is naturally offered here.

The spatial resolution of the analyzed grid (500 m) remains a fundamental limitation for a more precise definition of the position of the zero isochion. Thus, spatial refinement, in addition to process automation, is necessary for a deeper implementation of the zero isochion in the calculation of snow water storage. One possibility could be the differentiation of the reclassification of products with NDSI values according to different factors, which has proven to be successful in Austria according to [40]. However, the precondition is that the length of the derivation of the zero isochion will satisfy the requirement of the CHMI operational hydrology to have this result within 24 hours. More accurate spatial data currently exist, but again with a considerable time delay between acquisition and availability. Some promise, in this decade, can be seen in local observing systems or in the European COPERNICUS programme with Sentinel missions (see, e.g., [41]). It will certainly be an equally important task to study the snow cover properties separately for the accumulation, melting and remaining phases of the winter season, because – as the results of this study have shown – this division makes sense.

Last but not least, the question arises whether it is more advantageous to map the snow cover area directly using MODIS imagery. This would only be possible under ideal cloud-free conditions, when an overview of the whole Czech territory, or at least all regions with snow cover, is guaranteed. Such situations are in fact only minimal, on the order of units of days during the season. For this reason, MODIS imagery cannot currently be implemented in snow cover area calculations as a regularly used tool, but only as a supplement to the information obtained from the relatively dense snow gauging network of the CHMI. On the contrary, some potential can be found just in the calibration of the model based on the available zero isochion altitude series and its ability to predict for the "invisible" locations.

Acknowledgements

Both authors are supported within the so-called Long-Term Concept of Development of the Research Organization CHMI. The statistical work of O. Ledvinka is also supported by the Technology Agency of the Czech Republic (project SS01020366 "Use of remote sensing data for assessment of negative impacts of torrential rainfall"). The authors would like to express their gratitude for this support.

References

[1] BERCHA, Š. Vyhodnocování zásob vody ve sněhové pokrývce v ČHMÚ. In: KIMLOVÁ, M., ŘIČICOVÁ, P.BERCHA, Š (eds.). *XXI. stretnutie snehárov: sborník príspevkŭ ze semináře: Žítková 1.–3. 3. 2016 + vybrané nevydané příspěvky z předchozích setkání* [on-line]. Praha: Český hydrometeorologický ústav, 2017, p. 55–56. ISBN 978-80-87577-75-2. Available from: http://www.uh.sav.sk/en-gb/Research/Conferences/Snow-Meetings

[2] ČHMÚ. Hlásná a předpovědní povodňová služba. *Informace o velikosti sněhových zásob na území České republiky* [on-line]. 4. květen 2021 [accessed November 23, 2021]. Available from: https://www.chmi.cz/files/portal/docs/poboc/CB/snih/aktual.htm

[3] DUCHÁČEK, L. Vertikální variabilita nulové izochiony v rámci geomorfologických oblastí Česka. *Geografie* [on-line]. 2014, 119(2), p. 145–160. ISSN 1212-0014, 2571-421X. Available from: doi: 10.37040/geografie2014119020145

[4] Česká meteorologická společnost. Meteorologický slovník. *Elektronický meteorologický slovník* [on-line]. 2017 [accessed November 25, 2021]. Available from: http://slovnik.cmes.cz/

[5] NASA NSIDC. *About Us | National Snow and Ice Data Center* [on-line]. 2021 [accessed November 23, 2021]. Available from: https://nsidc.org/about/overview

[6] HALL, D. K., RIGGS, G. A. *MODIS/Terra Snow Cover 5-Min L2 Swath 500m, Version 61* [on-line]. B.m.: NASA National Snow and Ice Data Center DAAC. 2021 [accessed November 23, 2021]. Available from: doi: 10.5067/MODIS/MOD10_L2.061

[7] *Moderate Resolution Imaging Spectroradiometer* [on-line]. 2021 [accessed November 26, 2021]. Available from: https://en.wikipedia.org/w/index.php?title=Moderate_Resolution_Imaging_Spectroradiometer&oldid=1048616305

[8] NASA. *Terra Spacecraft | NASA* [on-line]. 4th August [accessed November 23, 2021]. Available from: https://www.nasa.gov/mission_pages/terra/spacecraft/index.html

[9] *Hierarchical Data Format* [on-line]. 2021 [accessed November 26, 2021]. Available from: https://en.wikipedia.org/w/index.php?title=Hierarchical_Data_Format&oldid=1049571370

[10] NASA. *HEG: HDF-EOS to GeoTIFF Conversion Tool – Data Access Services – Earthdata Wiki* [on-line]. 22nd April [accessed November 23, 2021]. Available from: https://wiki.earthdata.nasa.gov/display/DAS/HEG%3A++HDF-EOS+to+GeoTIFF+Conversion+Tool

[11] BOHÁČ, P., KOLÁŘ, J. *Vyšší geomorfologické jednotky České republiky*. Praha: Český úřad zeměměřický a katastrální, 1996. Geografické názvoslovné seznamy OSN – ČR, A1. ISBN 978-80-901212-7-0.

[12] ČÚZK. ČÚZK: Geoportál. *Data200* [on-line]. 20. leden 2020 [accessed November 23, 2021]. Available from: https://geoportal.cuzk.cz/(S(eew4l3agpixe2uphizmomaed))/Default.aspx?mode=TextMeta&side=mapy_data200&text=dSady_mapyData200&head_tab=sekce-02-gp&menu=229

[13] MARDIA, K. V. *Statistics of Directional Data*. London, New York: Academic Press, 1972. Probability and Mathematical Statistics. ISBN 978-0-12-471150-1.

[14] AGOSTINELLI, C., LUND, U. *R Package „Circular": Circular Statistics* [on-line]. English. B. m.: Pacific Climate Impacts Consortium, 2017. Available from: https://r-forge.r-project.org/projects/circular/

[15] PEBESMA, E. Simple Features for R: Standardized Support for Spatial Vector Data. *The R Journal* [on-line]. 2018, 10(1), p. 439. ISSN 2073-4859. Available from: doi: 10.32614/RJ-2018-009

[16] HIJMANS, R. J. *Terra: Spatial Data Analysis* [on-line]. 2021. Available from: https://CRAN.R-project.org/package=terra

[17] VIO, R. WAMSTEKER, W. Tersts of Irregularly Sampled Stochastic Time Series for AGN. In: MAOZ, D., STERNBERG, A., LEIBOWITZ, E. M. (eds). *Astronomical Time Series: Proceedings of The Florence and George Wise Observatory 25th Anniversary Symposium held in Tel-Aviv, Israel, 30 December 1996–1 January 1997* [on-line]. Dordrecht: Springer Netherlands, 1997 [accessed June 8, 2019], Astrophysics and Space Science Library, 218, p. 167–170. ISBN 978-90-481-4895-0. Available from: http://link.springer.com/10.1007/978-94-015-8941-3

[18] JUNGER, W. L., PONCE DE LEON, A. Imputation of Missing Data in Time Series for Air Pollutants. *Atmospheric Environment* [on-line]. 2015, 102, p. 96–104. ISSN 1352-2310. Available from: doi: 10.1016/j.atmosenv.2014.11.049

[19] JUNGER, W. PONCE DE LEON, A. *Mtsdi: Multivariate Time Series Data Imputation* [on-line]. 2018. Available from: https://CRAN.R-project.org/package=mtsdi

[20] ZVÁRA, K. *Základy statistiky v prostředí R* [online]. Praha: Karolinum, 2013 [accessed February 27, 2017]. Biomedicínská statistika, IV. ISBN 978-80-246-2447-1. Available from: http://site.ebrary.com/id/10852905

[21] AKAIKE, H. A New Look at the Statistical Model Identification. *IEEE Transactions on Automatic Control* [on-line]. 1974, 19(6), p. 716–723. ISSN 0018-9286. Available from: doi: 10.1109/TAC.1974.1100705

[22] KUTNER, M. H., NACHTSHEIM, Ch. J., NETER, J., LI, W. *Applied Linear Statistical Models*. 5th ed. Boston: McGraw-Hill/Irwin, 2005. Operations and Decision Sciences. ISBN 0-07-238688-6.

[23] VENABLES, W. N., RIPLEY, B. D. *Modern Applied Statistics with S*. 4th ed. New York: Springer, 2002. Statistics and Computing. ISBN 978-0-387-95457-8.

[24] MEYER, H. *CAST: „Caret" Applications for Spatial-Temporal Models* [on-line]. 2021. Available from: https://CRAN.R-project.org/package=CAST

[25] MEYER, H., REUDENBACH, Ch., HENGL, T., KATURJI, M., NAUSS, T. Improving Performance of Spatio-Temporal Machine Learning Models Using forward Feature Selection and Target-Oriented Validation. *Environmental Modelling & Software* [on-line]. 2018, 101, p. 1–9. ISSN 1364-8152. Available from: doi: 10.1016/j.envsoft.2017.12.001

[26] MEYER, H., REUDENBACH, Ch., WÖLLAUER, S., NAUSS, T. Importance of Spatial Predictor Variable Selection in Machine Learning Applications – Moving from Data Reproduction to Spatial Prediction. *Ecological Modelling* [on-line]. 2019, 411, 108815. ISSN 0304-3800. Available from: doi: 10.1016/j.ecolmodel.2019.108815

[27] KUHN, M. *Caret: Classification and Regression Training*. [on-line]. 2021. Available from: https://CRAN.R-project.org/package=caret

[28] KUHN, M., JOHNSON, K. *Applied Predictive Modeling* [on-line]. New York, NY: Springer New York, 2013 [accessed September 15, 2020]. ISBN 978-1-4614-6848-6. Available from: http://link.springer.com/10.1007/978-1-4614-6849-3

[29] LIAW, A., WIENER, M. Classification and Regression by RandomForest. *R News*. 2002, 2(3), p. 18–22. ISSN 1609-3631.

[30] BRONAUGH, D., WERNER, A. *Zyp: Zhang + Yue-Pilon trends package* [online]. B.m.: Pacific Climate Impacts Consortium, 2019. Available from: https://CRAN.R-project.org/package=zyp

[31] KENDALL, M. G. A New Measure of Rank Correlation. *Biometrika* [on-line]. 1938, 30(1), p. 81–93. ISSN 0006-3444. Available from: doi: 10.2307/2332226

[32] MANN, H. B. Nonparametric Tests against Trend. *Econometrica* [on-line]. 1945, 13(3), p. 245–259. ISSN 00129682. Available from: doi: 10.2307/1907187

[33] KENDALL, M. KEITH, J. ORD. *Time Series*. 3rd ed. Sevenoaks: Arnold, 1993. ISBN 978-0-340-59327-1.

[34] WILKS, D. S. *Statistical Methods in the Atmospheric Sciences* [on-line]. 4th ed. B.m.: Elsevier, 2019 [accessed October 1, 2019]. ISBN 978-0-12-815823-4. Available from: https://linkinghub.elsevier.com/retrieve/pii/C20170039216

[35] MAŤAŠOVSKÁ, V., KOTHAN, F., LEDVINKA, O., PUMANN, P., FOJTÍK, T., MAKOVCOVÁ, M., BENDAKOVSKÁ, L. Využití metod dálkového průzkumu Země pro monitoring stavu koupacích míst. *Vodohospodářské technicko-ekonomické informace* [on-line]. 2021, 63(1), p. 37–45. ISSN 0322-8916. Available from: doi: 10.46555/VTEI.2020.12.003

[36] SEN, P. K. Estimates of the Regression Coefficient Based on Kendall's Tau. *Journal of the American Statistical Association* [on-line]. 1968, 63(324), p. 1379–1389. ISSN 01621459. Available from: doi: 10.2307/2285891

[37] DENG, G., TANG, Z., HU, G., WANG, J., SANG, G., LI, J. Spatiotemporal Dynamics of Snowline Altitude and their Responses to Climate Change in the Tienshan Mountains, Central Asia, during 2001–2019. *Sustainability* [on-line]. 2021, 13(7), 3992. ISSN 2071-1050. Available from: doi: 10.3390/su13073992

[38] KRAJČÍ, P., HOLKO, L., PARAJKA, J. Variability of Snow Line Elevation, Snow Cover Area and Depletion in the Main Slovak Basins in Winters 2001–2014. *Journal of Hydrology and Hydromechanics* [on-line]. 2016, 64(1), p. 12–22. ISSN 0042-790X. Available from: doi: 10.1515/johh-2016-0011

[39] PARAJKA, J., BEZAK, N., BURKHART, J., HAUKSSON, B., HOLKO, L., HUNDECHA, Y., JENICEK, M., KRAJČÍ, P., MANGINI, W., MOLNAR, P., RIBOUST, P., RIZZI, J., SENSOY, A., THIREL, G., VIGLIONE, A. MODIS Snowline Elevation Changes during Snowmelt Runoff Events in Europe. *Journal of Hydrology and Hydromechanics* [on-line]. 2019, 67(1), p. 101–109. ISSN 0042-790X. Available from: doi: 10.2478/johh-2018-0011

[40] TONG, R., PARAJKA, J., KOMMA, J., BLÖSCHL, G. Mapping Snow Cover from Daily Collection 6 MODIS Products over Austria. *Journal of Hydrology* [on-line]. 2020, 590, 125548. ISSN 0022-1694. Available from: doi: 10.1016/j.jhydrol.2020.125548

[41] Koordinační rada ministra dopravy pro kosmické aktivity. Informační stránky Koordinační rady ministra dopravy pro kosmické aktivity. *Mapová aplikace | CollGS* [on-line]. 2021 [accessed November 26, 2021]. Available from: https://collgs.czechspaceportal.cz/mapova-aplikace/

The authors

Mgr. Libor Ducháček[1]
✉ libor.duchacek@chmi.cz
ORCID: 0000-0001-6646-3399

Mgr. Ondřej Ledvinka, Ph.D.[2]
✉ ondrej.ledvinka@chmi.cz
ORCID: 0000-0002-0203-7064

[1] Czech Hydrometeorological Institute,
Applied Hydrology Department, Jablonec nad Nisou
[2] Czech Hydrometeorological Institute,
Hydrology Database and Water Budget Department, Prague

The paper has been peer-reviewed.

DOI: 10.46555/VTEI.2021.11.004

Possibilities of using spectroscopy for the evaluation of forest soil properties

JOSEF KRATINA, VÁCLAVA MAŤAŠOVSKÁ

Keywords: forest soil — VNIR spectroscopy — prediction of soil properties

SUMMARY

The aim of this study was to objectively evaluate the applicability of VNIR spectroscopy (spectroscopy in the visible and near-infrared region of the electromagnetic spectrum) for the prediction of forest soil properties. The most appropriate combinations of statistical pre-processing (no pre-processing, continuum removal, 1st and 2nd derivative) and processing (PLSR – partial least squares regression, PCR – principal component regression, SVM – support vector machines) methods in specific spectral bands were sought for each soil property. The combination of the 1st derivative and SVM methods proved to be generally the most successful in the whole VNIR spectral band (400–2500 nm). However, in some cases (different forms of magnesium, manganese, iron, or aluminium) other models have proved to be successful. The best predictable properties (R^2 > 0.6) include soil pH, oxidizable carbon content, and the contents of aluminium, iron, silicon, or calcium (at higher concentrations). Not very high prediction success (R^2 < 0.3) was found for parameters that take on low values (the content of sodium, manganese, or divalent aluminium complexes). The results show that VNIR spectroscopy is a useful method for the prediction of forest soil properties. It cannot completely replace classical analysis, but it can complement it very well, especially in practice. For example, it can help to thicken the data network in soil mapping and refine the information better than other spatial estimation methods. It can be used in cases where a significant amount of data is needed in a short time frame and at minimum cost. It is suitable for monitoring trends over time or for rapid exploration of an area.

INTRODUCTION

Information on soil properties is required for a variety of purposes, such as precision agriculture or forestry, soil quality assessment, soil mapping or soil conservation. It is necessary to collect a large amount of analytical data within soil examination. The collection and subsequent analysis of soil samples using traditional methods is time consuming and costly [1, 2]. Therefore, indirect measurements and predictions of soil properties using mathematical models are increasingly being used. Several studies have shown that spectroscopy in the visible (VIS) and near-infrared (NIR) region of the electromagnetic spectrum is a suitable method for assessing soil properties. The models published so far are not universal and are only relevant under specific conditions and for certain soil groups. This study aims at assessing the applicability of spectroscopy in the evaluation of properties of forest soils in the Czech Republic based on the relationships between spectral features and soil properties determined by traditional laboratory methods. More than 4,500 samples taken from whole soil profiles were used for this assessment. Appropriate combinations of data preparation methods (1st and 2nd derivatives [3], continuum removal) and statistical techniques of partial least squares regression (PLSR), support vector machines (SVM) and principal component regression (PCR) were tested to develop predictive models.

THE METHODS

The study was carried out using 4,680 samples taken from whole soil profiles using a soil probe or from excavated soil material. Some of the soil samples were obtained from the Department of Soil Science and Soil Protection at the Czech University of Life Sciences in Prague, the rest were borrowed from other departments. The sampling sites were chosen to cover the whole territory of the Czech Republic and to include different forest soil types. The sampling sites were located at different altitudes and in forests with different species composition. The study did not deal with field measurements; only dried samples treated to fine soil I (particle size < 2 mm) were used [4]. This eliminated the influence of soil moisture, which is essential on the spectral curves and hinders the field application of the method to a great extent. Selected analyses were performed with soil samples using conventional methods (*Tab. 1*).

Fig. 1. FieldSpec 3 spectrometer (photo: Josef Kratina)

Tab. 1. Used methods of conventional analysis

Property	Units	Description of analysis
pH_H_2O	–	Soil pH (H_2O) [4]
pH_$CaCl_2$	–	Soil pH – $CaCl_2$ [5]
pH_KCl	–	Soil pH – KCl [6]
Cox	%	Oxidizable carbon content using modified Tyurin method [4]
KVK	mmol.100 g^{-1}	Cation exchange capacity (Bower) [4]
BS	mmol.100 g^{-1}	Saturation of sorption complex with basic cations [4]
N	mg.kg^{-1}	NIR spectroscopic determination [7]
P_M3	mg.kg^{-1}	Phosphorus extracted with Mehlich III solution [4]
P_AR	mg.kg^{-1}	Phosphorus extracted with aqua regia [8]
K_M3	mg.kg^{-1}	Potassium extracted with Mehlich III solution [4]
K_AR	mg.kg^{-1}	Potassium extracted with aqua regia [8]
K_$BaCl_2$	mg.kg^{-1}	Exchangeable cations (potassium), leachate – $BaCl_2$ [9]
Ca_M3	mg.kg^{-1}	Calcium extracted with Mehlich III solution [4]
Ca_AR	mg.kg^{-1}	Calcium extracted with aqua regia [8]
Ca_$BaCl_2$	mg.kg^{-1}	Exchangeable cations (calcium), leachate – $BaCl_2$ [9]
Mg_M3	mg.kg^{-1}	Magnesium extracted with Mehlich III solution [4]
Mg_AR	mg.kg^{-1}	Magnesium extracted with aqua regia [8]
Mg_$BaCl_2$	mg.kg^{-1}	Exchangeable cations (magnesium), leachate – $BaCl_2$ [9]
Na_AR	mg.kg^{-1}	Sodium extracted with aqua regia [8]
Na_$BaCl_2$	mg.kg^{-1}	Exchangeable cations (sodium), leachate – $BaCl_2$ [9]
Mn_$BaCl_2$	mg.kg^{-1}	Exchangeable cations (manganese), leachate – $BaCl_2$ [9]
Mn_AR	mg.kg^{-1}	Mangan extracted with aqua regia [8]
Mn_KCl	mg.kg^{-1}	Mangan extracted with KCl solution [10]
Mn_ox	mg.kg^{-1}	Mangan extracted with oxalate [11]
Mn_dit	mg.kg^{-1}	Mangan extracted with dithionite [12]
Fe_$BaCl_2$	mg.kg^{-1}	Exchangeable cations (iron), leachate – $BaCl_2$ [9]
Fe_AR	mg.kg^{-1}	Iron extracted with aqua regia [8]
Fe_KCl	mg.kg^{-1}	Iron extracted with KCl solution [10]
Fe_ox	mg.kg^{-1}	Iron extracted with oxalate [11]
Fe_dit	mg.kg^{-1}	Iron extracted with dithionite [12]
Al_$BaCl_2$	mg.kg^{-1}	Exchangeable cations (aluminium), leachate – $BaCl_2$ [9]
Al_AR	mg.kg^{-1}	Aluminium extracted with aqua regia [8]
Al_KCl	mg.kg^{-1}	Aluminium extracted with KCl solution [10]
Al_ox	mg.kg^{-1}	Aluminium extracted with oxalate [11]
Al_dit	mg.kg^{-1}	Aluminium extracted with dithionite [12]
Al (X) 1+	mg.kg^{-1}	Aluminium forms in KCl leachate [10]
Al (Y) 2+	mg.kg^{-1}	Aluminium forms in KCl leachate [10]
Al 3+	mg.kg^{-1}	Aluminium forms in KCl leachate [10]
VA	mmol.kg^{-1}	Exchangeable acidity Al+H [13]
Si_ox	mg.kg^{-1}	Silicon extracted with oxalate [11]
Si_dit	mg.kg^{-1}	Silicon extracted with dithionite [12]

The spectra were measured in samples treated to fine soil I in Petri dishes using a FieldSpec 3 spectrometer (ASD Inc., USA) with a High Intensity Contact Probe (*Fig. 1*). The range of the spectrometer is 350–2,500 nm.

The program Statistica 12 (StatSoft) was used to determine basic statistical descriptive characteristics. The program ViewSpec Pro 6.0 (ASD Inc.) was used to pre-process the spectral data, namely, to smooth the spectral curves (splice correction). The R program (R Core Team) was used to adjust the spectra using continuum removal. The programs Unscrambler X 10.3 (CAMO Software) and R (R Core Team) were used for their calibration (partial least squares regression, support vector machines, principal components regression).

The relationship between spectral features and soil properties, which were obtained using traditional laboratory methods, was evaluated statistically. The appropriateness of using different data preparation methods such as 1st and 2nd derivative or continuum removal (unification of spectral curves obtained with different instruments or under different light conditions) was tested. Published models for predicting soil characteristics from spectral features were tested, their parameters were adjusted, or new models were created using statistical methods of PLSR, PCR and SVM. For the statistical evaluation, not only all the data were used together, but they were also divided into subsets by sampling area and by horizon to describe the most appropriate data entry method for successful prediction. The effect of the spectral band used on the success of the prediction was also tested. Some properties are better predicted using the entire VNIR spectrum, while for others it is more appropriate to use only a selected spectral band, which is chosen either experimentally or based on the literature [14–17].

The new models have been validated. The reported predictions, expressed in terms of R^2 (coefficient of determination) and RMSE (root mean square error) values, are the result of the cross validation process in which the data set is divided into several subsets, one (10% of the whole) is removed and the remaining ones are used for model calibration. The model is then applied to the previously removed set, the values predicted by the model are compared with those measured in the laboratory. This is repeated for all subsets. The R^2 and RMSE parameters are then calculated. The model was calibrated for the groups formed in this way. Subsequently, the new models were subjected to external validation, in which the model was applied to a different data set and the success of the prediction was determined.

RESULTS AND DISCUSSION

Success of a method in predicting soil properties is highly dependent on the appropriate way of entering the input data, their statistical pre-processing and evaluation. The aim of this study was to find the most suitable combination of data entry method, statistical pre-processing, and spectral data processing to obtain the best results for soil property prediction.

The whole dataset and its division by horizons and regions

The first statistically evaluated dataset was the whole dataset regardless of sampling area or horizon. Spectra without pre-processing in the entire 350–2,500 nm range were used. The statistical method used was partial least squares regression (PLSR), which is often recommended in the literature. In *Fig. 2*, which shows all spectra together, we can see the large variability of their course. This may be due to different soil properties, e.g. different amounts of soil organic matter in the mineral and organic horizons.

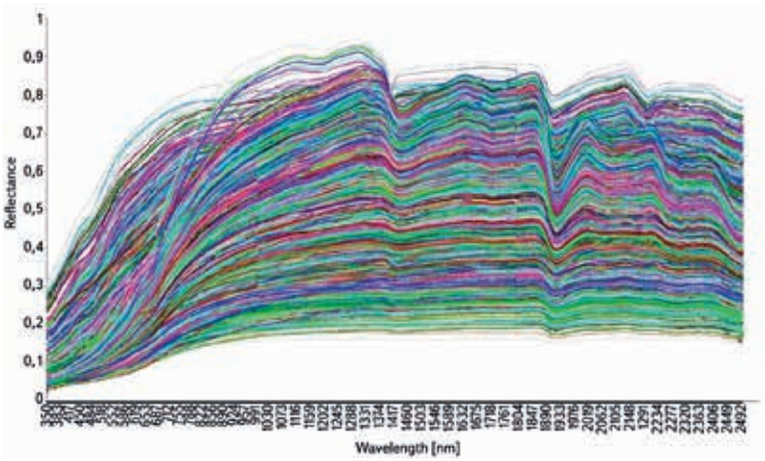

Fig. 2. Spectra representation – the summary data set

Properties common to as many measured samples as possible were sought. Specifically, it concerned the amount of oxidizable carbon – Cox, total nitrogen content and pH_$CaCl_2$. The results seem to be very good (Cox – R^2 = 0.92, nitrogen content – R^2 = 0.77, pH_$CaCl_2$ – R^2 = 0.51), but their publication would only be correct in the case of the pH_$CaCl_2$. According to the frequency distribution of the data of the individual properties, the normal distribution is only in the case of pH_$CaCl_2$. The results for oxidizable carbon and nitrogen content form two clusters. These give a high value of the coefficient of determination when fitted through the regression line. However, the results are biased and cannot be interpreted correctly. The pH_$CaCl_2$ prediction is more successful despite the lower value of the coefficient of determination. Since normal distribution of the data is a prerequisite for the application of PLSR, the set had to be subjected to a different statistical treatment.

Tab. 2. Predictions according to horizons

	R^2	RMSE
pH_$CaCl_2$ – whole set	0.51	0.46
N [mg.kg^{-1}] – whole set	0.77	0.31
pH_$CaCl_2$ – mineral horizons	0.32	0.44
pH_$CaCl_2$ – organic horizons	0.64	0.44
N [mg.kg^{-1}] – mineral horizons	0.44	0.11
N [mg.kg^{-1}] – organic horizons	0.37	0.25

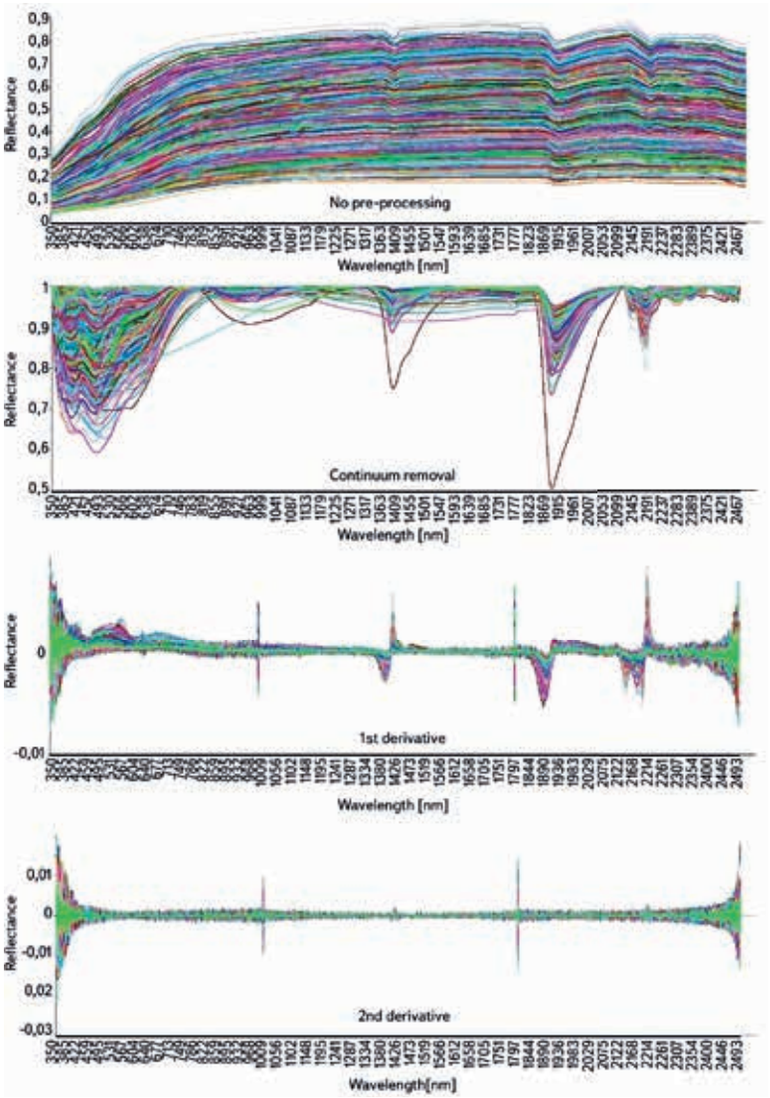

Fig. 3. The course of spectral curves – various pre-processing methods

Tab. 2 shows the results of the prediction of pH_$CaCl_2$ and nitrogen content using the whole set and when it is divided into organic and mineral horizons. It can be seen from the results that, in contrast to the previous results, the whole set shows a higher R^2 value, but the root mean square error (RMSE) increases along with it, although it should ideally decrease.

The preliminary results show that division of the dataset by sampling areas does not always provably increase the success rate of soil property prediction and, therefore, this data preparation method cannot be recommended unequivocally. The conclusion is more complicated when it comes to division of the data by soil horizon. In some cases, such a division appears to be more advantageous, while in other cases the prediction success rate, expressed by the coefficient of determination, is significantly better in favour of the undivided set. In such a situation, however, another variable describing the success of the prediction, the root mean square error, should be observed. The RMSE, unlike the coefficient of determination, should be decreasing, which does not happen in the above cases.

Tab. 3. The best predictions by method and band – summary

Property	Horizon (area)	Pre-processing	Statistical method	Spectral band [nm]	R^2 validation	RMSE validation
pH_H_2O	min. hor.	1st derivative	SVM	400–2,500	0.46	0.40
pH_$CaCl_2$	min. hor.	1st derivative	SVM	400–2,500	0.45	0.40
pH_$CaCl_2$	org. hor.	1st derivative, CR	SVM	400–2,500	0.72	0.39
pH_KCl	A horizons	1st derivative	SVM	400–2,500	0.55	0.12
Cox	min. hor.	1st derivative	SVM	400–2,500	0.68	1.85
Cox	org. hor.	1st derivative	SVM	400–2,500	0.84	3.71
Cox	A horizons	1st derivative	SVM	400–2,500	0.48	1.63
KVK	A horizons	None	PLSR	400–2,500	0.37	14.37
KVK	min. hor.	1st derivative	SVM	400–2,500	0.64	22.52
BS	min. hor.	1st derivative	SVM	400–2,500	0.44	20.65
N	min. hor.	1st derivative	SVM	400–2,500	0.57	0.10
N	org. hor.	1st derivative	SVM	400–2,500	0.62	0.19
P_M3	min. hor.	1st derivative	SVM	400–2,500	0.10	26.68
P_AR	org. hor.	1st derivative	SVM	400–2,500	0.34	243.91
K_M3	min. hor.	1st derivative	SVM	400–2,500	0.31	54.00
K_AR	org. hor.	1st derivative	SVM	400–2,500	0.57	657.13
K_$BaCl_2$	min. hor.	1st derivative	SVM	400–2,500	0.51	20.29
K_$BaCl_2$	A horizons	1st derivative	SVM	750–2,500	0.42	0.87
Ca_M3	min. hor.	CR	PLSR	1,100–2,500	0.36	687.14
Ca_AR	org. hor.	1st derivative	SVM	400–2,500	0.76	2,198.70
Ca_$BaCl_2$	A horizons	None	PLSR	1,100–2,500	0.33	0.19
Ca_$BaCl_2$	min. hor.	1st derivative	SVM	400–2,500	0.27	13.33
Mg_M3	min. hor.	CR	PLSR	1100–2,500	0.32	146.92
Mg_AR	org. hor.	1st derivative	SVM	400–2,500	0.43	1,303.50
Mg_$BaCl_2$	A horizons	1st derivative	PLSR	400–2,500	0.43	15.18
Mg_$BaCl_2$	min. hor.	1st derivative	SVM	400–2,500	0.32	3.00
Na_AR	org. hor.	1st derivative	SVM	400–2,500	0.23	40.40
Na_$BaCl_2$	min. hor.	1st derivative	SVM	400–2,500	0.35	0.18
Na_$BaCl_2$	A horizons	1st derivative	SVM	400–2,500	0.16	7.93
Mn_$BaCl_2$	min. hor.	1st derivative	SVM	400–2,500	0.28	1.49
Mn_$BaCl_2$	A horizons	1st derivative	SVM	400–2,500	0.51	32.22
Mn_AR	org. hor.	1st derivative	SVM	400–2,500	0.51	1,141.80
Mn_KCl	A horizons	1st derivative	SVM	400–2,500	0.48	58.28
Mn_ox	A horizons	CR	PLSR	400–2,500	0.56	107.65

Property	Horizon (area)	Pre-processing	Statistical method	Spectral band [nm]	R^2 validation	RMSE validation
Mn_dit	A horizons	1st derivative	SVM	400–750	0.55	121.04
Fe_$BaCl_2$	min. hor.	1st derivative	SVM	400–2,500	0.38	1.38
Fe_$BaCl_2$	A horizons	None	PLSR	400–2,500	0.65	44.59
Fe_AR	org. hor.	1st derivative	SVM	400–2,500	0.51	5,757.50
Fe_KCl	A horizons	None	PCR	400–2,500	0.67	68.64
Fe_ox	A horizons	None	PLSR	1,100–2,500	0.68	2,033.40
Fe_dit	A horizons	None	PLSR	750–2,500	0.69	2,370.50
Al_$BaCl_2$	min. hor.	1st derivative	SVM	400–2,500	0.59	14.99
Al_$BaCl_2$	A horizons	None	PLSR	400–800	0.58	120.53
Al_AR	org. hor.	1st derivative	SVM	400–2,500	0.70	2,395.20
Al_KCl	A horizons	None	PCR	400–2,500	0.62	106.41
Al_ox	A horizons	None	PLSR	400–2,500	0.63	617.01
Al_dit	A horizons	1st derivative	SVM	400–2,500	0.45	824.18
Al (X) 1+	A horizons	None	PCR	600–800	0.63	15.56
Al (Y) 2+	A horizons	1st derivative	SVM	1,100–2,500	0.44	19.21
Al 3+	A horizons	None	PCR	400–2,500	0.58	91.29
VA	min. hor.	1st derivative	SVM	400–2,500	0.58	16.58
VA	A horizons	None	PCR	400–2,500	0.49	16.64
Si_ox	A horizons	1st derivative	SVM	400–2,500	0.35	120.40
Si_dit	A horizons	2nd derivative	SVM	400–750	0.59	979.57

Organic and mineral horizons are fundamentally different in nature and different properties are usually determined for them in the laboratory. If some properties are determined together for the horizons of the whole soil profile, the differences are clearly visible. The data do not have a normal distribution (it is bimodal) and the results cannot be interpreted correctly. This preliminary conclusion was further verified using the SVM method, which is not as fundamentally sensitive to the data distribution as regression (linear) methods.

Effect of the statistical method used on the success of the prediction

The data were subjected to various combinations of pre-processing (no pre-processing, 1st and 2nd derivatives, continuum removal) and statistical methods (PLSR, PCR, SVM). An example of the change in the spectral curves according to the pre-processing method used is shown in *Fig. 3*. The two most effective combinations were always selected for each property and they were refined individually.

In their paper [18], Viscarra Rossel and Behrens identified SVM and PLSR as the two most successful methods. The results of this study confirm this, especially in favour of SVM, and provide additional information by combining these methods with different pre-processing methods. In most cases, the highest prediction success was found when combining the 1st derivative of spectral data and SVM, followed by PLSR on data without pre-processing and SVM after continuum removal. Another successful combination in some cases was the use of the 2nd derivative and SVM. In contrast, regression methods applied to data pre-processed with the 2nd derivative were clearly the least successful. The regression methods of PLSR and PCR provide very similar results, mostly in slight favour of PLSR.

Prediction of individual properties

Based on the literature [14, 15, 17] and the above findings, the best combinations of the type of pre-processing used, the statistical method and, more recently, the spectral band selected were sought. For each property, the most successful combinations of methods were selected according to previous findings and subjected to further testing. The modification of the spectra by clipping the 350–400 nm band, which is significantly interfered by noise at the UV-visible interface, was common to all properties. In general, the combination of the 1st derivative spectral data pre-processing method and the support vector machine statistical method using the entire VNIR spectral band (400–2,500 nm) appears to be the best. However, there are cases where other combinations of methods and other (narrower) spectral bands have proven to be most appropriate. For

Tab. 4. The best versatile statistical models for the prediction of individual properties

Property	Pre-processing	Statistical method	Spectral band [nm]
pH_H_2O	1st derivative	SVM	400–2,500
pH_$CaCl_2$	1st derivative	SVM	400–2,500
pH_KCl	1st derivative	SVM	400–2,500
Cox	1st derivative	SVM	400–2,500
KVK	1st derivative	SVM	400–2,500
BS	1st derivative	SVM	400–2,500
N	1st derivative	SVM	400–2,500
P	1st derivative	SVM	400–2,500
K	1st derivative	SVM	400–2,500
Ca	1st derivative	SVM	400–2,500
Mg_M3	continuum removal	PLSR	1,100–2,500
Mg_AR	1st derivative	SVM	400–2,500
Mg_vym ($BaCl_2$)	1st derivative	SVM	400–2,500
Na	1st derivative	SVM	400–2,500
Mn_AR, KCl	1st derivative	SVM	400–2,500
Mn_ox	continuum removal	PLSR	400–2,500
Mn_dit	1st derivative	SVM	400–750
Fe_vym ($BaCl_2$)	1st derivative	SVM	400–2,500
Fe_AR	1st derivative	SVM	400–2,500
Fe_KCl	1st derivative	SVM	400–2,500
Fe_ox	No pre-processing	PLSR	1,100–2,500
Fe_dit	No pre-processing	PLSR	750–2,500
Al_vym ($BaCl_2$)	1st derivative	SVM	400–2,500
Al_AR	1st derivative	SVM	400–2,500
Al_KCl	No pre-processing	PLSR	400–2,500
Al_ox	No pre-processing	PLSR	400–2,500
Al_dit	1st derivative	SVM	400–2,500
Al (X) 1+	No pre-processing	PCR	600–800
Al (Y) 2+	2nd derivative	SVM	1,100–2,500
Al 3+	No pre-processing	PLSR	400–2,500
VA	1st derivative	SVM	400–2,500
Si	1st derivative	SVM	400–2,500

example, calcium and magnesium determined in the aqua regia leachate were best predicted by the PLSR method applied to spectral data modified using the continuum removal function in the near-infrared region of the 1,100–2,500 nm spectrum. In most cases, the PLSR method (Mg, Mn, Fe, Al) instead of SVM was best for the elements determined in oxalate. The diversity of the models was particularly observed in the case of iron and aluminium prediction, i.e. for two elements that are highly monitored in forest soils. The spectral detectability of the different forms of aluminium varies considerably. The least successfully predicted divalent form, which binds to organic matter but is present in extremely small amounts, can alternatively be predicted by subtracting the content of the monovalent and trivalent complexes from the total content determined in a common leachate, in this case it is the KCl leachate. *Tab. 3* shows the best models for predicting each soil property, including the validation R^2 and RMSE. The set is divided by the soil horizon or group of horizons.

Testing and modification of found models

The found models were also applied to independent data sets. The prediction success rates of each property before and after the models´ application were compared. The data used as those "before model application" were subjected to standard statistical processing, i.e., the PLSR method across the whole VNIR band on the non-pre-processed spectra. The models that improved the prediction results were found to be appropriate and universal. In cases the prediction success increased very little, remained unchanged, or even decreased, other models were sought based on existing knowledge.

Tab. 4 shows the best models for predicting forest soil properties. In addition to the success of the prediction, emphasis was put on the versatility of the models. In case a property was determined in various ways, but the model is common to all these ways, only the given property is indicated in the table. If the determination method had an impact on the spectral detectability and therefore required the use of a different model, the properties are described individually together with the determination method.

CONCLUSION

The aim of the study was to objectively evaluate the applicability of spectroscopy in the visible and near-infrared region of the spectrum for predicting forest soil properties. These soils differ fundamentally from agricultural soils in their appearance, development, physical and chemical processes, presence of organic horizons, etc. They are also usually monitored for different properties. It has been found that the division of the data set by sampling area is not a significant input criterion; the distribution of the data is more important. Due to the large differences between organic and mineral horizons, it is recommended, on the basis of the results, to examine these horizons separately.

As a large amount of data was available, it was possible to split the data into a larger training set, on which the models were trained thoroughly one by one, and a testing set, on which the models were tested and further adjusted based on the results if necessary. In this way, the most appropriate combinations of statistical pre-processing and processing methods in specific spectral bands were found for each soil property. The combination of 1st derivative and support vector machine in the whole VNIR spectral band (400–2,500 nm) is generally found to be the most successful. However, in some cases, other models have proven successful. The best predictable properties ($R^2 > 0.6$) include soil pH, and the contents of oxidizable carbon, aluminium, iron, silicon, or calcium (at higher concentrations). Not very high prediction success ($R^2 < 0.3$) was found for parameters that take on low values (the content of sodium, manganese, or divalent aluminium complexes).

The results show that VNIR spectroscopy is a useful method for the prediction of forest soil properties. It cannot completely replace classical analysis, but it can complement it. For example, in soil mapping, it can help to thicken the data network and refine the information better than other spatial estimation methods. It can be used in cases where large amounts of data are needed in a short time frame and at minimum cost. It is suitable for monitoring trends over time or for rapid examination of samples from an area.

Acknowledgements

The authors would like to thank the Department of Soil Science and Soil Protection at the Czech University of Life Sciences in Prague for providing technical equipment and assistance in the preparation of this study, which was carried out as part of PhD studies.

References

[1] KOOISTRA, L., WEHRENS, R., LEUVEN, R. S. E. W., BUYDENS, L. M. C. Possibilities of Visible-Near-Infrared Spectroscopy for the Assessment of Soil Contamination in River Floodplains. *Analytica Chimica Acta*. 2001, 446, p. 97–105.

[2] JIANG, Q. et al.: Estimation of Soil Organic Carbon and Total Nitrogen in Different Soil Layers Using VNIR Spectroscopy: Effects of Spiking on Model Applicability. *Geoderma*. 2017, 293, p. 54–63.

[3] MARTENS, H., NAES, T. Multivariate Calibration, 2nd ed. Chichester, UK: John Wiley and Sons Ltd, 1989. 419 p.

[4] ZBÍRAL, J. Analýza půd I. Brno: Ústřední kontrolní a zkušební ústav zemědělský, 2002. 197 p.

[5] WHITE, R. E. On the Measurement of Soil pH. *Journal of the Australian Institute of Agricultural Science*. 1969, 35, p. 3–14.

[6] GILLMAN, G. P., SUMPTER, M. E. Modification of the Compulsive Exchange Method for Measuring Exchange Characteristics of Soils. *Australian Journal of Soil Research*. 1986, 17, p. 61–66.

[7] SHEPHERD, K. D., WALSH, M. G. Development of Reflectance Spectral Libraries for Characterization of Soil Properties. *Soil Science Society of America Journal*. 2002, 66, p. 988–998.

[8] *ISO 11466:1995. Soil Quality — Extraction of Trace Elements Soluble in Aqua Regia. ISO/TC 190/SC 3 Chemical and Physical Characterization*. 1995-03.

[9] BERNHARDT, C. Particle Size Analysis – Classification and Sedimentation Methods. London: Springer, 1994. 428 p.

[10] DRÁBEK, O., BORŮVKA, L., MLÁDKOVÁ, L., KOČÁREK, M. Possible Method of Aluminium Speciation in Forest Soils. *Journal of Inorganic Biochemistry*. 2003, 97, p. 8–15.

[11] COURCHESNE, F., TURMEL, M. C. Extractable Al, Fe, Mn and Si. In: CARTER, M. R., GREGORICH, E. G. (eds.), *Soil Sampling and Methods of Analysis*. 2nd ed. Canadian Society of Soil Science. CRC Press, 2008, p. 307–315.

[12] MCKEAGUE, J. A., BRYDON, J. E., MILES, N. M. Differentiation of Forms of Extractable Ion and Aluminum in Soils. *Soil Science Society of America Journal*. 1971, 35, p. 33–38.

[13] GILLMAN, G. P., SUMPTER, M. E. Modification of the Compulsive Exchange Method for Measuring Exchange Characteristics of Soils. *Australian Journal of Soil Research*. 1986, 17, p. 61–66.

[14] VISCARRA ROSSEL, R. A., WALVOORT, D. J. J., McBRATNEY, A. B., JANIK, L. J., SKJEMSTAD, J. O. Visible, Near Infrared, Mid Infrared or Combined Diffuse Reflectance Spectroscopy for Simultaneous Assessment of Various Soil Properties. *Geoderma*. 2006, 131, p. 59–75.

[15] BROWN, D. J., SHEPHERD, K. D., WALSH, M. G., MAYS, M. D., REINSCH, T. G. Global Soil Characterization with VNIR Diffuse Reflectance Spectroscopy. *Geoderma*. 2006, 132, p. 273–290.

[16] BILGILI, A. V., VAN ES, H. M., AKBAS, F., DURAK, A., HIVELY, W. D. Visible-Near Infrared Reflectance Spectroscopy for Assessment of Soil Properties in a Semi-Arid Area of Turkey. *Journal of Arid Environments*. 2010, 74, p. 229–238.

[17] GHOLIZADEH, A. et al. Soil Organic Carbon Estimation Using VNIR–SWIR Spectroscopy. The Effect of Multiple Sensors and Scanning Conditions. *Soil and Tillage Research*. 2021, 211. ISSN 0167-1987.

[18] VISCARRA ROSSEL, R. A., BEHRENS, T. Using Data Mining to Model and Interpret Soil Diffuse Reflectance Spectra. *Geoderma*. 2010, 158, p. 46–54.

The authors

Ing. Josef Kratina, Ph.D.
✉ josef.kratina@vuv.cz
ORCID: 0000-0001-6095-586X

Ing. Bc. Václava Maťašovská
✉ vaclava.matasovska@vuv.cz
ORCID: 0000-0001-9229-463X

T. G. Masaryk Water Research Institute, Prague

The paper has been peer-reviewed.

DOI: 10.46555/VTEI.2021.11.003

Practical examples of using GIS in hydrology at the Czech Hydrometeorological Institute

PETR ŠERCL, RADOVAN TYL, PAVEL KUKLA, MARTIN PECHA

Keywords: GIS — hydrology — watershed divide — physical-geographical characteristics — flash floods

SUMMARY

GIS technologies are widely used in the Hydrology Department of the Czech Hydrometeorological Institute (CHMI). The processing of geospatial data, which are used in hydrology for analytical tasks, and the development of GIS technologies in the last two decades have contributed to the spread of GIS in the CHMI practice. The use of GIS tools is shown in four examples.

The first one focuses on the creation of GIS data. One of the basic source materials for analytical work in hydrology is the polygon layer of four-order watershed divides. Since 2018, these data have been updated, or re-created, on the basis of the *Digital Relief Model 5th Generation* (DMR 5G) and the updated Polyline layer of watercourses ZABAGED (Basic Geographic Data Base), the geometry and attributes of which are harmonised in cooperation with the watercourse administrators, Czech Geodetic and Cadastral Office and T. G. Masaryk Water Research Institute.

The second example concerns the preparation of input source data for the derivation of the hydrological characteristics of *M-day* discharge, which, according to Czech Standard 75 1400 *Surface water hydrological data*, are among the basic hydrological data. The example describes the procedure of deriving a raster layer of long-term annual runoff for the reference period 1981–2010. In this case, a regression relationship between the average annual runoff depth, average annual precipitation, and the average annual amount of potential evapotranspiration over the period was used.

The third example describes the use of GIS in the preparation of hydrological assessments according to the above-mentioned standard (75 1400), which usually result in *M-day* or *N-year-flood* discharges in a specified profile of a certain watercourse. For this purpose, a special application has been developed that allows not only to derive the basic physical-geographical characteristics of the watershed from the digital relief model (watershed slope, length and slope of thalweg), but also to determine other necessary characteristics, e.g. the proportion of a certain type of land use in the watershed or the average values of other watershed features (precipitation, CN – runoff curve numbers, etc.).

The fourth example focuses on the use of GIS in operational hydrological service, specifically in the development of the Flash Flood Indicator, which determines the level of risk of flash flood formation or occurrence based on current land saturation and radar rainfall estimates. The scripting and development tools that GIS offers are mentioned here.

INTRODUCTION

Since the data provided by the CHMI have its spatial component, it is impossible to imagine the Institute´s operation without the application of GIS technology. For a long time, GIS has been used not "only" to produce simple static map outputs, but mainly as a tool for data processing and analysis. The trend is to move away from static maps on the CHMI website and in publications, which of course remain a standard part of the use of GIS technology, to dynamic web maps, which have added value in the form of, for example, displaying additional information on map features, searching by addresses or other attributes, zoom tools and possibly other tools integrated into web map applications.

The use of GIS technology in the hydrology of the CHMI is demonstrated in four specific examples in separate chapters. The examples include sophisticated data acquisition in a multi-user database, derivation of raster data from point observations, preparation of data for hydrological modelling and hydrological assessment processing, and demonstration of the use of scripting tools to create automatically launched tasks that include the process from data retrieval, subsequent processing and publication of results in a web environment.

That the path to the above was quite difficult and lengthy is described in the following chapter on history.

HISTORY OF USING GIS IN HYDROLOGY OF THE CZECH HYDROMETEOROLOGICAL INSTITUTE

The GIS technology appeared in the CHMI in the late 1990s, based on the international project "*Monitoring and information resources management*" funded by the U.S. Environmental Protection Agency (EPA) in 1993-1997. As part of the project, the CHMI Hydrology Department received for free an AV 400 workstation and ArcView and ARC/INFO software licenses (UNIX platform), including system support and training opportunities. The CHMI staff also visited the EPA centre in the USA.

In the initial period, i.e. 1993–1995, GIS was only a peripheral issue in the CHMI hydrology, as it was concentrated in a single workplace and an institute-wide computer network had not yet been built to make the data available to more staff.

A significant improvement of the situation occurred in 1996 and 1997, when the institute-wide computer network was completed and the purchase of additional ArcView licenses together with the necessary hardware improvements led to the expansion of GIS users not only at the central Hydrology Department in Prague, but also at selected branches. These other GIS sites, which were gradually built up during this period, were already PC-based (ArcView, Windows 95 or Windows NT). Thus, as is clear from the above, the GIS technology used in the CHMI hydrology from the very beginning was the ESRI technology.

Data layers, either vector or raster, are essential for working with GIS of course. Compared to the present, there was a shortage of data usable in GIS, especially detailed data that would allow sophisticated analysis.

In 1994, under a grant from the Ministry of Environment of the Czech Republic, the data layers DMÚ200 (vector data 1 : 200,000: waters, roads and railways, energy infrastructure, administrative arrangement, etc.) and DMR-2 (digital relief model, 100 × 100 m raster) were acquired under a contract with the then Military Topographic Institute in Dobruška[1]. The digital equivalent of topographic maps (DETM) in the form of TIF files at scales of 1 : 50,000, 1 : 500,000, 1 : 1,000,000 and 1 : 2,000,000 was also obtained under the contract with the Military Topographic Institute. While the acquisition of these data was significant, the degree of resolution did not allow for significant analysis.

Therefore, the acquisition of GIS data layers within the CHMI working capacities started in 1997. These were mainly point layers of surface-water and groundwater observation objects and rainfall gauge observations. The most extensive work was carried out in the acquisition of a polygon layer of watershed divides of basic watersheds[2] (scale 1 : 25,000, polygon area from 5 km^2), in which the CHMI branch offices also participated. The course of the watershed divides had to be first drawn on paper military topographic maps 1 : 25,000 and then digitised.

Once the watershed divide layer was processed, it was possible to perform more detailed analyses and create the first applications using the Avenue programming language that was part of ArcView GIS version 3.x. One of the first applications was the interpolation of point measurements (rainfall) with the incorporation of their regression dependence on the elevation (using the ArcView Spatial Analyst extension), and therefore the first creation of own derived raster data that could be further analysed, e.g. by applying zonal statistics to the watershed area.

A major breakthrough was the acquisition of a digital version of the military topographic maps called DMU25 (Digital Territory Model at a scale of 1 : 25,000) in 2001. This version contained vector layers of feature positions, but also elevation in the form of contour lines. Using the contour line layer, it was not only possible to refine the watershed divide layer of the basic watersheds, but also, based on it, to derive a raster terrain elevation layer with a resolution of 25 × 25 m. This more detailed terrain model (DMR) already allowed its analysis and, in particular, the derivation of the watershed´s physical-geographical characteristics, which include the average watershed slope, the slope and length of the thalweg and other important inputs for hydrological calculations.

Another major milestone in the acquisition of GIS data was the research projects QD1368 "*Verification of methods for deriving hydrological source data for assessing the safety of hydraulic structures during floods*" (2001–2004) and R&D 1D/1/5/05 "*Development of methods for predicting drought and flood situations based on infiltration and retention properties of the land cover in the Czech Republic*", which ran from 2004 to 2007. Within the project QD1368, raster layers of N-year maximum precipitation of 1-, 2- and 3-days duration were derived in cooperation between hydrologists and the CHMI Climatology Department. Other very important data for hydrological modelling were obtained in cooperation with the Research Institute of Land Reclamation and Soil Protection in Zbraslav and in the framework of the above-mentioned research projects, namely vector layers of infiltration capacity and water retention capacity of soils (1 × 1 km resolution), which resulted in a layer of so-called hydrological soil groups. Combined with the updated land use vector layer from the European CORINE (Corine Land Cover) project, it was possible to derive a raster layer of CN (Curve Number) values, which is a key parameter for determining runoff depth from rainfall [1]. The acquisition of these data enabled the full preparation of inputs to hydrological rainfall-runoff modelling and the preparation of hydrological assessments, which is the subject of a separate chapter. The ArcView GIS 3.x software was gradually replaced by the more modern ArcGIS Desktop at the end of the first decade of the 21st century.

Since January 2013, ZABAGED data have become the primary digital GIS foundation, from which – or rather on top of which – new layers of DMR and watershed divides of basic watersheds have been derived or updated. In parallel with the production of the updated Corine Land Cover layers, the raster layers of CN values were also updated. The watershed divides over the ZABAGED data were used in the preparation of so-called *M-Day* discharge cadastre.

Currently (November 2021), the layer of watershed divides of basic watersheds is being refined, using the Digital Relief Model of 5th Generation (DMR 5G) and the verified layer of waters, i.e. watercourse lines and water area polygons from the Czech Geodetic and Cadastral Office, as a basis.

The use of GIS has not left aside the web GIS technology in the CHMI. The ArcGIS Online product is used for publishing dynamic map outputs for the public and ArcGIS Enterprise, Standard version, was purchased for sharing GIS data within the CHMI.

ADMINISTRATION OF THE 4TH ORDER WATERSHED DIVIDE DATASET

The watershed area is the basic and necessary source for the derivation of standard and non-standard hydrological data according to the Czech standard 75 1400 *Surface water hydrological data*. The watershed area is delimited by a watershed divide, which is an imaginary boundary separating two adjacent watersheds, or an orographically defined area from which water flows to the respective outlet section.

The first subdivision of watercourses according to hydrological sequence was made as part of the preparation of the Hydrological Conditions of the Czechoslovak Socialist Republic in 1965. Here, watercourses with their own developed beds and a watershed area greater than 5 km^2 were singled out [2]. The hydrological subdivision is presented in the tabular summary of the publication and in the attached maps at a scale of 1 : 200,000 (see *Fig. 1*). The overview of the basic watershed areas also includes information on the name of the watercourse, its order, its length, shape of the watershed, forest cover and whether it is a left or right tributary. At that time, the hydrological order number was in the format of eight digits (1-22-33-444), which determined the watercourse´s affiliation to the European watershed divides (the Elbe, Danube, Vistula, Oder) and to more detailed sub-watersheds. This also defined the division of the hydrological arrangement of the watercourses into individual orders (i. e. first- to fourth-order watersheds).

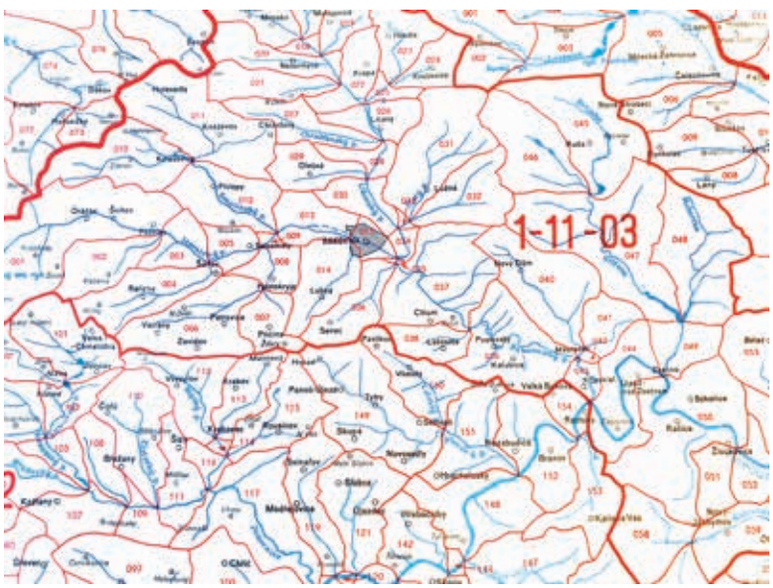

Fig. 1. Map of watershed divides in the book *Hydrologické poměry* [2]

Since then, there have been three major updates to the watershed divide dataset. First was the digitization of the 1 : 25,000 scale watershed divides from military topographic maps. At the same time, the hydrological arrangement number was expanded by one digit to nine positions (1-22-33-4444). The second update was carried out in 2008–2012, when the DIBAVOD (Digital Water Data Base) structure of watercourses was used for the 1 : 10,000 reference scale and the hydrological arrangement number was simultaneously extended to the current 14 digits (1-22-33-4444-5-66-77). This made it possible to structure the division of watersheds to the profiles of hydrological structures´ dams, out-of-level crossings and to the profiles of water gauging stations. The update was performed over an expanded set of fourth-order watersheds, from which the lower-order watershed divides are subsequently generated by the primary key, which is the hydrologic arrangement number.

The last update of the watershed divide dataset started after the completion of the DMR 5G and refinement of the watercourse layer based on aerial laser scanning at the Czech Geodetic and Cadastral Office in early 2018. The ESRI platform with all its components and database-desktop application-server links was used to update the watershed divides.

The actual editing/updating of the watershed divides is done through the ArcGIS Pro desktop application, Advanced license, at the hydrology departments of the CHMI branches and at the Surface Water Department of the CHMI central office. All necessary source data are stored in the Oracle database with ESRI SDE superstructure and shared via ArcGIS Enterprise. Its use through the SDE database or ArcGIS Enterprise ensures the up-to-dateness and consistency of data across the different processors. There is no need to split the watershed divide layer into individual parts based on the territorial scope of the branches and merge them back together after updating. The editing is done over one whole layer. Topological rules are set over the watershed divide dataset in the SDE database to ensure homogeneity of the edited data. Aerial photographs and the 1 : 10,000 base map provided as services of the Czech Geodetic and Cadastral Office´s ArcGIS Server are used, too. Binding work instructions have been created to ensure a uniform workflow for updating the fourth-order watershed divide dataset across branches. All data are converted and used in the WGS 1984 UTM 33N coordinate system.

The primary source for updating the fourth-order watershed divides is the Digital Relief Model Generation 5 (DMR 5G) of the Czech Geodetic and Cadastral Office with a 2 × 2 m raster resolution. Other necessary supporting sources include information on the structural and geometric layout of the watercourses. The geometry of the watercourses is taken from the data of ZABAGED state mapping work. The structure of the backbone watercourses is also determined by the ZABAGED watercourse dataset. The differences between the Central Watercourse Register dataset, which is used by watercourse administrators and the state enterprise Forests of the Czech Republic, and the ZABAGED watercourse layer are solved within harmonization of backbone watercourses covered by the "*ISVS Water*" project. The agreed changes are then incorporated into the ZABAGED watercourse dataset in approximately six-month cycles.

Other ZABAGED layers are indispensable sources, such as water areas, culverts or a point layer called "*River network nodal point*", where information on crossings, confluences, springs, or pseudo-conjunctions (fictitious confluences or crossings) of watercourses are included in the attributes. At the same time, other data sources provided within harmonization of backbone watercourses covered by the "*ISVS Water*" project are used, especially foreign watercourses mediated by the Czech Geodetic and Cadastral Office and the Main Drainage Facilities dataset from the State Land Office.

In the territory of the Capital City of Prague, data on the storm sewer network and adjacent drainage areas of the Prague Water Management Authority and detailed data on watercourses managed by the Department of Environmental Protection of the Capital City of Prague are also used to update the watershed divides.

One of the main and most important bases for the creation of watershed divides are contour lines. Since contour lines derived from the DMR 5G from the Czech Geodetic and Cadastral Office are currently not available for the whole territory of the Czech Republic, the watershed divides are updated over contour lines generated "on the fly" with the same parameters at all branches using the raster tool "Contour" in ArcGIS Pro. This is *de facto* a raster layer that is redrawn dynamically according to the map scale. Based on the analyses, the basic scale for updating the watershed divides was set at 1 : 1,000 to match the accuracy of the digital relief model and, at the same time, to correspond to further processing of hydrological data. Nevertheless, when updating watershed divides in certain areas, editing at a higher resolution than the established scale is necessary.

The second necessary basis for updating the watershed divides is the shaded relief that is generated dynamically as well as the contour lines over the DMR 5G using the raster analysis "Hillshade".

The Hydrologic Raster Analysis Toolkit uses the selected digital relief model to calculate and determine the hydrologic features of the watershed – including the river network and watershed divides. It is difficult to determine the correct course of watershed divides in some flat areas of the Czech Republic, so an extension in the form of a toolbox called HydroDEM was developed and incorporated into ArcGIS Pro by the Surface Water Depatment. This tool allows the automatic generation of watershed divides using DMR 5G raster analyses while defining boundary conditions (parameters and layers used). However, the automatically generated watershed divide is derived purely on top of the digital relief model and does not take into account anthropogenic interventions on watercourses, such as artificial flumes, off-channel crossings, underground sections or culverts that divert water under elevated roads. Therefore, the automatically generated watershed divide serves as an auxiliary tool in the actual updating of the watershed divide layer.

The process of updating the watershed divide dataset using DMR 5G is being funded under the institutional support for long-term conceptual development and will continue in 2022. The update is expected to be completed in late 2022. In the subsequent period, we expect to update the watershed divide dataset on an approximately annual cycle by incorporating changes related to changing watercourse structure impacting the watershed divide structure.

PREPARATION OF INPUT SOURCE DATA FOR DERIVATION OF M-DAY DISCHARGES

The *M-day* discharges, according to Czech standard 75 1400 *Surface water hydrological data,* are among the basic hydrological data provided for any river network profile. They are always determined for a specific reference period.

The calculation of the hydrological characteristics of the *M-day* discharges for the reference period 1981–2010 was preceded by the derivation of several climatological characteristics. The primary climatic factor that has the greatest influence on runoff patterns is precipitation. The long-term annual rainfall over a watershed is the amount of water from precipitation falling on the surface of a given area over a given time interval. It is expressed as the height of the water layer (in millimetres) distributed uniformly over the area.

The long-term annual rainfall over a watershed is one of the basic climatological and hydrological characteristics determining the long-term hydrological balance of the watershed. It can be determined using GIS tools by overlaying a polygon layer of watershed divides over a raster layer of rainfall derived from observations at rainfall gauging stations.

Therefore, deriving a raster of long-term annual precipitation using the maximum available data was one of the main objectives of the processing. The methodology for deriving the average annual rainfall for the reference period at the rainfall gauging stations is described in detail in reference [3].

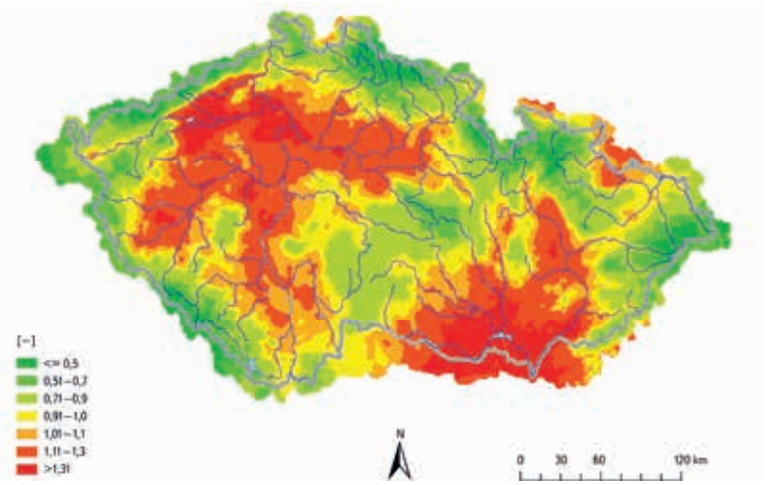

Fig. 2. Aridity index for the period 1981–2010

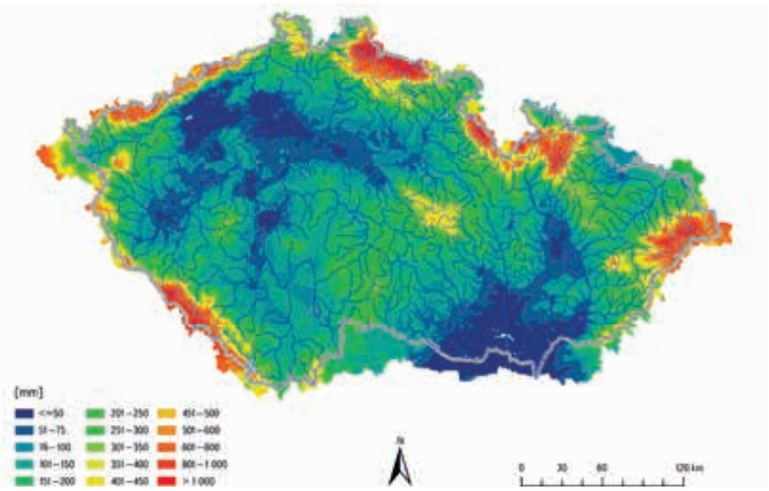

Fig. 3. Long-term annual runoff for the period 1981–2010 obtained from regression relationships between long-term average annual rainfall totals and long-term annual potential evapotranspiration

The point data of long-term annual rainfall were interpolated to a raster layer using the orographic interpolation method developed at the CHMI [4]. A raster of terrain elevations at a 1 × 1 km step smoothed[3] in the vicinity of 3 × 3 km was used as a basis. The advantages of the method used include the simplicity of use and the identification of regression relationships on a local (regional) level, while the disadvantage is the derivation of purely linear regression relationships where the magnitude of precipitation depends on only one variable. However, the use of smoothed terrain partially eliminates this disadvantage, because by smoothing the terrain, stations of the same elevation but representing completely different climatic conditions, e. g. Milešovka and Pec pod Sněžkou, are given different "relative" elevations due to average elevation change in relation to their surroundings.

A great contribution to the derivation of the raster layer of long-term annual rainfall was the use of data from foreign sources, which helped to refine the data in border areas, especially in the area of the Šumava and Krušné Mts., as well as in foreign territories where a significant part of Czech rivers´ watersheds lie (e. g. the Ohře, the Dyje).

By deriving the long-term annual rainfall together with the value of the long-term annual potential evapotranspiration, the so-called aridity index (see *Fig. 2*), which is the ratio of the annual potential evapotranspiration to the annual rainfall, can be calculated. This index is the basis for estimating the long-term runoff depth on unobserved watersheds.

Data from 234 climatological stations with at least eight years of observation were used to derive the annual potential evapotranspiration raster for the period 1981–2010. First, monthly potential evapotranspiration values were calculated, and the annual sums were derived. The shorter series were complemented by means of the linear regression method using the analogue (stations with a complete series of observations) with the highest coefficient of determination.

Using orographic interpolation [4], a raster of annual potential evapotranspiration was derived for each year from the 1981–2010 period in a GIS environment and a raster of mean values for 1981–2010 was calculated.

The methodology for deriving the long-term annual runoff for the period 1981–2010 using regression relationships from the long-term average annual rainfall and long-term annual potential evapotranspiration is described in [3]. The derivation used map algebra functions applied to the above-mentioned raster layers of climatological features. The resulting map of long-term annual runoff depth is shown in *Fig. 3*.

ELABORATION OF HYDROLOGICAL ASSESSMENTS

Hydrological assessments mean the provision of standard hydrological data according to Czech standard 75 1400 *Surface water hydrological data*. The standard hydrological data include, *inter alia*, the time series of hydrological variables observed at the gauging stations, the previously mentioned *M-day* discharges, *N-year* discharges and theoretical flood waves with peak flow rate of a given recurrence interval. Unlike the time series, the *M-day* and *N-year* discharge values and theoretical flood waves are provided for any river network profile. This fact, i. e., providing data for any river network profile, has led to the use of GIS technology to derive physical and geographic characteristics of the watershed and other variables that serve as the basis for determination of standard hydrological data in unobserved profiles.

The third generation of the application has been used for these purposes, successively called AVPosudek (for ArcView GIS 3.x), AGPosudek (for ArcGIS Desktop), and AGPosudek Pro (for ArcGIS Pro), with the functionality of each version of the applications being modified and developed as needed. The following description will cover the latest generation of this application, namely AGPosudek Pro.

AGPosudek Pro is an application in the form of an add-in for ArcGIS Pro developed in VB.NET using the ArcGIS Pro SDK for Microsoft.NET. Creating add-ins is facilitated by the integration of SDK into Microsoft Visual Studio and

Fig. 4. ArcGIS Pro window with a map showing the watershed, contour lines and watercourses being assessed

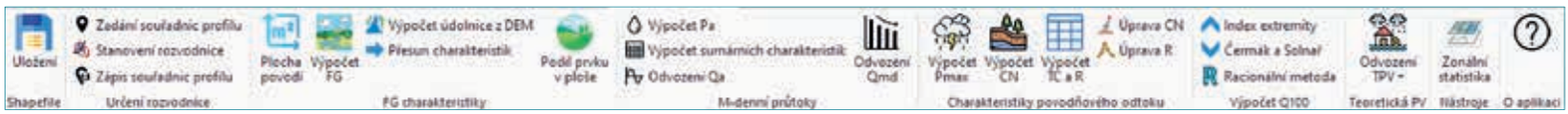

Fig. 5. AGPosudek Pro application ribbon bar

templates for the individual objects that make up the application (dialog windows and other controls). It is available at https://pro.arcgis.com/en/pro-app/latest/sdk/ (verified on November 5, 2021), including a large number of examples that are, however, written in C#. There is a C# converter for VB.NET, available at https://codeconverter.icsharpcode.net/ (verified on 5 November 2021).

Fig. 4 shows a cut-out of an ArcGIS Pro window with the AGPosudek Pro add-in loaded. The window shows a map with the watershed divide layer of the watershed under assessment for the profile shown by the point. It also shows detailed watershed divides of the basic watersheds, ZABAGED contour lines, and ZABAGED watercourses. A ribbon bar showing the various application tools is in *Fig. 5*.

The creation of a full version of the ArcGIS Pro application was only possible in version 2.6, which enabled the incorporation of user graphics (points, lines and polygons) into the map graphics layer.

The functionality of AGPosudek Pro can be briefly summarised as follows:

- Saving the selected watershed polygon: the user selects from the basic watershed divides layer a watershed polygon in which to process the assessment and saves it in a separate shapefile.
- Determination of the watershed divide: Based on the coordinates (usually in S-JTSK), the user plots a profile on the watercourse as a point on the map in the graphics layer and plots the line of the watershed divide that passes through the point in the graphics layer. Then, using the "Determine watershed divide" tool, the user splits the polygon in the shapefile of the selected watershed. The user can delete the downstream part of the watershed (below the profile) and continue working only with the polygon of the watershed to the profile under consideration. All results of the tools below are written in the attribute table of the selected watershed layer.
- Calculation of the watershed area: The watershed polygon area is recalculated from the map projection to the ETRS89 / LAEA Europe planar projection (code 3035).
- Calculation of physical-geographical characteristics: The tool calculates the average slope of the watershed based on the selected DMR layer and, if the thalweg line is plotted, it also calculates its length and slope. The tool uses the GIS function "Slope" inter alia.


Fig. 6. Hand-drawn (black arrows) and calculation-derived (green line) thalweg

- Deriving the thalweg line from the DMR: Based on the selected DMR layer, a line is derived that connects the outlet section and the hydraulically furthest point in the watershed. The tool uses the GIS hydrological functions (Flow Direction, Flow Accumulation, Flow Length, etc.) and the CostPath function, see *Fig. 6*[4]. The length and slope of the thalweg are also calculated. In addition to an attribute table, the results are displayed in dialogue windows from where the user can copy them into any document.
- Calculation of the feature´s share in the area: Based on the Corine Land Cover layer, the tool calculates the proportion of the area of the selected land cover to the watershed total area. It is most used to calculate the proportion of the area covered by forests. The tool uses the GIS function "Tabulate Area".
- The application also uses the zonal statistics function based on the selected raster layer, e.g. to calculate average values per a watershed. These are the average long-term annual rainfall, the N-year maximum rainfall of a given duration, the CN value, etc.
- Other functions of the application are used to derive specific hydrological characteristics, e.g. 100-year flow values, using various methods. For this purpose, the results of the previous tools are used to derive physical-geographical characteristics, average N-year rainfall values, CN values, forest cover ratio, etc.

The AGPosudek and the new AGPosudek Pro applications are used by hydrologists preparing assessments at the CHMI branch offices.

FLASH FLOOD INDICATOR

The operational hydrological service, called the Flood Forecasting Service, issues important outputs for the public. They are available on the website https://hydro.chmi.cz/hpps/ (verified on 7 November 2021).

A flood event that is both potentially dangerous and difficult to predict is flash flooding. It is not possible to accurately predict both the time and place of occurrence of a flash flood because the location and time of the causative factor, which is torrential rainfall, are difficult to predict. Despite these difficulties, it is possible to monitor and evaluate in real time certain parameters and phenomena from which the level of risk of flash flooding occurrence or localised flooding can be assessed.

One of these phenomena is the level of current soil saturation. If the soil is more saturated, it can hold less water and its infiltration capacity is reduced. Therefore, in areas with higher soil saturation, the risk of flash flooding in the event of torrential rainfall is significantly higher. Using rainfall-runoff modelling, it is possible to determine the approximate amount of rainfall that, if it fell over a certain period, would potentially cause significant surface runoff.

Torrential rainfall is one of the potentially dangerous concomitants of convective storms. The occurrence of convective storms in time and space is monitored by weather radars. The radar does not directly measure rainfall, but reflectivity. Based on the relationship between the reflectivity and the hourly rainfall intensity, it is possible to estimate approximately how much rainfall has fallen or will possibly fall over an area based on a short-term forecast, called nowcasting [5]. Precipitation estimates can be refined significantly using a combination of rainfall observations and radar measurements. By means of rainfall-runoff modelling, it is then possible to approximate the magnitude of the runoff response and therefore the risk of flash flood occurrence.

Tab. 1. Matrix for the derivation of the general risk for the municipalities with extended jurisdiction according to the flash flood risk and the local flooding risk

		Flash flood risk			
	Risk level	**No risk**	**Medium risk**	**High risk**	**Very high risk**
Local flooding risk	**No risk**	No risk	Medium risk	Medium risk	High risk
	Medium risk	Medium risk	Medium risk	Medium risk	High risk
	High risk	Medium risk	High risk	High risk	High risk
	Very high risk	High risk	Very high risk	Very high risk	Very high risk

Based on the above-mentioned facts, the development of the so-called Flash Flood Indicator (FFI), which started within the R&D project SP/1c4/16/07 "*Research and implementation of new tools for flood and runoff forecasting within providing the flood forecasting service in the Czech Republic*" (2007–2011), was inspired by the "Flash Flood Guidance" system operated by the U. S. National Weather Service (NWS) [6].

The FFI system was in experimental operation until 2016 and was gradually improved. The outputs for the period 2017–2019 were evaluated in detail, and since 2020 the FFI has been part of the CHMI forecast service. The system is in operation from approximately mid-April to mid-October, which is the period with convective precipitation. It is described in detail in paper [7], and a translation of this paper into English has now been completed (November 2021), together with a major update of its content [8].

Development of FFI began on the ArcView GIS 3.x platform in the Avenue programming language and was transferred to ArcGIS Desktop system and reprogrammed in Python during 2011. Individual tools can be run interactively (from within the GIS environment) or automatically using the system task scheduler, either in a daily step or in a defined shorter step.

Configuration files containing many parameters are available to configure the running of the procedures. It is possible to specify input data paths, directories, or geodatabases for storing the results, time step interval of input rainfall data in minutes, length of time in minutes for both rainfall and nowcasting, threshold values for determining individual risk levels, etc.

The following data are the basic input in the daily step:

- A raster of 24-hour rainfall totals as a combination of radar measurements and rainfall observations, called MERGE, see [9].
- Point values of the current evapotranspiration, which are interpolated by the IDW (Inverse Distance Weighing) method into the raster.

The output of the procedures in the daily step is:

- A raster of current soil saturation values represented by CN values at 1 × 1 km resolution, derived from the balance of rainfall and evapotranspiration. The saturation indicator is defined by relating the current CN values to the extreme (limiting) CN values.
- Polygon layer with the potentially hazardous precipitation totals of 1-, 3- and 6-hours duration for a 3 × 3 km area.

The calculations in daily step are run several times during the day, leaving room for sometimes necessary adjustments of the input data and recalculation of the outputs.

The main input to the procedures, which are run in a shorter time step (every 20 minutes in 2021), are 15-minute sums of radar precipitation estimates that are adjusted based on rain-gauge observations. Until 2021, a single value of the adjustment coefficient was derived for the whole territory of the Czech Republic. Since 2022 onwards, it is expected to use an area-varying adjustment coefficient and to use the MERGE product at time intervals when this product is already available. The modification of the adjustment coefficient calculation method was addressed within the research project VI20192021166 "*Hydrometeorological risks in the Czech Republic – changes in risks and improvement of their prediction*" (2019–2021) and is described in detail in the article [10].

The risk of flash flood occurrence is calculated in a network of hydrologically connected watershed features and river reaches, in which the basic source layer is a polygon layer of the basic watersheds, where physical and geographic characteristics (watershed slope, thalweg slope and length, current CN value, etc.) are calculated for each watershed. These linked features form a hydrological model in which the hydrological response to actual rainfall is calculated, as well as to expected rainfall, which is predicted by nowcasting. The risk of flash flood occurrence is calculated in the outlet section of each watershed.

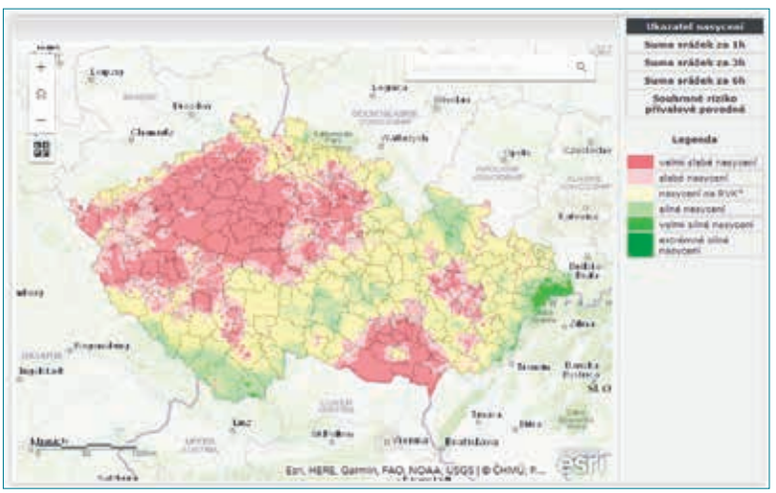

Fig. 7. Soil saturation indicator valid for June 30, 2020 at 6:00 UTC as seen on the CHMI website, see legend in *Tab. 2*

Tab. 2. Legend of the soil saturation layer

Description
very low saturation
low saturation
saturation at field capacity
strong saturation
very strong saturation
extremely strong saturation

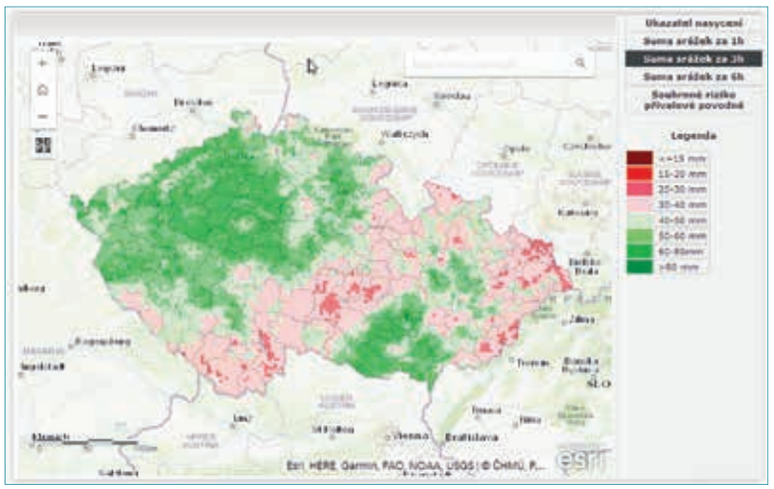

Fig. 8. Map of potential risk rainfall amounts with the duration of 3 hours valid for June 30, 2020 at 6:00 UTC as seen on the CHMI website

In the 3 × 3 km polygon layer, the local flooding risk is calculated based on the two-hour sum of the precipitation that has already fallen, or the one-hour sum of the precipitation that has fallen and the one-hour sum of the precipitation from nowcasting. Physical and geographic characteristics including the current CN value are derived for each polygon, like all watersheds.

A total of three thresholds, which are linked to the theoretical value of the specific 100-year flow, are set for the flash flood risk calculated in the hydrological model of the linked watersheds and river reaches, as well as for the local flood risk determined for polygons of constant size. These threshold values can be changed in configuration files.

The main result is the determination of the risk of flash flooding and local flooding for the municipalities with extended jurisdiction, for which the so-called general risk of flash flooding is also determined according to the following *Tab. 1*.

For the purposes of Flood Forecasting Service, an XML file with information on the risk of flash flood or local flooding is generated for each municipality with extended jurisdiction and this output is also used in the mobile application of the Czech Hydrometeorological Institute.

All outputs are also stored in ESRI file geodatabases in the form of raster and vector layers or tables. Selected data are transferred to cloud storage on ArcGIS Online and displayed as web maps and interactive web applications.

The following two images show the web maps that are embedded in the Flood Reporting and Forecast Service site. *Fig. 7* shows the saturation indicator, and *Fig. 8* shows the totals of potentially hazardous rainfall lasting 3 hours. Both maps are fully interactive.

Fig. 9 shows the window of the web mapping application where all relevant and up-to-date outputs from the FFI system can be viewed:

- saturation indicator,
- potentially risky rainfall events with durations of 1, 3 and 6 hours,
- risk of local flooding for municipality with extended powers,
- risk of flash floods for municipality with extended powers,
- the general risk of flash flooding as a combination of the risks of local flooding and flash flood (see above),
- the sum of the adjusted radar estimates of rainfall in 3 × 3 km polygons over the previous 2 hours, if the sum was higher than 10 mm or this sum posed a risk of local flooding,
- the sum of the adjusted radar estimates of rainfall in 3 × 3 km polygons over the previous 1 hour plus 1 hour of nowcasting if the sum was higher than 10 mm or this sum posed a risk of local flooding,

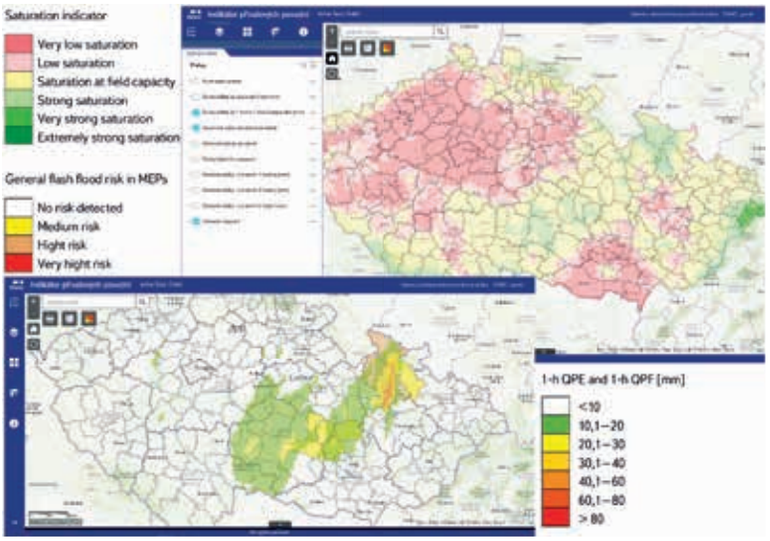

Fig. 9. The outputs from web map application 'Flash Flood Indicator' running on the ArcGIS Online platform. It depicts the soil saturation indicator layer (upper-right), radar rainfall estimates (QPE and QPF) ≥ 10 mm/2 h and actual general flash flood risk (bottom left) in municipalities with extended jurisdiction

- the risk of flash floods in a watershed system where a filter can be applied for those watersheds where peak flow is yet to be reached.

The application currently runs on ArcGIS Online in two versions. The older one is based on the Web Application Builder template, the newer one is based on the Experience Builder template, which has more advanced options in relation to optimizing the view for different devices (PC, tablets, mobile phones).

The Flash Flood Indicator is a comprehensive system based on the ESRI GIS technology platform. It consists of quite extensive Python scripts that make use of many GIS functions ranging from interpolations, map algebra and advanced geoprocessing functions (overlays or intersections of layers) to publishing data layers in a web environment. In particular, the "arcpy" library, which is licensed with ArcGIS Desktop or ArcGIS Pro products, and the "arcgis" library, which is a freely available library for working with GIS layers published on the web, are used.

CONCLUSION

Presenting specific examples, this paper demonstrates the use of GIS technology in solving various hydrological tasks at the Czech Hydrometeorological Institute. It is clear that GIS has long been used not only to create cartograms or carto-diagrams, but it is a comprehensive tool that includes the creation and administration of data in multi-user geodatabases, geospatial data processing and analysis, the possibility of creating user-tailored applications or creating scripts to solve complex tasks.

Although the focus of work in GIS is likely to remain on working with data in a heavy client environment, the publication of results is shifting from static maps to dynamic maps and online map applications that can be accessed from a standard web browser. This will allow to extend the use of GIS technology to users who do not normally work with GIS technology, and it is also an opportunity for organisations (in this case the CHMI) to effectively publish data and results of their employees' work.

Notes

1. At present it is The Military Geographic and Hydrometeorological Office in Dobruška

2. This includes fourth-order watersheds and watersheds related to other important profiles (reservoir dams, water gauging stations, etc.)

3. The "Aggregate" function was used to calculate the average values of the original 100 × 100 m raster at 1 × 1 km resolution, and then the "Block Statistics" function was applied to create a raster of average values over a 3 × 3 km radius while maintaining the 1 × 1 km raster resolution.

4. The differences between the automatically derived thalweg and the thalweg determined "manually" are due both to the distinction of the basis DMR and the choice made by the user-hydrologist, who usually respects the actual course of the watercourse line when determining the thalweg.

References

[1] JANEČEK, M. *Použití metody čísel odtokových křivek CN k navrhování protierozních opatření.* Praha, VÚMOP 1998. p. 1–35.

[2] Kolektiv pracovníků Hydrologické služby HMÚ. *Hydrologické poměry Československé socialistické republiky. Díl I. Text.* Josef ZÍTEK (ed.). Praha 1965. 414 p.

[3] BUDÍK, L., ŠERCL, P., KUKLA, P., LETT, P., PECHA, M. Odvození základních hydrologických údajů za referenční období 1981–2010. In: *Sborník prací Českého hydrometeorologického ústavu*, 65, 2018, p. 60.

[4] ŠERCL, P. Hodnocení metod odhadu plošných srážek. *Meteorologické zprávy.* 2008, 61(2), p. 33–43.

[5] NOVÁK, P. The Czech Hydrometeorological Institute's Severe Storm Nowcasting System. *Atmospheric Research* 2007, 83, p. 450–457.

[6] SWEENEY L. T. *Modernized Areal Flash Flood Guidance.* Office of Hydrology, Silver Spring, Md. NOAA Technical Memorandum NWS HYDRO 44, Silver Spring, MD, 1992. Available from https://repository.library.noaa.gov/view/noaa/13498

[7] ŠERCL, P. Indikátor přívalových povodní. Možnosti predikce přívalových povodní v podmínkách České republiky. In: *Sborník prací Českého hydrometeorologického ústavu*. 2015, 60, p. 10–28. ISBN 9788087577271.

[8] ŠERCL, P., PECHA, M., NOVÁK, P., KYZNAROVÁ, H., SVOBODA, V., LEDVINKA, O., DAŇHELKA, J. *Flash Flood Indicator.* Praha, ČHMÚ, [2022].

[9] NOVÁK, P., KYZNAROVÁ, H. Progress in Operational Quantitative Precipitation Estimation in the Czech Republic. In: *Proceedings of 8th European Conference on Radar in Meteorology and Hydrology (ERAD2014), Garmisch-Partenkirchen, Germany,1–5 September 2014.* Available from: http://www.pa.op.dlr.de/erad2014/programme/ExtendedAbstracts/067_Novak.pdf

[10] NOVÁK, P., KYZNAROVÁ, H., PECHA, M., ŠERCL, P., SVOBODA, V., LEDVINKA, O. Utilization of Weather Radar Data for the Flash Flood Indicator Application in the Czech Republic. *Remote Sens.* 2021, 13(16), 3184. Available from: https://doi.org/10.3390/rs13163184

The authors

Ing. Petr Šercl, Ph.D.
✉ petr.sercl@chmi.cz
ORCID: 0000-0003-1581-961X

Ing. Radovan Tyl, Ph.D.
✉ radovan.tyl@chmi.cz
ORCID: 0000-0002-5270-3248

RNDr. Pavel Kukla
✉ pavel.kukla@chmi.cz

Mgr. Martin Pecha
✉ martin.pecha@chmi.cz
ORCID: 0000-0003-0294-8981

Czech Hydrometeorological Institute, Prague

The paper has been peer-reviewed.

DOI: 10.46555/VTEI.2021.11.001

Photo: 123rf.com

The Authors

Mgr. Libor Ducháček

Czech Hydrometeorological Institute, Jablonec nad Nisou

✉ libor.duchacek@chmi.cz
www.chmi.cz

Libor Ducháček graduated from the Faculty of Science at Charles University in Prague with a degree in physical geography and geoecology. In 2008, he began working as a hydrologist in the regional department of the Czech Hydrometeorological Institute (CHMI) in Jablonec nad Nisou, which takes care of seven experimental watersheds in the Jizera Mountains. The regular field collection of hydrological data (hydrometering, snow water measurements) was gradually joined by the testing of new flow measurement methods. He has been the main methodologist for flow measurement at the CHMI since 2016 and he has been part of the WMO hydrometering expert group since 2020.

Ing. Josef Kratina, Ph.D.

TGM Water Research Institute, Prague

✉ josef.kratina@vuv.cz
www.vuv.cz

Josef Kratina graduated from the master's programme in soil evaluation and protection and the PhD programme in natural resource utilisation and protection at the Czech University of Life Sciences in Prague. He completed his dissertation in 2015. He is a member of the Czech Pedological Society. In 2015 – 2016, he was employed as an environmental assessment specialist (nature, landscape, forests, agriculture) at the Czech Environmental Information Agency (CENIA). Since 2018, he has been employed at the TGM Water Research Institute as a researcher at the Department of Hydrochemistry, where, in addition to hydrochemistry, he also focuses on pedology and sewage sludge management issues. He is involved in several research projects as a principal researcher or team member, and he also dedicates himself to publishing activities.

Ing. Petr Šercl, Ph.D.

Czech Hydrometeorological Institute, Prague

✉ petr.sercl@chmi.cz
www.chmi.cz

Petr Šercl has been working as a hydrologist at the Czech Hydrological Institute since 1989, now as the Head of the Surface Water Department. He graduated in water management and water structures at the Faculty of Civil Engineering of the Czech Technical University. In 2007, he completed his PhD in physical geography and geoecology at the Department of Physical Geography, Faculty of Science, Charles University in Prague. He specializes in the use of GIS in hydrology, rainfall-runoff modelling, and extreme hydrological phenomena, especially flash floods.

Bc. Vít Šťovíček

Czech Hydrometeorological Institute, Prague

✉ vit.stovicek@chmi.cz
www.chmi.cz

Vít Šťovíček has been an employee of the Czech Hydrometeorological Institute (CHMI), Hydrology Database and Water Budget Department, since 2021. He graduated with a bachelor's degree in geography and cartography at the Faculty of Science, Charles University, and since 2019 he has been a student of the master's programme in hydrology and hydrogeology. Currently, he is involved in the project "*Water Systems and Water Management in the Czech Republic under Climate Change*" (2020-2026) at the Czech Hydrometeorological Institute. His research interests include snow hydrology, GIS analyses and hydrological modelling.

Interview with Ing. Lucie Orlíková, Ph.D., an assistant professor at the Department of Geoinformatics, Technical University of Ostrava (VSB)

Generally speaking, the field of geoinformatics is relatively new and the GIS community is still rather small in the Czech Republic. So, the first question will probably not be very original, but it suggests itself at the very beginning – what brought you to this field?

Ever since I was at grammar school, I have been inclined to geography and working with maps. At that time, however, I had no idea about the existence of geographic information systems, so my initial idea was to begin studying physical geography after graduation. Nevertheless, I attended an open day at our faculty where I was filled with enthusiasm by my today´s colleague, Associate Professor Petr Rapant, and his introduction to geoinformatics. At that time, the combination of information technology and geography was very unusual. That day determined my future career. After completing my Ph.D., I stayed on as an academic in our department. I have been able to combine my passion for geoinformatics with the opportunity to pass on the knowledge I had gained to younger students.

Since 2007, you have been working at the Department of Geoinformatics at the Technical University of Ostrava, where you teach some of the core specialised subjects. What is your opinion about the development of the educational system in GIS over the past ten years? Can we say that the conditions for teaching have changed?

The development in the field of geoinformatics has been rapid over the last ten years. Our studies and the structure of our courses undergo changes and updates quite often, as it is necessary to constantly reflect current developments and the employers´ requirements for our graduates. At the same time, it is necessary for us, the academics, to keep up, so we try to educate ourselves constantly. We attend courses and conferences, study foreign literature and pass on the acquired knowledge to our students. The teaching conditions themselves have also gone through major changes. Nowadays, it is quite common for students to have their own, high-quality technical equipment, and there is a lot of online support materials available, so teaching is easier in this respect.

I would like to pay attention to the topics of the final theses now. There is also a noticeable dynamism in the development of the field, in terms of the complexity of processing, technologies used or trends. Do you feel that the current society´s requirements and possible application of the results obtained are reflected sufficiently in the assignment of the theses?

We always try to focus our final theses on topical issues, and the theses are often prepared on the basis of requirements related to practice. When working on the theses, the students cooperate with companies closely. Currently, many theses cover environmental issues such as bark beetle calamity, monitoring glacier movement, land use, mapping of floods using satellite imagery, using unmanned aerial vehicles to locate subsurface drainage networks, etc... We have also tried to respond to the COVID-19 pandemic and some of the works are focused on it.

As already mentioned, you teach several subjects ranging from basic geoinformatics to remote sensing. Could you reveal which of the many GIS branches is closest to your heart?

For me personally, it is remote sensing. The planet Earth itself has fascinated people since time immemorial and today, in the age of satellites, the internet and modern technology, it is much easier to explore.

Your past activities included, among other things, work on water management issues, specifically the projects "TRANSCAT" and "Research and development of a modular system for the creation of applications in integrated water management". Could you tell us more about them?

The aim of the "TRANSCAT" project was to develop an operational and integrated comprehensive Decision Support System in order to achieve optimum water management in river catchments encompassing border regions within the application of the Water Framework Directive 2000/60/EC of the European Parliament and of the Council. It also aimed to prevent extensive contamination of aquifers, to improve groundwater quality and reduce the risk of flooding.

What specifically are you working on at present?

I am currently training in machine learning and its use, especially in satellite image processing. This year I have attended machine learning workshops and studied with Professor Kanevsky at the University of Lausanne. I would like to work on water management applications, such as determining water and hydrological balance of a landscape or flood monitoring using both optical and radar data. We have good equipment at our Department, e.g., we work with unmanned aerial vehicles with hyperspectral cameras at present, so we are able to obtain very detailed and high-quality data quite quickly.

Under the current conditions, i.e., with the availability of satellite and reference data, possible automation and integration of advanced modelling techniques into GIS tools and development of machine learning algorithms, do you see a real potential in the use of satellite data in water management?

The availability and especially the ever-increasing number of satellites provides us with an essentially continuous view of planet Earth. Machine learning, artificial intelligence and other related technologies are increasingly being applied in science, and their importance is bound to grow – even in many conservative fields. We have a unique and immense dataset to process. We can thus monitor phenomena on the Earth's surface over the long term, study water quality, search for new water sources, observe sea currents, study run-off conditions in the landscape, plan better for flood protection, and use these technologies to our advantage and to improve the ever-deteriorating environmental situation.

This sounds like an interesting incentive for potential cooperation, which can bring remarkable opportunities and results and is certainly worth considering. Thank you very much for taking the time for this interview, I wish you every success in your research and teaching activities, and I look forward to any future interview, for example on collaborative projects.

Ing. Bc. Václava Maťašovská

Ing. Lucie Orlíková, Ph.D.

Ing. Lucie Orlíková, Ph.D., has been an employee of the Department of Geoinformatics at the Faculty of Mining and Geology since 2007. In 2012 she completed her PhD studies in geoinformatics at the Faculty of Mining and Geology, Technical University of Ostrava (VSB). In the years 2017-2021, she was the main researcher and co-researcher of projects supported by the Technology Agency and Grant Agency of the Czech Republic as well as foreign projects, e.g., "Research and development of a modular system for the creation of applications in integrated water management" or "Use of geoinformation technologies to particularise rainfall-runoff relationships". She focuses on the application of machine learning methods in remote sensing, namely in water management and forestry.

IAHS International Commission on Remote Sensing

The International Commission on Remote Sensing (ICRS), as one of the current ten scientific commissions under the umbrella of the International Association of Hydrological Sciences (IAHS; [1]), has emerged as a logical response to the availability of spatial data associated with the launch of the first satellites in the 1970ˢ that were designed to observe the Earth's landscape sphere from space, providing a completely new perspective in which the spatial extent of the territory under observation played the major role. In fact, hydrologists have seen great potential in such data since those early days, as the data have allowed the scientists to continue improving their understanding of the hydrological cycle, including its components, some of which being otherwise very difficult to measure on the Earth's surface for a variety of reasons. Moreover, this is underlined by the fact that ground-based observations are unlikely ever to provide such a comprehensive insight into the ongoing process for a single point in time in terms of the large territory captured. The beginnings of the use of remote sensing (RS) products in hydrology and water management are very often associated with collecting information about the cryosphere. That would not even be otherwise possible if we were dependent merely on ground-based observation, which (if it is being done anywhere in these landscapes at all) is inevitably burdened with a wide range of errors and uncertainties, and sometimes even periodic outages in seasons that are not conducive to such observations. Therefore, it is not surprising that the need for a predecessor of the ICRS has been seriously discussed since the turn of the 1970ˢ and 1980ˢ. Especially hydrologists who study snowy and glaciated areas have required the use of RS data. Let us give an example of the then perspective of the related International Commission on Snow and Ice Hydrology (ICSIH), which concerned large-scale studies of snow and built precisely on the potential of RS products (see paper [2], whose author was also an ICRS president). Similarly, the use of RS products within the ICSIH is mentioned in retrospective article [3] and more generally, concerning the needs of the whole IAHS, also in article [4].

The contribution, which was written on the occasion of the 90th anniversary of the IAHS, dates the origins of the ICRS more precisely to the year 1979 when the 17th General Assembly of the International Union of Geodesy and Geophysics (IUGG), of which the IAHS is a part, was held in Canberra, Australia. At that time, a committee was established, which met for the first time in 1981 in Denver, Colorado [5]. The Symposium on Hydrological Applications of Remote Sensing and Remote Data Transmission was held in Hamburg, Germany, in April 1983, as part of the 18th IUGG General Assembly. One of the outcomes of this Symposium was at book [6], the preface to which mentions the fact that the Symposium was organized by the International Commission on Remote Sensing and Data Transmission (ICRSDT), i.e. the predecessor of today's ICRS. However, according to the ICRS officials themselves, the first independent meeting of the Commission took place at the International Workshop on Hydrologic Applications of Space Technologies which was held in Cocoa Beach, Florida, in August 1985 [7] and resulted in publication [8]. It can be deduced from the name (ICRSDT) that data transmission was very essential and important for hydrologists, especially for those in the filed of operational hydrology. Indeed, the very first meetings of the ICRSDT were held in the presence of representatives of the World Meteorological Organization (WMO) and other UN organizations (e.g. UNESCO). This is evidence of the hydrologists' assumption that it is the RS products (not only radars but also satellites) that will help improve hydrological forecasts by providing a more precise picture of spatial differentiation of the landscape that forms a catchment. This resulted in further development of microcomputer software to process such data (e.g. geographical information systems, GIS), as well as development and adaptation of hydrological models, as estimated well by Askew of the WMO [9] (see also contribution [10], whose ideas are expanded in [11]).

It was 15 years before the second independent ICRS meeting took place. As the preface to publication [7] says, that did not mean that ICRS members and supporters had not been active during that period. On the contrary, several joint symposia (i.e. with other IAHS commissions) were organized within the IUGG assemblies and IAHS scientific assemblies, which normally take place two years after the IUGG assemblies. It certainly does not make sense to list all these meetings here. It is much more sensible to refer those interested in a deeper study directly to the website from where it is possible to download the individual articles published in the IAHS "red books", which, by the way, are very rich in detailed information [12]. As an example, let us mention at least the book based on the International Symposium on Integrated Methods in Catchment Hydrology, which took place in Birmingham, UK, in June 1999, where the 22nd IUGG General Assembly was just held at that time. These joint symposia only emphasise the importance of RS applications overlapping to various areas of hydrology and water management. Contribution [5] also mentions that the ICRS was transformed in 1998. At that time, the ICRS, judging at least by the change of the name, presumably lost interest in data transmissions as these became the focus of other expert groups.

The third ICRS meeting, again a symposium with a focus on RS in hydrology, was held in Jackson Hole, Wyoming, in late September 2010 [13]. In the meantime, however, a number of issues were identified that necessitated separate international conferences or, again, symposia to be included in the agenda of the IUGG assemblies, or IAHS scientific assemblies. The GIS applications in hydrology for the purposes of flood forecasting, runoff simulation, (integrated) water management, and environmental modelling thus came to the fore [14, 15]. Hand in hand with the latter, change detection through RS data also gained importance, both in hydrological terms and in general with respect to all environmental components and the needs of human society [14–16]. At these meetings, hydrogeologists also demonstrated their skills, not for the first time. They come together under the umbrella of the International Association of Hydrogeologists (IAH), which is a separate body alongside the IAHS, although it does not form the IUGG. Incidentally, hydrogeologists also stressed the importance of hydroinformatics for the whole hydrology, including RS data processing. Hydroinformatics has gradually been brought into hydrology through hydraulics, which resulted in the formation of the Joint Committee on Hydroinformatics in Cardiff in July 2002 [17]. The Jackson Hole ICRS symposium itself then indicated the continuation of estimating the following hydrological parameters using RS: soil moisture, evapotranspiration, surface temperature, distribution and characteristics of vegetation (including crops and invasive species), and snow pack properties. For these purposes, the combined use of satellite- and airborne instruments was emphasized. It was also found that the above-mentioned hydrological parameters can be well obtained if lidar images taken from the aircraft and the ground are used additionally. Finally, advances in understanding and modelling the hydrological cycle in relation to the start of surface energy balance flux measurements using scintillometers and eddy covariance systems were mentioned [13].

The current ICRS (the present incumbents are listed in [18]) has two sections, one for RS and the other for GIS [5]. Experts from both sections first combined their symposia and conferences, which originally focused separately more on RS and separately more on GIS, into one in Guangzhou, China in 2014.

The purpose of this merged event, or in other words, two events held in one location, was to review and report on advances in GIS and RS technologies as well as their applications in hydrology, water management and the environment, and to share experience of scientists, engineers, NGOs and policy makers worldwide in the fields of meteorology, hydrology, water management, environment, flood forecasting and management, GIS and RS [19].

So far, the most recent stand-alone symposium entitled "Remote Sensing and Hydrology Symposium" (RSHS) has been organized in Córdoba, Spain, in May 2018. The potential to obtain relatively long time series using RS was highlighted there. To achieve this goal, however, it is necessary to consider the merging of data coming from different instruments with different accuracies, including those located on the Earth's surface. The symposium was divided into several thematic areas:

1. current and future missions for water cycle observation,
2. observations of water cycle components,
3. Earth Observation retrievals and data products linked to the water cycle,
4. applications of RS data in water resources management,
5. crop irrigation management by RS,
6. water quality and soil cover assessment from RS data.

Throughout the symposium, emphasis was placed on integrated water and basin management with regard to potential environmental changes [20]. It should be anticipated in the future that spatial resolution of RS products will increase primarily, which can be used successfully in hydrology. However, if the final information obtained from the data is to be relevant, it is necessary to adapt established approaches and methods to these data, and to be aware of the fact that longer time series derived from RS products may be burdened with different uncertainties in different sections.

We can already look forward to presentations of further activities and outcomes given by ICRS experts. For instance, further symposia are being prepared for the 11th IAHS Scientific Assembly, which is scheduled to take place in Montpellier, France, at the turn of May and June 2022, while celebrating the 100th IAHS anniversary (cf. e.g. [4]). The agenda to date has demonstrated that the interest of the world's hydrologists in the RS technologies and methods is not waning [21]. Therefore, the author of this informative paper firmly hopes that Czech hydrologists or water managers will not be left behind and he will also be very glad if this paper is of interest to those who have not been aware of ICRS activities so far.

References

[1] IAHS. *International Association of Hydrological Sciences* [on-line]. 20th October 2021 [accessed November 28, 2021]. Available from: https://iahs.info/

[2] RANGO, A. An International Perspective on Large-Scale Snow Studies. *Hydrological Sciences Journal* [on-line]. 1985, 30(2), p. 225–238. ISSN 0262-6667, 2150-3435. Available from: doi: 10.1080/02626668509490986

[3] RADOK, U. The International Commission on Snow and Ice (ICSI) and its Precursors, 1894–1994. *Hydrological Sciences Journal* [on-line]. 1997, 42(2), p. 131–140. ISSN 0262-6667, 2150-3435. Available from: doi: 10.1080/02626669709492015

[4] ROSBJERG, D., RODDA, J. IAHS. A Brief History of Hydrology. *History of Geo- and Space Sciences* [on-line]. 2019, 10(1), p. 109–118. ISSN 2190-5029. Available from: doi: 10.5194/hgss-10-109-2019

[5] NEALE, Ch. Remote Sensing and Hydrology. In: *Celebrating 90 Years of International Scientific Cooperation and Activity* [on-line]. Delft: International Association of Hydrological Sciences, 2012, p. 6–7. Available from: https://iahs.info/uploads/IAHS%2090th%20Anniversary%20screen-res.pdf

[6] GOODISON, B. E. (ed.). *Hydrological Applications of Remote Sensing and Remote Data Transmission*. Wallingford, Oxfordshire, UK: IAHS Press, 1985. IAHS Red Book 145. ISBN 978-0-947571-10-8.

[7] OWE, M., BRUBAKER, K., RITCHIE, J., RANGO, A. (eds.). *Remote Sensing and Hydrology 2000. A Selection of Papers Presented at the Conference on Remote Sensing and Hydrology 2000 Held at Santa Fe, New Mexico, USA, April 2000*. Wallingford, Oxfordshire, UK: IAHS Press, 2001. IAHS Red Book 267. ISBN 978-1-901502-46-6.

[8] JOHNSON, A. I. (ed.). *Hydrologic Applications of Space Technology: Proceedings of an International Workshop on Hydrologic Applications of Space Technology Held in Cocoa Beach, Florida, USA, 19–23 August 1985*. Wallingford, Oxfordshire, UK: IAHS Press, 1986. IAHS Red Book 160. ISBN 978-0-947571-85-6.

[9] ASKEW, A. J. Closing Discussion. In: JOHNSON, A. I. (ed.). *Hydrologic Applications of Space Technology: Proceedings of an International Workshop on Hydrologic Applications of Space Technology Held in Cocoa Beach, Florida, USA, 19–23 August 1985*. Wallingford, Oxfordshire, UK: IAHS Press, 1986, p. 485–488. IAHS Red Book 160. p. 485–488. ISBN 978-0-947571-85-6.

[10] SCHULTZ, G. A., ENGMAN, E. T. Present Use and Future Perspectives of Remote Sensing in Hydrology and Water Management. In: OWE, M., BRUBAKER, K., RITCHIE, J., RANGO, A. (eds.). *Remote Sensing and Hydrology 2000. A Selection of Papers Presented at the Conference on Remote Sensing and Hydrology 2000, Held at Santa Fe, New Mexico, USA, April 2000*. Wallingford, Oxfordshire, UK: IAHS Press, 2001, p. 545–551. IAHS Red Book 267. ISBN 978-1-901502-46-6.

[11] SCHULTZ, G. A., ENGMAN, E. T. (eds.). *Remote Sensing in Hydrology and Water Management*. Berlin: Springer, 2000. ISBN 978-3-642-64036-0.

[12] *IAHS. International Association of Hydrological Sciences. Publications* [on-line]. 20th October 2021 [accessed November 30, 2021]. Available from: https://iahs.info/Publications-News/

[13] NEALE, Ch. M. U., COSH, M. H. (eds.). *Remote Sensing and Hydrology: Proceedings of a Symposium Organized by the International Commission on Remote Sensing of IAHS, Held at Jackson Hole, Wyoming, USA, 27–30 September 2010*. Wallingford, Oxfordshire, UK: IAHS Press, 2012. IAHS Red Book 352. ISBN 978-1-907161-27-8.

[14] CHEN, Y., TAKARA, K., CLUCKIE, I. D., DE SMEDT, F. H. (eds.). *GIS and Remote Sensing in Hydrology, Water Resources and Environment*. Wallingford, Oxfordshire, UK: IAHS Press, 2004. IAHS Red Book 289. ISBN 978-1-901502-72-5.

[15] BLÖSCHL, G., VAN DE GIESEN, N., MURALIDHARAN, D., REN, L., SEYLER, F., SHARMA, U., VRBA, J. (eds.). *Improving Integrated Surface and Groundwater Resources Management in a Vulnerable and Changing World. Proceedings of Symposium JS.3 at the Joint Convention of the International Association of Hydrological Sciences (IAHS) and the International Association of Hydrogeologists (IAH) Held in Hyderabad, India, 6–12 September 2009*. Wallingford, Oxfordshire, UK: IAHS Press, 2009. IAHS Red Book 330. ISBN 978-1-907161-01-8.

[16] OWE, M., NEALE, Ch. (eds.). *Remote Sensing for Environmental Monitoring and Change Detection. A Compilation of Papers Presented at the IAHS Symposium on Remote Sensing for Environmental Monitoring and Change Detection, in Perugia, as Part of the 24th IUGG General Assembly, 2007*. Wallingford, Oxfordshire, UK: IAHS Press, 2007. IAHS Red Book 316. ISBN 978-1-901502-24-4.

[17] CLUCKIE, I. D., CHEN, Y., BABOVIC, B., KONIKOW, L., MYNETT, A., DEMUTH, S., SAVIC, D. A. (eds.). *Hydroinformatics in Hydrology, Hydrogeology and Water Resources. Proceedings of Symposium JS.4 at the Joint Convention of the International Association of Hydrological Sciences (IAHS) and the International Association of Hydrogeologists (IAH) Held in Hyderabad, India, 6–12 September 2009*. Wallingford, Oxfordshire, UK: IAHS Press, 2009. IAHS Red Book 331. ISBN 978-1-907161-02-5.

[18] *IAHS. International Association of Hydrological Sciences. ICRS | Remote Sensing International Commission* [on-line]. 20th October 2021 [accessed November 30, 2021]. Available from: https://iahs.info/Commissions--W-Groups/ICRS-Remote-Sensing.do

[19] CHEN, Y., NEALE, Ch., CLUCKIE, I., SU, Z., ZHOU, J., HUAN, Q., XU, Z. (eds.). *Remote Sensing and GIS for Hydrology and Water Resources* [on-line]. Wallingford, Oxfordshire, UK: IAHS Press, 2015. IAHS Red Book 368. ISBN 978-1-907161-46-9. Available from: https://piahs.copernicus.org/articles/368/index.html

[20] GONZÁLEZ-DUGO, M. P., NEALE, C., ANDREU, A., PIMENTEL R., POLO, M. J. (eds.). *Earth Observation for Integrated Water and Basin Management: New Possibilities and Challenges for Adaptation to a Changing Environment* [on-line]. Wallingford, Oxfordshire, UK: IAHS Press, 2018. IAHS Red Book 380. ISBN 978-1-5108-8294-2. Available from: https://piahs.copernicus.org/articles/380/index.html

[21] IM2E. *IAHS 2022 Montpellier* [on-line]. 2020 [accessed November 30, 2021]. Available from: http://www.iahs2022.org/index.asp

The author

Mgr. Ondřej Ledvinka, Ph.D.
✉ ondrej.ledvinka@chmi.cz
ORCID: 0000-0002-0203-7064

Czech Hydrometeorological Institute,
Hydrology Database and Water Budget Department, Prague

Photo: Shutterstock.com

GIS and cartography at the T. G. Masaryk Water Research Institute

Keywords: GIS — geographic information systems — cartography — DIBAVOD — information system — spatial data — analyses — web map application — T. G. Masaryk Water Research Institute

FROM HISTORY TO THE PRESENT

Geographic information systems (GIS), data processing, evaluation and interpretation are an essential and integral part of research at present as most information can be related to a specific location on the Earth's surface. The GIS and Cartography Department at the T. G. Masaryk Water Research Institute deals with research and commercial projects by means of the application of GIS tools. However, it is not just a matter of using specialised software; valid data and qualified staff who can apply their knowledge correctly are also essential. The GIS and Cartography Department has been working at the Institute for many years. In the 1990s, there was a cartography and remote sensing unit, which was part of the Water Management Department. The unit provided not only mapping source documents and data for the state administration (these activities are being carried out within the project "*Support for the state administration in the field of water*" after the transformation into a public research institution), but also the updating and printing of the Base Water Management Map 1 : 50 000. As part of its research activities, the Department later participated in the projects "*Evaluation of the flood situation in July 1997*" within the subtask "*Geodetic documentation for flood evaluation and the creation of a digital model of the river system in the affected areas*" and "*Integration of the information on landfills, facilities and old contaminated sites, evaluation of their environmental risks and impacts*" [1]. The need for quality and accessible data resulted in the creation of the Digital Water Management Data Base (DIBAVOD) as a source of geodata for water management and protection [2]. Subsequently, the staff of the Department participated in the research project, specifically in its sub-part "*Development and application of procedures using geographic information systems technologies in relation to the Digital Water Management Data Base*". At present, the activities of the GIS and Cartography Department are very diverse. It deals with national and international research projects, administers and updates data for the government, develops online mapping applications, analytical tools, and procedures. It also prepares cartographic outputs and cooperates with all the other departments within the T. G. Masaryk Water Research Institute, for which it also administers the data warehouse and GIS devices. Last but not least, it provides expertise in the field of geographic information systems and cartography. And despite this wide range of activities, the Department tries to keep up with the fast-developing trends in GIS, which it then puts into practice.

TASTING OF OUR ACTIVITIES

Base Water Management Map of the Czech Republic

This unique cartographic work, the Base Water Management Map of the Czech Republic at the scale of 1 : 50 000, is the most detailed national water management map. It was prepared as a part of the Directional Water Management Plan and published by the Czech Geodetic and Cadastral Office as a thematic national map for the Ministry of Environment of the Czech Republic. The T. G. Masaryk Water Research Institute is in charge of the thematic content and its updating. The territory of the Czech Republic is covered by 211 map sheets in the arrangement of medium-scale base maps.

The first systematic subject-focused mapping in water management for the Czech Republic´s territory was done within the State Water Management Plan of Czechoslovakia (1st edition of the Plan) in 1949–1954. The beginnings of the development of the Base Water Management Map date back to 1961, when the Ministry of Agriculture, Forestry and Water Management commissioned the Water Management Directorates in Prague and Bratislava, in cooperation with other water management organisations, to draw up the "Base Water Management Map of the Czechoslovak Socialist Republic" (1964 edition). In 1971–1976, a new set of the Base Water Management Map of the Czechoslovak Socialist Republic was prepared again in terms of authorship, cartography, and reproduction on the basis of the Base Map of the Czechoslovak Socialist Republic (1 : 50 000). This set is referred to as the 1st edition in the history of the creation and updating of the Base Water Management Map (1 : 50 000). The second updated edition of the Base Water Management Map of the Czechoslovak Socialist Republic was published in 1980–1988. The last, third updated edition of the Base Water Management Map of the Czech Republic was published in 1989-1999. Since 1999, further development of the Base Water Management Map has been directed towards the transformation of the analogue map into a digital map in the form of the DIBAVOD geographic reference database. The process of digitisation of the Base Water Management Map (1 : 50 000) was carried out in the T. G. Masaryk Water Research Institute by vectorising objects from scanned sheets of the Base Water Management Map (1 : 50 000). Since 1995, the base map (1 : 10 000) has been digitised by the Czech Geodetic and Cadastral Office in the same way into layers of the Basic Geographic Data Base (ZABAGED®) [3]. The updated course of watercourses and catchment divides was obtained on a sheet-by-sheet basis from ZABAGED®. The watercourses and catchment divides were gradually processed topologically into the form of a structural model of the Czech Republic´s catchments and watercourses. The layers of watercourses and catchment divides were then incorporated into DIBAVOD, which was subsequently the source of the thematic content of the updated edition of the Base Water Management Map (1 : 50 000) [4].

Eight test sheets were issued in 2008. The catalogue of map symbols was revised, and the legend became part of the map sheet (*Fig. 1*). Due to the lack of funding and the different responsibilities for the thematic layers, merely the printing technology line was set up and tested in cooperation with the Czech Geodetic and Cadastral Office in Sedlčany.

Fig. 1. Test sheet of the Base Water Management Map (1 : 50 000)

The original printed Base Water Management Map (1 : 50 000) is currently distributed only in the digital raster form created by scanning the original printed maps (TIFF format with LZW compression, 400 DPI resolution). More information is available at https://www.dibavod.cz/63/puvodni-tistena-zakladni-vodohospodarska-mapa-1:50-000.html

Digital Water Management Data Base

The need for a unified spatial data base for water management and water protection led to the development of a major database, known as DIBAVOD, namely as a thematic extension of ZABAGED®. It is intended, inter alia, for the creation of thematic cartographic outputs focused on water management and water protection on top of the Base Map of the Czech Republic 1 : 10 000 or 1 : 50 000. The first mention of DIBAVOD appeared within the R&D project 650/8/01 "*Methodology for creating cartographic outputs from digital data*". In pursuance of this project, the DIBAVOD Object Catalogue was defined, which consists of a list of object types in the category of water and a set of catalogue sheets, each of which being dedicated to one object type. A draft document "*Instructions for the creation, updating and publishing of the Water Management Map of the Czech Republic 1 : 50 000*" with a catalogue of the Base Water Management Map (1 : 50 000) symbols and a sample sheet (15–32) were created inter alia. A similar material has been created for the Map of Flood-Prone Areas: "*Instructions for the creation, updating and publication of the Map of Flood-Prone Areas in the Czech Republic 1 : 10 000*" with the catalogue of map symbols of the Map of Flood-Prone Areas (1 : 10 000) and the sample sheet for the Map of Flood-Prone Areas (1 : 10 000) (15-32-20). The technological solution was appropriate for its time – it was an Intergraph MGE environment. The aim was to keep all defined objects (datasets) up-to-date and freely available to the public if possible. This goal could not be achieved because several ministries and some private sector entities are responsible for the data at the same time. Stable funding for updating the database in its entirety is not guaranteed at present. For these reasons, some objects are inaccessible, and some have not been updated for a long time. Nevertheless, it can be hoped that the situation will change, and that all data will be up-to-date, guaranteed and available to all and that the production of the cartographic visualisation of the Base Water Management Map (1 : 50 000) will be resumed.

Data not only for state administration

As mentioned above, quality and guaranteed data are the cornerstone of any successful and responsible research activity. The same applies to the performance of government and other related agendas. The GIS and Cartography Department and the entire T. G. Masaryk Water Research Institute are proud partners involved in the administration, updating and publication of selected spatial data used by the state and public administration. A small taste of the data and activities is given in the following paragraphs.

The watercourse data set is one of the core data sets in water protection and water management. It is therefore vital that these data are kept neat and in the best accordance with reality. As the agendas related to watercourses are divided among several actors from different ministries, several different watercourse data sets have been created over the years. To correct this inconsistency, a cross-ministerial working group has been established to address "harmonisation of the river network in the Czech Republic" since 2019. In cooperation with the Ministry of Environment (T. G. Masaryk Water Research Institute, Czech Hydrometeorological Institute), Ministry of Agriculture (catchment administration enterprises (Povodí), Forests of the Czech Republic, State Land Office) and the Czech Geodetic and Cadastral Office, the springs, estuaries and possibly the course of the main watercourses in all more than nine thousand 4th order river catchments are being checked. The result should be a single guaranteed network of watercourses, which will have an agreed structure, contain all relevant information and, where appropriate, be linkable with thematic databases of stakeholders via linking identifiers. This data set should be administered by the Czech Geodetic and Cadastral Office within ZABAGED® as a unified source of information.

Another important activity is updating the database of water resource protection areas in the Czech Republic, which the GIS and Cartography Department has been working on with several breaks for about 20 years. A comprehensive revision of the database was carried out within the project "*Support for State Administration Performance*" under the Ministry of Environment in 2015–2017. The database now contains more than 17,000 polygons of protection areas. Almost 15,000 of them have been validated by the competent water administration authority of the respective municipality and are accompanied by the document on the establishment of the water resource protection area in digital form. The remaining 2,000 areas are either no longer valid or have not been verified by the relevant authority. Currently, updating work is being carried out at annual intervals [5]. A user-friendly online mapping application has been developed, available at https://www.dibavod.cz/ochranna-pasma (*Fig. 2*), to make visualisation of the water resource protection area database easier. At the turn of the year, the database is always published and available for viewing and downloading via web services on the DIBAVOD and HEIS portals [6] and on the National INSPIRE geoportal [7].

Fig. 2. Web map application showing the current status of the water resource protection area

INSPIRE is a European directive that simplifies the way spatial data should look, how they should be described and how they should be shared so that they are usable by all users [8]. Although European directives may not always be popular, it is at least an interesting challenge to create uniform data models across European countries so that all users understand and can share, compare, and harmonise the data with each other. The Directive is therefore a good first step in this endeavour. The T. G. Masaryk Water Research Institute is responsible for several data sets that are subject to this Directive. Metadata are thus provided for these data and users can view or download them using web mapping services.

The T. G. Masaryk Water Research Institute is also a key player in international cooperation concerning water protection and it puts great emphasis on correct and harmonised data being collected, updated, and shared with domestic and international users. The Institute is also an important partner for foreign entities, not only in activities related to spatial data. One of the main partners, as mentioned above, is the European Commission and its organisations to which spatial data and information are reported according to the relevant European directives [9–12]. Other important partners are the International Commissions for the Protection of the Elbe, Danube and Oder rivers [13–15]. The Institute collaborates with these Commissions and its partners in the development of strategic key documents and shares with them mutually relevant data related to water management and protection.

Use of remote sensing methods to monitor bathing sites in the Czech Republic

The project TJ02000091 "*The use of remote sensing methods to monitor bathing sites in the Czech Republic*" was implemented in the period 2019–2021. It was funded by the Czech Technology Agency, specifically from the Zeta II programme for the support of junior researchers in innovative activities. The primary objective of the project was to find a relevant relationship between the values of selected indicators of bathing water status and quality which resulted from field surveys and subsequent laboratory work on one hand, and the values from the processed *Copernicus* (Sentinel-2) satellite data on the other. Using GIS tools and modern statistical techniques, six predictive models were constructed and applied to 40 selected bathing water sites (*Fig. 3*). The project´s most important outputs include the online map application "*Indicators of the state and quality of bathing waters in the Czech Republic*" and the printed publication "*Atlas of bathing waters in the Czech Republic*". Information on the achieved results and the project´s other parameters is presented on the website https://www.dibavod.cz/201/vyuziti-metod-dalkoveho-pruzkumu-zeme-pro-monitoring-stavu-a-kvality-koupacich-mist-v-ceske-republice.html. The results and findings obtained within the project confirmed the initial hypothesis that satellite data can support and improve existing monitoring significantly [16].

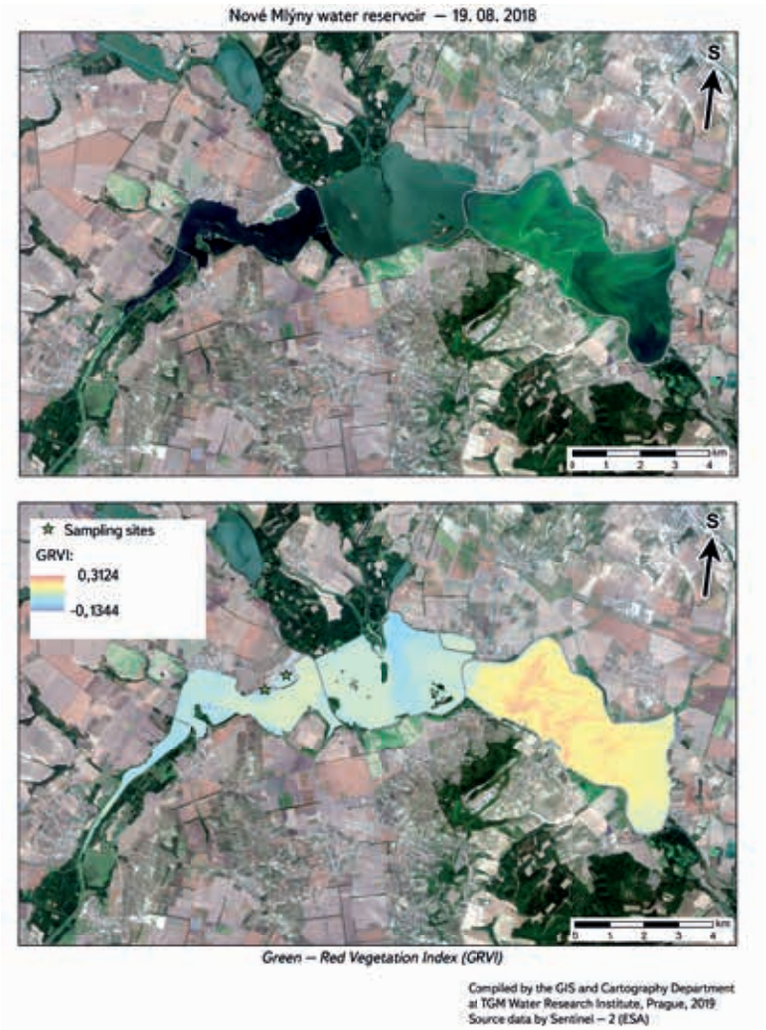

Fig. 3. Example of remote sensing data evaluation

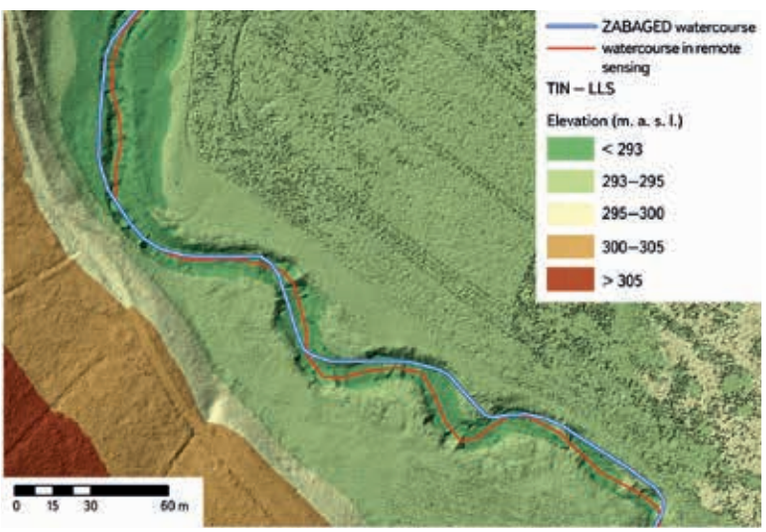

Fig. 4. Testing the use of RS 5G in the context of water management and water protection

Research using altimetry data

In the past, the GIS and Cartography Department worked on several important projects using the then new product 5th-Generation Digital Model of the Czech Republic´s Relief (DMR 5G) [17]. It concerned very detailed data acquired by the Czech Geodetic and Cadastral Office in cooperation with other organisations using the airborne laser scanning. Within the research project VZ 0002071101, the then new detailed relief model was used to identify transverse obstacles in the beds of small watercourses and to revise the data sets of catchment boundaries and watercourses. The Ministry of Interior's security research VG20102014010 enabled testing of the modern RS 5G technology in relation to flood-prone areas delimitation accuracy in 2010-2014 (*Fig. 4*).

Fig. 5. Online mapping application Type-based Drought Mitigation Measures

Fig. 6. Example of a bathing place

Type-based drought mitigation measures — online mapping application

The online mapping application *Type-based Drought Mitigation Measures* was developed to make information available to the public on how to address adaptation of an area of interest to ongoing climate change and associated increased drought events. It is available at https://www.dibavod.cz/typova-opatreni-sucho (*Fig. 5*). Possible solutions are presented by means of selected sample sites where some measures to mitigate the negative impacts of drought have been implemented. The specific measures themselves can be viewed, as well as the whole set of taken measures, including a description of the expected impact on drought via a fact sheet. The application is based on a combination of the R programming language (including extension packages) and HTML 5, CSS and Javascript technologies. The application includes a clear help and a detailed user manual.

Growth pole I and II

A survey of potential opportunities to expand bathing and water recreation sites in the Capital City of Prague was carried out within the project "*Water Recreation Opportunities in the Capital City of Prague (from History to the Present), Prague – Growth Pole II*" in 2018–2020. Water quality was monitored, and the condition and potential were assessed in 57 sites selected out of approximately 150 sites found. The main outputs of the project were a database, a set of maps (https://koupanivpraze.vuv.cz/) and an online map application (https://www.dibavod.cz/vodni-rekreace-praha), which present the project results in a clear way and increase public awareness of the current opportunities for recreation by water in the Prague area (*Fig. 6*) [18].

Sustainable recycling of plastics in Mongolia

The project aims at contributing to economic prosperity and poverty reduction as well as supporting the development of a green economy and the transition to a low-carbon, resource-efficient and circular economy in Mongolia. Waste management is a key issue in Mongolia due to urbanization, industrialization, and the increasing consumption of packaged products. Plastic waste is a particularly serious problem as it causes extensive pollution and is also often dumped illegally by both citizens and companies. The project, funded by the European Union (SWITCH-Asia Programme), is led by The Charity of the Czech Republic. The T. G. Masaryk Water Research Institute, together with three other partners, is a co-operating institution. Experts from the Waste Management Centre are the main researchers within the Institute. The GIS and Cartography Department is mainly responsible for data analysis and publication of results using cartographic outputs and online mapping applications [19].

WHAT (ELSE) CAN THE GIS AND CARTOGRAPHY DEPARTMENT DO FOR YOU?

Remote Sensing

The popularity of satellite data, i.e. the results of unconventional remote sensing methods, is currently on the rise. The reason for this growing interest is caused not only by their distinctive characteristics, but especially by the fact that recently some satellite system operators have released their data in open-source mode, i.e., for free use. It should be noted here that, thanks to the very high frequency and large extent of sensing of the Earth's surface, it is easy to create relatively dense time series and thus build up a relatively complete picture of the evolution of the object or phenomenon under observation. For this reason, satellite data are generally considered a tool that is suitable for

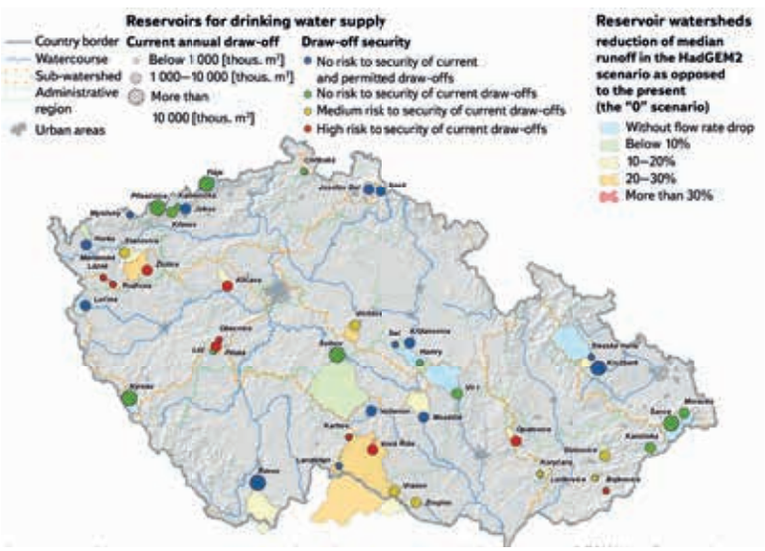

Fig. 7. Illustration of the map output

increasing efficiency but also for reducing the cost of certain activities. The relevance of the results obtained from remote sensing data is ensured by the necessary calibration and subsequent validation with terrestrial data (obtained *in situ*). Since 2018, the GIS and Cartography Department has been testing specific tasks with European Space Agency (ESA) optical data, both at low spatial resolution (Sentinel-3) and at very high spatial resolution (Sentinel-2). Attention is also given to data acquired in the thermal band of the electromagnetic spectrum (Landsat 7, 8 and the TERRA satellite system). Radar data (Sentinel-1) should not be overlooked either. Specific applications we address include e.g., monitoring of some indicators of bathing water status and quality, snow cover detection, soil moisture monitoring, determination of landscape surface temperature and water levels.

Cartographic outputs

Map works or overview maps (*Fig. 7*) are the outputs of many research and commercial projects. The GIS and Cartography Department ensures that the map output is of a standard that meets basic cartographic rules, is easy to understand and presents project results appropriately. In addition to "classic" analogue maps, it also deals with online cartography.

Online map applications

The online map application is a well-arranged interactive tool for publishing data and services with on-line access via a web browser. It is an integral part of modern sharing of individual project outputs with the general public or stakeholders. It can contain raster and vector datasets (lines, points, polygons) with an attribute table supplemented by additional information (e.g., photo, graph, animation, website). Analytical and publishing tools can also be used within the application. Some links to online map applications developed at the T. G. Masaryk Water Research Institute have been provided in the text of this article. Here are a few more:

- Water Recreation Opportunities in the City of Prague (from History to the Present) (https://www.dibavod.cz/vodni-rekreace-praha)
- Indicators of the status and quality of selected bathing waters of the Czech Republic (https://geoportal.vuv.cz/aplikace/dpz-koupaci-vody-zeta/)
- Water recreation – bathing in natural swimming pools and other surface waters (https://www.dibavod.cz/koupaci-vody)

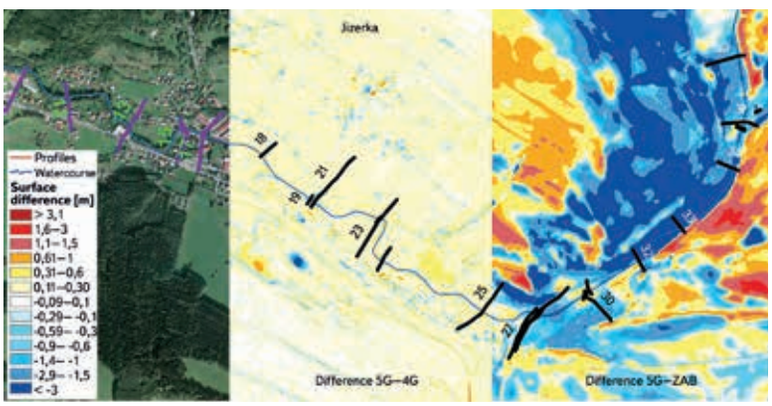

Fig. 8. Analysis of raster data in combination with vector data

Data analysis, data availability and user support

The strength of geographic information systems lies primarily in the variety of analytical tools that can be used to extract many insights from the data under study. Although it may not seem so at first glance, GIS and its analyses can be applied to almost any data because most of the information can be located in place or over time. Both vector (points, lines, polygons) and raster data or combinations of both can be analysed (*Fig. 8*). The results of the analyses cannot be of good quality unless they are based on updated and guaranteed data and are interpreted correctly. This is also a challenge for the GIS and Cartography Department that strives to ensure unified and up-to-date datasets and guaranteed data sources within and outside the Institute. Equally important is communicating with and educating project workers and researchers so that they can make sure that GIS can make their work easier, help them extract the most information from the data they explore, and visualize the results in an elegant way.

WHAT TO SAY IN CONCLUSION?

As can be seen from the above (brief) overview, the scope of the GIS and Cartography Department is very broad. Through the use of GIS, geoinformatics, cartography and other similar disciplines, it implements research and commercial projects, both nationally and internationally. It is an important segment in supporting the performance of the state administration, especially the Ministry of Environment. It carries out these activities both independently, as the key research entity, and in cooperation with experts from various fields of human activity. Therefore, it has a unique opportunity to apply its knowledge and GIS in diverse and interesting projects (*Fig. 9*). In addition, the Department strives to provide other staff at the T. G. Masaryk Water Research Institute with a quality database, up-to-date and functional software and, above all, user support in their daily work. The work of the Department thus requires not only expertise in the software, but also knowledge of the specialised data and context. In the future, the Department would like to develop and extend these activities by using other dynamically developing analytical, visualisation and publishing tools and applications. In fact, its staff believe that GIS is not just a misunderstood expense, but above all a valuable investment with a high return.

Fig. 9. Link to the website of the GIS and Cartography Department of the T. G. Masaryk Water Research Institute

References

[1] KULT, A. et al. (2020): Sto let činnosti Výzkumného ústavu vodohospodářského od jeho založení v roce 1919. Praha: VÚV TGM, v. v. i. 2020, p. 198–199. ISBN 978-80-87402-74-0.

[2] VÚV TGM. *Digitální báze vodohospodářských dat (DIBAVOD)* [on-line]. Available from: http://www.dibavod.cz

[3] ČÚZK. *Základní báze geografických dat České republiky (ZABAGED®)* [on-line]. Available from: https://geoportal.cuzk.cz/(S(d4gf3q3ih23q2ldznuevgfa1))/default.aspx?lng=CZ&mode=TextMeta&text=dSady_zabaged&side=zabaged&menu=24&head_tab=sekce-02-gp

[4] ZBOŘIL, A., FOJTÍK, T., KURFIŘTOVÁ, J. *Vývoj aplikací pro tvorbu kartografických výstupů ve vodním hospodářství – Historie a analýza současného stavu, Závěrečná zpráva.* 2018.

[5] NOVÁKOVÁ, H., FOJTÍK, T., ZBOŘIL, A. *Databáze ochranných pásem vodních zdrojů v České republice.* Vodohospodářské technicko-ekonomické informace. 2019, 61(2), p. 12–19. ISSN 0322-8916.

[6] VÚV TGM. *Hydroekologický informační systém VÚV TGM (HEIS VÚV)* [on-line]. Available from: https://heis.vuv.cz

[7] CENIA. *Národní geoportál INSPIRE* [on-line]. Available from: https://geoportal.gov.cz

[8] *Směrnice Evropského parlamentu a Rady 2007/2/ES o zřízení Infrastruktury pro prostorové informace v Evropském společenství (INSPIRE)*

[9] *Směrnice Evropského parlamentu a Rady 2000/60/EC ustavující rámec pro činnost Společenství v oblasti vodní politiky*

[10] *Směrnice Evropského parlamentu a Rady 2007/60/ES o vyhodnocování a zvládání povodňových rizik*

[11] *Směrnice Rady 91/676/EEC o ochraně vod před znečištěním dusičnany ze zemědělských zdrojů*

[12] *Směrnice Rady 91/271/EEC o čištění městských odpadních vod*

[13] *MKOL. Mezinárodní komise pro ochranu Labe* [on-line]. Available from: https://www.ikse-mkol.org/cz/

[14] *MKOOpZ. Mezinárodní komise pro ochranu Odry před znečištěním* [on-line]. Available from: http://www.mkoo.pl/index.php?lang=CZ

[15] *MKOD. Mezinárodní komise pro ochranu Dunaje* [on-line]. Available from: https://www.icpdr.org/main/

[16] MAŤAŠOVSKÁ, V., KOTHAN, F., LEDVINKA, O., PUMANN, P., FOJTÍK, T., MAKOVCOVÁ, M., BENDAKOVSKÁ, L. *Využití metod dálkového průzkumu Země pro monitoring stavu koupacích míst*. Vodohospodářské technicko-ekonomické informace. 2021, 63(1), p. 37–45. ISSN 0322-8916.

[17] ČÚZK. *Digitální model reliéfu České republiky 5. generace (DMR 5G)* [on-line]. Available from: https://geoportal.cuzk.cz/(S(qadwqsinrfyoginq0zbwzu3p))/Default.aspx?lng=CZ&mode=TextMeta&side=vyskopis&metadataID=CZ-CUZK-DMR5G-V&mapid=8&menu=302

[18] MLEJNKOVÁ, H., JAŠÍKOVÁ, L., FOJTÍK, T., MAKOVCOVÁ, M., JURANOVÁ, E., PUMANN, P. *Vodní rekreace v Praze od historie po současnost*. Vodohospodářské technicko-ekonomické informace. 2019, 61(5), p. 12–21. ISSN 0322-8916.

[19] Caritas Czech Republic. *Sustainable Plastic Recycling in Mongolia* [on-line]. Available from: https://mongolia.charita.cz/what-we-do/Ongoing%20projects/sustainable-plastic-recycling-in-mongolia/

The authors

Ing. Tomáš Fojtík
✉ tomas.fojtik@vuv.cz
ORCID: 0000-0001-6480-3900

Mgr. Lucie Jašíková, Ph.D.
✉ lucie.jasikova@vuv.cz
ORCID: 0000-0001-5209-406X

Jindra Kurfiřtová
✉ jindra.kurfirtova@vuv.cz

Ing. Marcela Makovcová
✉ marcela.makovcova@vuv.cz
ORCID: 0000-0002-1060-4188

Ing. Bc. Václava Maťašovská
✉ vaclava.matasovska@vuv.cz
ORCID: 0000-0001-9229-463X

Pavel Mayer
✉ pavel.mayer@vuv.cz

Ing. Hana Nováková, Ph.D.
✉ hana.novakova@vuv.cz
ORCID: 0000-0002-5946-4796

Judita Zavřelová
✉ judita.zavrelova@vuv.cz

Aleš Zbořil
✉ ales.zboril@vuv.cz
ORCID: 0000-0001-8202-3879

VTEI/2022/1

Since 1959

VODOHOSPODÁŘSKÉ
TECHNICKO-EKONOMICKÉ INFORMACE

WATER MANAGEMENT
TECHNICAL AND ECONOMIC INFORMATION

A scientific bimonthly journal specialising in water research. It is included in the List of Peer-Reviewed Non-Impacted Periodicals Published in the Czech Republic.

Volume 64

VTEI.cz

Published by: the TGM Water Research Institute,
Podbabská 2582/30, 160 00 Prague 6

Sources of photographs for this issue:
VÚV, Shutterstock.com, 123RF.com

Graphic design, typesetting and printing:
ABALON s. r. o., www.abalon.cz

Number of copies: 700 ks
Since 2022, the VTEI journal has been published in English at https://www.vtei.cz/en/

The next isuue will be published in April 2022.
Instructions for authors are available at www.vtei.cz

ISSN 0322-8916
ISSN 1805-6555 (on-line)
MK ČR E 6365

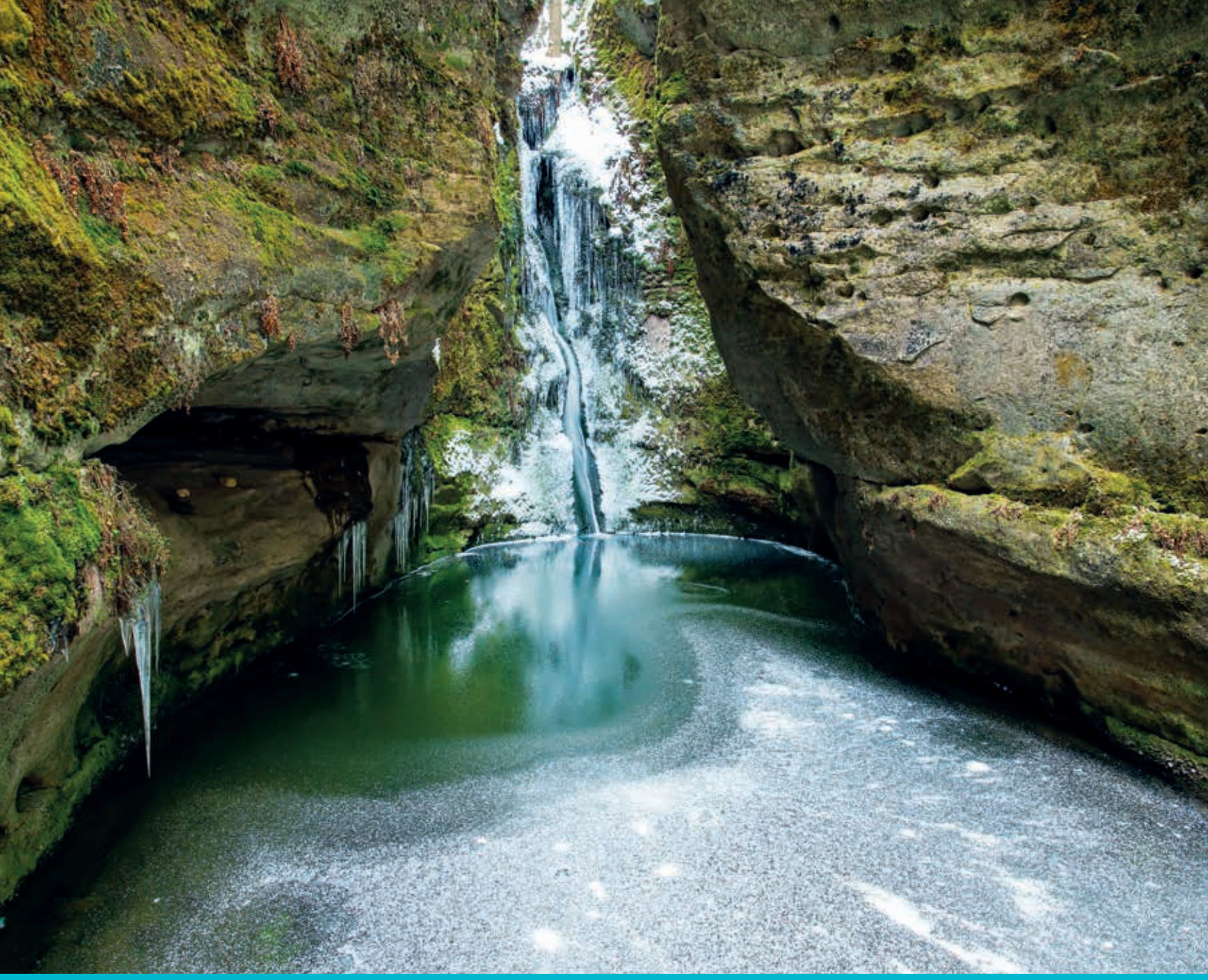

THE SPRING OF HAPPINESS

The waterfall on the *Kachní* Stream, which is called the Spring of Happiness, is located near the quay where it is possible to start boating through the Wild Gorge (*Divoká soutěska*) of the *Kamenice* river in the Bohemian Switzerland National Park. Similarly to other popular tourist spots, the small lake below the waterfall is also full of coins. The sandstone rocks that surround it contain up to 15 percent of water, which, due to gravity, permeates through them mostly from the top down. The tops of the rocks are therefore very dry in summer and the lower parts of the gorges are wet, full of trickles. Being a typical small watercourse in the middle of sandstone rocks, the *Kachní* Stream appears only after long rainy periods.
Text and photo by Václav Sojka, www.vaclavsojka.cz.

VÝZKUMNÝ ÚSTAV
VODOHOSPODÁŘSKÝ
T. G. MASARYKA
veřejná výzkumná instituce

VTEI.cz